University of Stavanger

FACULTY OF SCIENCE AND TECHNOLOGY

Bachelor's Thesis

Study program/specialization: **Energy and Petroleum Engineering**	The spring semester, 2022 Open access
Author: Audun Brenne Fehn	(Signature of the author)
Program coordinator: Supervisor(s): Mesfin Belayneh	
Title of bachelor's thesis: **Gas bubble dynamics and Pressure Build-up studies in Simulated Wellbore** Tittel på bacheloroppgave på norsk: **Gassbobledynamikk og trykkoppbyggingsstudier i simulert brønnboring**	
Credits: 20	
Keywords: • Viscosity • Resistivity • Water-based drilling fluid • Rheology • Nanoparticle • Silica • Aluminum Oxide • Pressure build-up • Simulated wellbore	Number of pages: xxx + Supplemental material/other: 0 Date/year xxx/xxx/2022 Stavanger

Acknowledgment

This task would never have been possible without the wonderful help and effort of my supervisor Mesfin Belayneh Agonafir. I big thank you to him! He has been involved in helping to choose the right task and helping to construct and build the physical and web-based simulation of the well that was used. He has also been available every time a problem has arisen and has helped solve it.

Thanks also to other employees at the University in Stavanger who have helped to weld together the pipe construction of the physical well and mechanical engineers who have found and constructed the pressure sensor on the well.

Abstract

This thesis work presents the gas bubble dynamics were studies experimental and in simulated computer simulation. A total of 13 fluids have been synthesized, which wide range of viscosity and density. The open well rig experimental study is in 178cm well, where the speed of bubble has been studies in three wellbore annuli clearance. In the close well, the experiment was conducted in 1m length and 50mm inner diameter, where the wellhead pressure was studied. The work was presented at the Oil and Energy Day for the industry and received a student prize.

Result showed that

- Gas bubble velocity depends on the rheological parameters
- Gas bubble velocity depends on the annular wellbore clearance
- The wellhead pressure build-up depends on the wellbore fluid rheological parameters, the type of kick influx and annular wellbore clearance
- The gas bubble speeds literature model requires a correlation factor. The parameter depends on the annular wellbore clearance and the rheological wellbore fluid. Wellhead pressure build-up pressure also depends on the type of kick influx

Contents

Acknowledgment I

Abstract II

Contents III

List of figures VI

List of tables X

List of Abbreviations XI

1 Introduction 12

1.1 Background and motivation 2

1.2 Problem formulation 4

1.3 Objective 6

1.4 Research Methods 6

2 Literature Study 7

2.1 Multiphase flow 7

2.2 Taylor bubble and slug 9

2.3 Bubble rise velocity in a Newtonian fluid 10

2.4 Bubble rise velocity in the non-Newtonian fluid 12

2.5 Materials description used in this thesis 12

2.5.1 CMC Polymer 13

2.5.2 Bentonite 13

2.5.3 Barite 13

2.5.4 NaCl 13

2.5.5 Aluminum oxide nano 13

2.5.6 Polymer -Xanthan gum 14

2.6 Fluid Characterization methods 14

2.6.1 Density measurements 14

2.6.2 Viscosity measurements 15

2.6.3 Rheometer measurements 15

2.7 Fluid Rheology methods 16

2.7.1 Newtonian Fluid Rheology model 16

2.7.2 Non-Newtonian Rheological models 17

2.7.2.1 Bingham 17

2.7.2.2 Power law 19

2.7.2.3 Herschel-Bulkley model and Unified model 20

2.7.3 Bubble velocity models 21

2.7.3.1 Wave analogy equation 21

2.7.3.2 Stokes or Hadamard-Rybczynski equation 22

2.7.3.3 Davies & Taylor equation 22

2.7.3.4 Li Zheng Model 23

2.7.3.5 Harmathy's equation 23

2.7.3.6 Slug flow gas migration regime 24

2.7.4 Boyle's law 24

3 Experimental works 26

3.1 Experimental Rig Construction 26

3.1.1 Top open rig 26

3.1.2 Top close rig 28

3.2 Bubble Behaviors 29

3.2.1 Slugs and Trails 29

3.2.2 Collision between bubbles 31

3.2.3 Bubble break with bentonite fluid 31

3.3 Experimental Fluid Synthesis and Characterization 33

3.3.1 Fluid 1-Water 33

3.3.2 Fluid 2-Viscous Fluid 34
3.3.3 Fluid 3-High Viscous 36
3.3.4 Fluid 4-Brine 38
3.3.5 Fluid 5-High Viscous with density modifier 40
3.3.6 Fluid 6-Bentonite 42
3.3.7 Fluid 7-Bentonite #2 44
3.3.8 Fluid 8-Modified fluid 48
3.3.9 Fluid 9-Ref + 0,2 Nano 50
3.3.10 Fluid 10-Ref Without Nano 51
3.3.11 Fluid 11-Bentonite and Barite 52
3.3.12 30 g cp with 500 g salt 53
3.3.13 Bentonite and barite #2 55
3.3.14 Nanofluid based drilling fluid 56

4 Results 56

4.1 Open system 57

4.1.1 Effect of density of the fluid and annular clearance 57
4.1.2 Effect of plastic viscosity and annular clearance 58
4.1.3 Effect of YIELD stress and LSYS and annular clearance 59
4.1.4 Effect of flow index parameter and annular clearance 60
4.1.5 Effect of LSYS effects in 2.5 mm clearance 61
4.1.6 Effect of H2O in Annular Clearance 62
4.1.7 Effect of density and viscosity and annular clearance 63

4.2 Closed system 64

4.2.1 Well Head pressure under different injection rate 64
4.2.1.1 Low injection rate 65
4.2.1.2 High injection rate 67
4.2.1.3 Continuous -average injection rate 68
4.2.1.4 Comparisons between BHP and Well head pressure under different injection rate 69

5 Gas bubble dynamics in closed well Computer Simulation 72

5.1 Simulation set up 73

5.2 Simulation results 76

5.2.1 Effect of kick intensity and kick types on wellhead pressure 76

5.2.2 Effect of annular Clearance 77

5.2.3 Effect of Methane vs Dry gas 79

6 Gas bubble speed modelling 83

6.1 Comparisons between gas bubble literature models and measurements 83

6.2 Correlation factor development 88

7 Summary and discussion 93

7.1 Summary of top open rig experimental works 96

7.2 Summary of top closed rig experimental works 102

8 Conclusion 104

9 References 106

10 Appendix 108

List of figures

Figure 1.1.1: Experimental rig design for a closed rig with a pressure sensor ..**Feil! Bokmerke er ikke definert.**

Figure 1.1.2: Simulated mud cake with fluid thru particles .. **Feil! Bokmerke er ikke definert.**

Figure 1.1.3: Experimental rig design for open well design with kick simulated pump gas-injection ..... **Feil! Bokmerke er ikke definert.**

Figure 1.3.1: The Research methods working prosses in this bachelor thesis 7

Figure 2.1.1: Reservoir pressure vs Reservoir temperature for hydrocarbons 8

Figure 2.2.1: Flow patterns Figure gathered from (Ghajar, 2005) 10
Figure 2.5.1: Simulated mud cake with fluid thru particles .. **Feil! Bokmerke er ikke definert.**
Figure 2.6.1: Newtonian fluid illustration 17
Figure 2.6.2: Bingham model that shows constant shear rate increase 18
Figure 2.6.3: Model of the Power law in Shear stress/shear rate 20
Figure 2.6.4: Model of Herschel-Bulkley law for Shear stress/Shear rate 21
Figure 2.6.5: Illustration of the Two-Plate-Model for the oscillatory test, [28](refref)..... **Feil! Bokmerke er ikke definert.**
Figure 2.6.6: Plot of the stress and strain curves against time [30] (refref)..... **Feil! Bokmerke er ikke definert.**
Figure 2.6.7: Illustration of amplitude sweep test result [27] (refref)..**Feil! Bokmerke er ikke definert.**
Figure 2.6.8: to the left the gas kick is at the bottom of the well, to the right the gas kick is at the top of the wellhead. (Hamarhaug, 2011; Vikra) 25
Figure 2.6.9: Baroid mud balance for measurements of fluid density ..**Feil! Bokmerke er ikke definert.**
Figure 3.1.1: a. Open wellbore physical rig construction with measuring illustration and bubble/slug illustration of the open wellbore rig simulation, b: picture of the picture/filming set-up 27
Figure 3.1.2: Slug/bubble illustration of measuring points and dynamic in the open wellbore rig, Illustration of bubble front and the corresponding time collection from the test 27
Figure 3.2.1: picture 1: bubble/slug dynamics from 1-3 measurements points, Picture 2: Slug combining point from 2-5 measurements points. 30
Figure 3.2.2: picture 3: bubble/slug dynamics from 8-11 measurements points, Picture 2: Slug ending point from 14-16 measurements points. 30
Figure 3.3.1: Experimental rig design for a closed rig with a pressure sensor ..**Feil! Bokmerke er ikke definert.**
Figure 3.4.1: Viscometer data at 22°C for Water 33
Figure 3.4.2: Viscoelastic data from at 22°C for Water 34
Figure 3.4.3: Viscometer data at 22°C for Viscous Fluid 35
Figure 3.4.4: Viscoelastic data at 22°C for Viscous Fluid 36
Figure 3.4.5: Viscometer data at 22°C for High Viscous Fluid 37
Figure 3.4.6: Viscoelastic data at 22°C for High Viscous Fluid 37
Figure 3.4.7: Viscometer data at 22°C for Brine 39

Figure 3.4.8: Viscoelastic data at 22°C for Brine 39
Figure 3.4.9: Viscometer data at 22°C for High Viscous Fluid with density modifier..... 41
Figure 3.4.10: Viscoelastic data at 22°C for High Viscous Fluid with density modifier..... 41
Figure 3.4.11: Viscometer data at 22°C for Bentonite Fluid 43
Figure 3.4.12 43
Figure 3.4.13: Viscometer data at 22°C for Bentonite Fluid nr 2 45
Figure 3.4.14: Viscometer data at 22°C for Modified Fluid 49
Figure 3.4.15: Viscometer data at 22°C for Ref+0,02 Nano..... 50
Figure 3.4.16: Viscometer data at 22°C for Ref without Nano..... 52
Figure 3.4.17: Viscometer data at 22°C for Bentonite and Barite 53
Figure 3.4.18: Viscometer data at 22°C for Fluid 12..... 54
Figure 3.4.19: Viscometer data at 22°C for Fluid 13..... 55
Figure 4.1.1: Average velocity between small and big bubbles in H2O vs in Brine. 58
Figure 4.1.2: Plastic Viscosity and Velocity of water(1cp), Fluid 2(6cp) and Fluid 3(13cp) with different clearance..... 58
Figure 4.1.3: Low shear yield stress and Velocity of water(0cp), Fluid 2(0,5cp) and Fluid 3(1,5cp) with different clearance..... 59
Figure 4.1.4: Yield stress and Velocity of water(0cp), Fluid 2(3cp) and Fluid 3(8,5cp) with different clearance..... 60
Figure 4.1.5: Flow index and Velocity of (form right to left) water (0), Fluid 2(0,73) and Fluid 3(0,68) with different clearance 61
Figure 4.1.6: LSYS and Velocity of Fluid 2(0,5cp) and Fluid 3(1,5) and Fluid 7(2,5cp) with the same clearance..... 62
Figure 4.1.7: Velocity of bubbles, Slugs and their average together in different clearance. ... 63
Figure 4.1.8: Velocity compared high- and low-density fluid (Water and brine) with different clearance..... 64
Figure 4.1.9: Change of velocity and clearance for water, brine and bentonite fluid 64
Figure 4.2.1: Fluid 1 and Fluid 12 with same low-rate injection and BHP 66
Figure 4.2.2: Fluid 4 and Fluid 5 with same high-rate injection and BHP 68
Figure 4.2.3: All fluids (use in closed rig physical simulation) in continuous injection rate .. 69
Figure 4.2.4: Water as fluid in the wellbore with BHP vs WHP, b, 2,5 CP as fluid in the wellbore with BHP vs WHP..... 69
Figure 4.2.5: Fluid 12 in the wellbore with BHP vs WHP, b, Fluid 5 in the wellbore with BHP vs WHP..... 69

Figure 4.2.6: Brine in the wellbore with BHP vs WHP, b, Bentonite fluid in the wellbore with BHP vs WHP 70
Figure 4.2.7: Weighted Bentonite in the wellbore with BHP vs WHP 70
Figure 4.2.8: The average measurements from BHP and WHP in continuous, low rate and high rate of gas injection. 71
Figure 4.3.1: 2 barrels injected with 2180 psi in bottom hole pressure **Feil! Bokmerke er ikke definert.**
Figure 4.3.2: 5 barrels injected with 2180 psi in bottom hole pressure.**Feil! Bokmerke er ikke definert.**
Figure 4.3.3: Well head pressure vs time for water as fluid with different BHP with real time lag from beginning ..... **Feil! Bokmerke er ikke definert.**
Figure 4.3.4: Well head pressure vs time for water as fluid with different BHP without the time lag ..... **Feil! Bokmerke er ikke definert.**
Figure 4.3.5: Comparisons between BHP/WHP with water as fluid ....**Feil! Bokmerke er ikke definert.**
Figure 4.3.6: All fluids compared for finish WHP and Kick intensity in Drillbench ..... **Feil! Bokmerke er ikke definert.**
Figure 4.3.7: Time of fluids to fill up 3m^3 Pit gain vs Kick intensity in Drillbench ..... **Feil! Bokmerke er ikke definert.**
Figure 4.3.8: Time of fluids to fill up 3m^3 Pit gain vs Kick intensity in Drillbench ..... **Feil! Bokmerke er ikke definert.**
Figure 4.3.9: Well head pressure dynamics for fluid 2 with different kick intensity..... **Feil! Bokmerke er ikke definert.**
Figure 4.3.10: Well head finish pressure for fluid 2 when gas kick (with different kick intensity) is at the well head ..... **Feil! Bokmerke er ikke definert.**
Figure 4.3.11: Dynamics in time for 3m^3 pit gain fill up for fluid 2 with different kick intensity ..... **Feil! Bokmerke er ikke definert.**
Figure 4.3.12: Time of fill up 3m^3 fill up of pit gain for fluid 2 with different kick intensity ..... **Feil! Bokmerke er ikke definert.**
Figure 4.3.13: Well head pressure dynamics for fluid 11 with different kick intensity..... **Feil! Bokmerke er ikke definert.**
Figure 4.3.14: Well head finish pressure for fluid 11 when gas kick (with different kick intensity) is at the well head ..... **Feil! Bokmerke er ikke definert.**

Figure 4.3.15: Dynamics in time for 3m^3 pit gain fill up for fluid 11 with different kick intensity ..... **Feil! Bokmerke er ikke definert.**
Figure 4.3.16: Time of fill up 3m^3 fill up of pit gain for fluid 11 with different kick intensity ..... **Feil! Bokmerke er ikke definert.**
Figure 4.3.17: Compered Dry Air and Methane gas with different kick intensity for fluid 2, 3, 8 and 11 ..... **Feil! Bokmerke er ikke definert.**
Figure 4.3.18: Dynamics in time to fill up 3m^3 pit gain for Fluid 2,3,8 and 11 with different kick intensity and with both Methane and Dry Air in the gas-kick ..... **Feil! Bokmerke er ikke definert.**
Figure 4.3.19: Time to fill up different Pit gain volume with constant kick intensity for Fluid 2,3 and 8 ..... **Feil! Bokmerke er ikke definert.**
Figure 4.3.20: Fluids compared by Well head finish pressure and kick intensity ..... **Feil! Bokmerke er ikke definert.**
Figure 5.2.1: Clearance of the open well demonstrated ..... **Feil! Bokmerke er ikke definert.**
Figure 5.2.2: Correlation factor/Clearance for Fluid 1 from Equation 33 and 35..... **Feil! Bokmerke er ikke definert.**
Figure 5.2.3: Correlation factor/Clearance for Fluid 2 from Equation 33 and 35..... **Feil! Bokmerke er ikke definert.**
Figure 5.2.4: Correlation factor/Clearance for Fluid 3 from Equation 33 and 35..... **Feil! Bokmerke er ikke definert.**
Figure 5.2.5: Correlation factor/Clearance for Fluid 4 from Equation 33 and 35..... **Feil! Bokmerke er ikke definert.**
Figure 5.2.6: Correlation factor/Clearance for Fluid 5 from Equation 33 and 35..... **Feil! Bokmerke er ikke definert.**
Figure 5.2.7: Correlation factor/Clearance from fluid 1 to Fluid 7 from Equation 33 and 35 ..... **Feil! Bokmerke er ikke definert.**
Figure 7.2.1: Fluid 11 Dynamics with Dry air as kick influx gas with different kick intensity ..... **Feil! Bokmerke er ikke definert.**
Figure 7.2.2: Fluid 11 Well head finish pressure dry air as kick influx gas with different kick intensity ..... **Feil! Bokmerke er ikke definert.**
Figure 7.2.3: Fluid 11 Dynamics with Methane as kick influx gas with different kick intensity ..... **Feil! Bokmerke er ikke definert.**
Figure 7.2.4: Fluid 11 Well head finish pressure Methane as kick influx gas with different kick intensity ..... **Feil! Bokmerke er ikke definert.**

Figure 7.2.5: Fluid 3 Well head pressure dynamics with regular clearance in annulus. ..... **Feil! Bokmerke er ikke definert.**

Figure 7.2.6: Fluid 3 Well head pressure dynamics with big clearance in annulus. ..... **Feil! Bokmerke er ikke definert.**

Figure 7.2.7: Well head finish pressure with different kick intensity for fluid 3 in regular clearance in annulus. ..... **Feil! Bokmerke er ikke definert.**

Figure 7.2.8: Well head finish pressure with different kick intensity for fluid 3 in big clearance in annulus. ..... **Feil! Bokmerke er ikke definert.**

Figure 7.2.9: Summarize BHP VS WHP for different pump injection rate for bentonite fluid ..... **Feil! Bokmerke er ikke definert.**

Figure 7.2.10: Summarize BHP VS WHP for different pump injection rate for brine fluid **Feil! Bokmerke er ikke definert.**

List of tables

Table 2.6.1: Viscoelastic behavior with changing angles. (refref) .....**Feil! Bokmerke er ikke definert.**

Table 3.4.1: Fluid 1 mixing recipe in mixing order 33

Table 3.4.2: Rheology Parameter data at 22°C for Water 34

Table 3.4.3: Fluid 2 mixing recipe in mixing order 35

Table 3.4.4: Rheology Parameter data at 22°C for Viscous Fluid 36

Table 3.4.5: Fluid 3 mixing recipe in mixing order 37

Table 3.4.6: Rheology Parameter data at 22°C for High Viscous Fluid 38

Table 3.4.7: Fluid 3 mixing recipe in mixing order 38

Table 3.4.8: Rheology Parameter data at 22°C for Brine 39

Table 3.4.9: Fluid 5 mixing recipe in mixing order 40

Table 3.4.10: Rheology Parameter data at 22°C for High Viscous Fluid with density modifier 41

Table 3.4.11: Fluid 6 mixing recipe in mixing order 42

Table 3.4.12: Rheology Parameter data at 22°C for Bentonite Fluid 43

Table 3.4.13: Fluid 7 mixing recipe in mixing order 44

Table 3.4.14: Rheology Parameter data at 22°C for Bentonite Fluid nr 2 45

Table 3.4.15: Fluid 8 mixing recipe in mixing order 48

Table 3.4.16: Rheology Parameter data at 22°C for Modified Fluid 49
Table 3.4.17: Fluid 9 mixing recipe in mixing order 50
Table 3.4.18: Rheology Parameter data at 22°C for Ref+0,2 Nano 50
Table 3.4.19: Fluid 10 mixing recipe in mixing order 51
Table 3.4.20: Rheology Parameter data at 22°C for Ref without Nano 52
Table 3.4.21: Fluid 11 mixing recipe in mixing order 52
Table 3.4.22: Rheology Parameter data at 22°C for Bentonite and Barite 53
Table 3.4.23: Fluid 12 mixing recipe in mixing order 54
Table 3.4.24: Rheology Parameter data at 22°C for Fluid 12 54
Table 3.4.25: Fluid 13 mixing recipe in mixing order 55
Table 3.4.26: Rheology Parameter data at 22°C for Fluid 13 55
Table 3.4.27: Mix composition for reference mud with and without nanoparticle with modified mud 56
Table 7.2.1: Summary of fluids type, Clearance I annulus, Rheology and measured velocity 95
Table 8.1.1: Summary of 96
Table 8.2.1: summary of fluids tested in the closed well simulation with rheology, BHP, WHP and difference between WHP and BHP (Delta) 103
Table 8.2.1: Table of average measurements units from BHP, continuous, low rate and high rate with procent of difference between BHP and WHP measurements 106

List of Abbreviations

API	American Petroleum Institute
BF	Base Fluid
BSc	Bachelor
C	Correlation factor
CMC	Carboxymethyl cellulose
CP	Carbopol
ECD	Equivalent circulating density
H-B	Herschel-Bulkley

ID	Inner Diameter
LSYS	Low Shear Yield Stress
MW	Mud Weight
Np	Nanoparticle
OBM	Oil-Based Mud
OD	Outer Diameter
PV	Plastic viscosity
Ref	Reference fluid
UiS	University of Stavanger
WBM	Water-Based Mud
WHP	Well head pressure
XG	Xanthan Gum
YS	Yield Stress

1 Introduction

This BSc thesis work deals with an experimental investigation of bubble flow dynamics in different drilling fluid properties (viscosity, density) and wellbore annular clearances. The experimental rigs were open and closed wells. In the open well, drilling fluids were filled in 170cm length and three annuli clearance (ODxID: 30mmx25mm, 40mmx25mm, 50mmx25mm) in which the gas bubble speeds were investigated. In the closed wells, fluids were filled up to 85 cm length and inner diameter of 50mm, where the well head pressure (WHP) build up were studied. Moreover, the fluid systems were used in computer simulation to study the WHP dynamics injected with Methane and Dry air. The study also evaluated the predictive power of literature models by comparing with the measurements and generated empirical correlations factors for different drilling fluid and annular clearance.

1.1 Background and motivation

Drilling fluid is an integral part of drilling operation. The main function of drilling fluids among others to mention are to maintain well pressure, bring cutting to the surface, cool wellbore, and drill bit (Skjeggestad, 1989). To mitigate the wellbore instability, the well pressure is normally designed to be between the fracture and collapse pressure. For instance, Figure 1.1.1 shows the Macondo well program and the red line indicates the BP's planned mud weight (The Bureau of Ocean Energy Managment, 2011).

When the well pressure is lower than collapse pressure, the wall of the formation will fall into the wellbore and resulting in solid induced drilling string sticking. On the other hand, when the well pressure exceeds the facture strength of the formation, the wellbore will fail by tensile failure and resulting in loss circulation. In reservoir section, when the well pressure is below the formation pressure, the formation fluid flow into the well will occur. This phenomenon is called Kick (Skjeggestad, 1989).

The behavior of kick dynamics in the OBM and WBM are different (Batchelor, 2012). As kick influx in WBM, it can be detected. However, there are cases where small concentration of kick in oil based becomes soluble and will not be detected. The undetected gas kicks are the main reason for many blowout incidents in the oil industry (Guangzhao Zhou, 2021). Figure 1.1.2 shows the collapse of the drilling rig after the biggest blowout incident and in addition, the hydrocarbon spilled into the ocean lasted for 87 days and damaged fauna and flora.

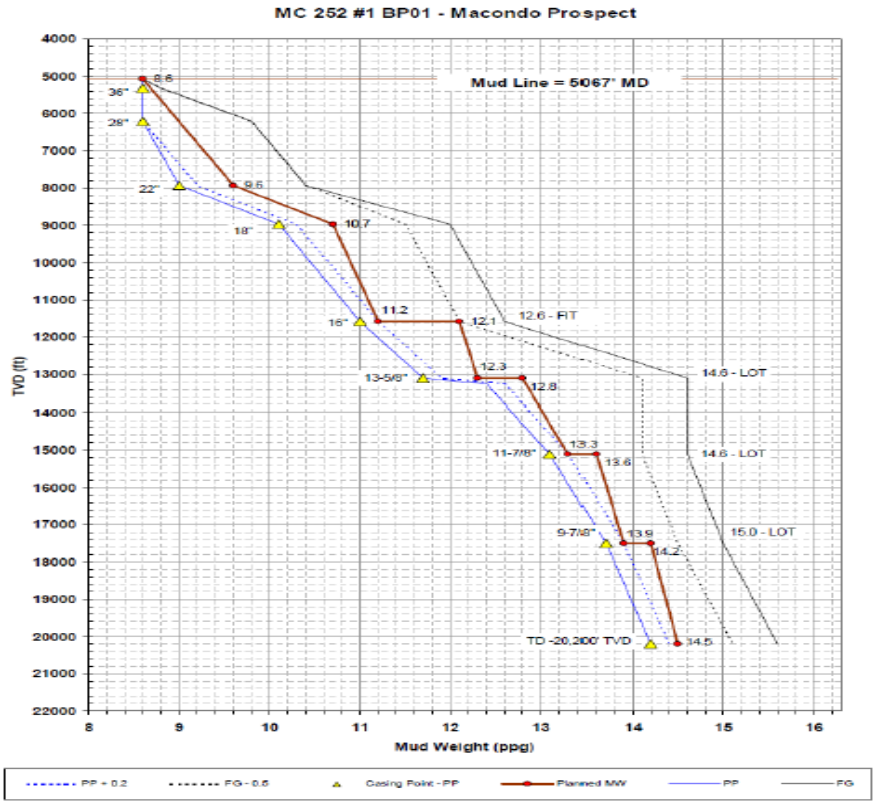

Figure 1.1.1: Macondo well drilling margin plot, (The Bureau of Ocean Energy Managment, 2011)

Figure 1.1.2: 1. The Macondo Blowout, 2. Environmental impact

Several experimental studies have been conducted to describe the gas -liquid two phase flow behaviour in wellbore for the purpose of understanding the well pressure and kick dynamics. Loyd (Warren L. Lloyd, 2000) have reported that the gas bubble rises depend on the rheological and physical properties of the drilling fluid and the gases including the fluid rheology (viscosity and gel strength), gas bubble geometry (size and shape), gas density and liquid density.

Like cutting suspension in drilling fluid, Johnson and Rezmer-Cooper 1995 (Ashley Johnson and lan Rezmer-Cooper, 1995) reported that gel strength of the drilling mud is the important

mud property that has a significant effect on gas suspension. According to Johann et al, for the gas concentration higher than 10%, the migration velocity is typically 100 feet/min (Ashley Johnson and lan Rezmer-Cooper, 1995).

Rommetveit et al have presented field test and data analysis of the ultra-Deepwater Hydraulics and Well Control Tests (Rolv Rommetveit, 2003). Johnson and Rezmer-Cooper 1995 have reported the work of Hovland and Roommvet (Frank Hovland, 1992) also as the gas slip velocity as 110m/ft.

Tarvin et al. (Tarvin, 1994) conducted experiments on gas rise test through drilling. The analysis of data showed that gas rises velocity faster than the migration velocity generally accepted in the drilling industry. Skalle et al. (P. Skalle, 1991) experimentally investigated the slip velocity of air in mud stagnant in vertical well and its impact on the Bottomhole pressure. They have developed empirical correlations of in-situ gas rise velocity and terminal settling velocity for dispersed bubbly flow and slug flow. The investigators have reported good downhole pressure estimation from the developed empirical correlations compared with the measurement. Lage et al's (A.C.V. Martins Lage, 1994) experimental results reported that the centre line gas front rise speed faster than the tail edge. The authors have indicated the surface pressure build up should consider the drilling fluids compressibility, the wellbore expansion and fluid lose.

Moreover, several theoretical modelling works are also developed for well control simulators to describe the kick phenomenon and predicting the well pressures.

Therefore, early kick detection allows for managing the well with the rig equipment as the gas enters the riser or choke line. On the other hand, as kick influx in water-based mud, and shut in the well, the well pressure increases as kick migrating up in the wellbore. It is evident that the kick rising speed affects the wellbore pressure at the open hole weakest point and the surface wellhead pressure development rate that may affect the well integrity at the wellhead.

1.2 Problem formulation

At the Louisiana state university, Santos (Otto L. A Santos, 2021) have conducted full scale experiment on the pressure buildup of gas injected in at the bottom of a close well. Fresh water is filled in 2-7 / 8 in and 5026 ft well. Nitrogen gas was used as a kick and injected at the bottom of the well with different injected rate. The pressure measured at the top of the well. Figure

1.2.1 show the wellhead pressure buildup in time for 2 barrel and 5 barrel injection with 2180 psi bottom hole pressure, respectively.

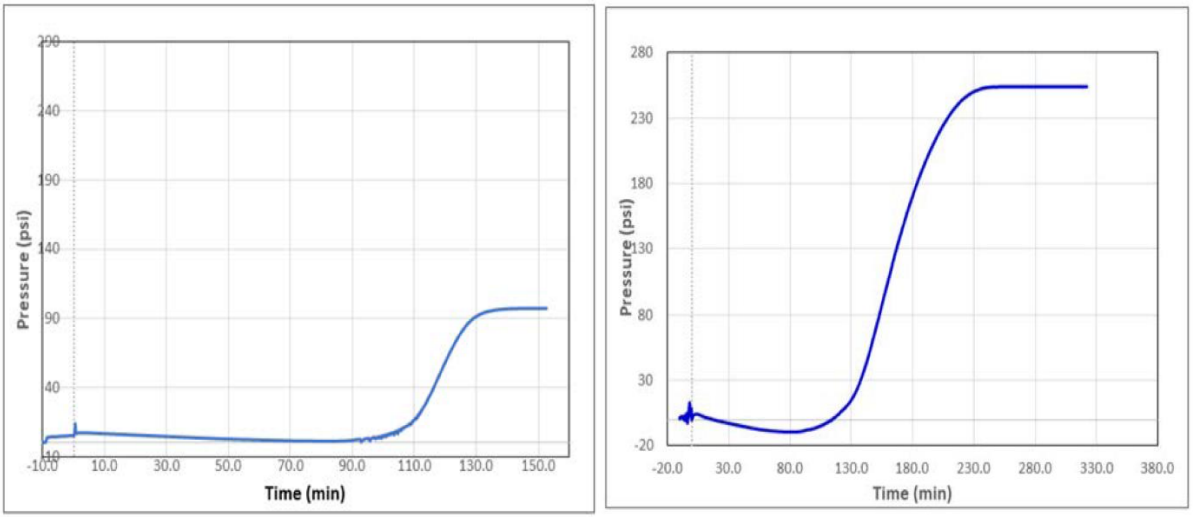

Figure 1.2.1: 1. Two barrels injected with 2180 psi in bottom hole pressure, 2. Five barrels injected with 2180 psi in bottom hole pressure, (Otto L. A Santos, 2021)

Results show the 2 barrels, and the 5 barrels doesn't carry the bottomhole pressure 2180psi all the way to the surface. The wellhead pressures rather recorded as 97 psi and 254 psi, respectively. This result clearly indicates the low of gas low, where the change in volume and gas pressure. Moreover, the change in volume gas indirectly reflect the compression of fluid. Therefore, the assumption of incompressible fluid in closed well is not valid and is more conservative.

Figure 1.2.1 shows the dynamic of the experimental work conducted in Newtonian fluid. Since drilling fluids are of non-Newtonian, this thesis work is designed to study the kick dynamics in non-Newtonian fluid.

In 1m long and 50mm ID closed well, this thesis work is therefore address research question such as

- Effect of viscosity on Wellhead pressure
- Effect of density on Wellhead pressure
- Combined effect of density and viscosity
- Injection rate and magnitude of injection pressure

In open hole, the main research tasks in this work are to explore the dynamics the velocity parameter in 17.5x5.0'', 12.25x5.0'' and 8.5x5.0'' annulus clearances

- Effect of viscosity
- Effect of density
- Their combined effects

Moreover, using the computer simulation studies, the thesis work is simulating the effect dynamics kick sizes, and kick intensity and annular clearances on wellhead pressure.

1.3 Objective

The objective of this thesis is to get a better understanding of bubble dynamics and wellhead pressure and how parameters have an impact and the trends from old formulas to today. Effect of wellbore fluid and geometry on the bubble dynamics in open and closed wells.

Run software simulation in closed / Open holes compared with experimental observations.

Develop empirical models that relate velocity and WHP with drilling fluid

The investigation is based on

- Experiments in open/closed wellbore
- Software kick dynamics simulation
- Empirical modeling of velocity and WHP.

1.4 Research Methods

Figure 1.4.1 shows the summary of the research program designed in this thesis work. The activities comprise two parts, namely experimental and computer-based simulation works. The computer-based simulation is called Drillbench (More information at below) and the program in this simulation is dynamic fluid.

During experimental works, two experimental rigs will be constructed. The experimental rigs will be filled with different drilling fluids having different physical and rheological properties.

The investigation of the kick dynamics and pressure build-ups in the open and closed rig systems respectively. The fluids are characterized by 13 fluids with water as the base fluid.

The second research is on the pressure dynamics in closed wells. In this simulation wellbore, dry gas and methane are simulated by filling the well with the formulated fluid systems.

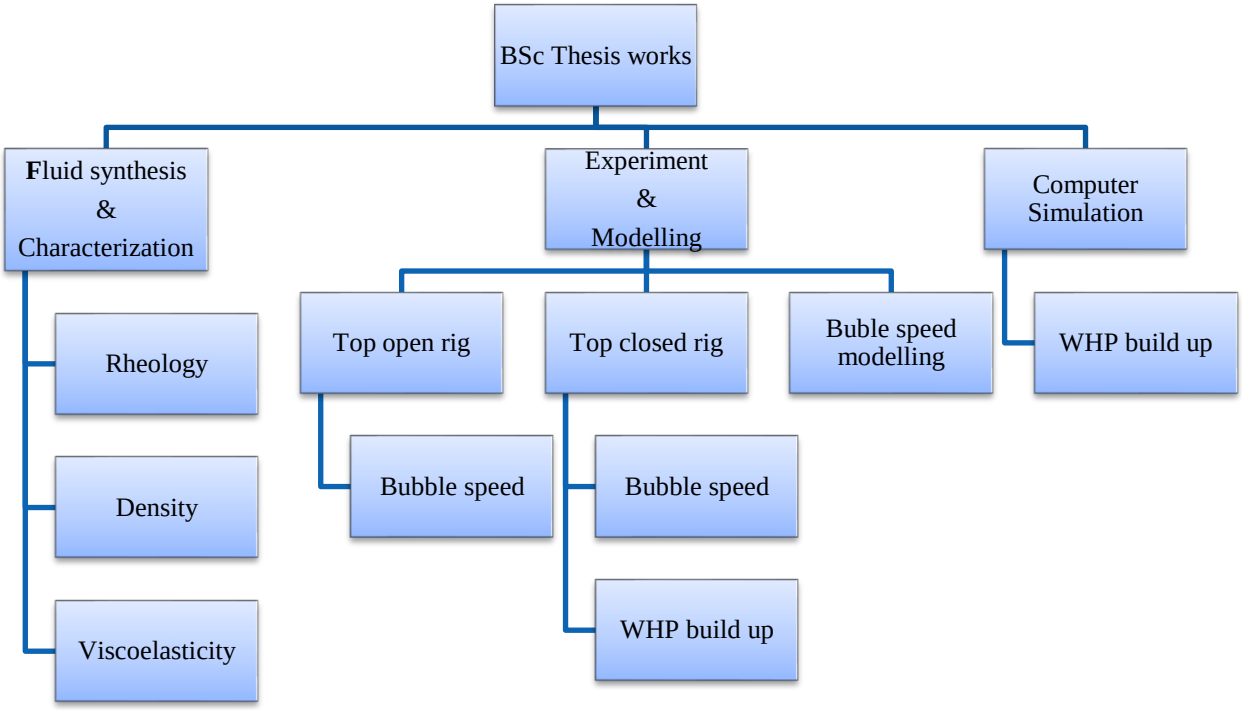

Figure 1.4.1: The Research methods working prosses in this bachelor thesis

2 Literature Study

The theoretical background study for flow and dynamics is complex. There is so many parameters for the fluid and wellbore to take to account. To keep things simple, just the factors that we tested and investigated are discussed in this chapter.

2.1 Multiphase flow

Multiphase flow is a description of different phases of flow materials can be liquid, gas, or solid. The main characterization with the multiphase flow is that it is combined into at least two phases. The parameters that affect the mineral or flow are temperature and pressure. In the petroleum industry, a three-phase flow of oil, water, and gas is a common situation that can

occur in a wellbore when drilling. When water or gas is pumped down to the reservoir to push hydrocarbons thru the pores of the rock and up the wellbore with pressure increases to one phase oil, production from the bottom of the wellbore can soon change to a multi-phase flow when pressure and temperature reduce on the way up to the surface. When the pressure is under the bubble or dew point the change will start as illustrated in Figure 2.1.1. The water in the oil can saturate and deflect into the wellbore (Hall, 1992).

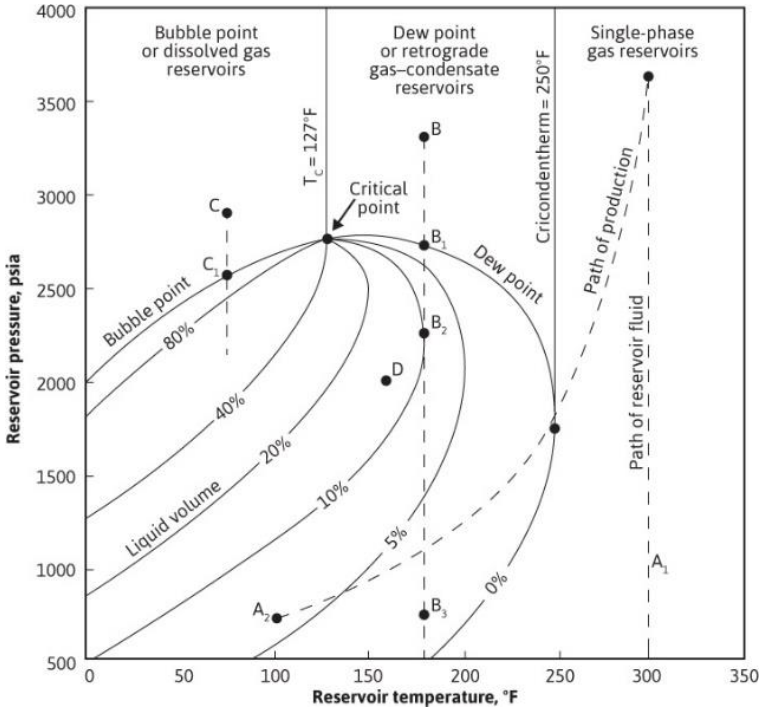

Figure 2.1.1: Reservoir pressure vs Reservoir temperature for hydrocarbons

Figure gathered from: (Terry, 2014)

In this thesis, the flow pattern for different bubble flow in still liquid in tubes will be the focus. There are different types of gas bubbles in a liquid phase. In tubes the bubbles can be characterized as bubbles, slug (Taylor bubble), churn, annular, and mist flow (Bugg, 2002).

What is important in terms of multiphase flow is how to develop the design of the drill pipe and this can have a big impact financially if this is done correctly. The hydrostatic components, pressure, and production rate in the well depend on the multiphase flow pattern. Rust and friction can form in the drill pipe, and it is therefore important to know about what is happening in the drill pipe. Since multiphase flow says a lot about the pressure, the temperature that can lead to an increase (or decrease) in volume, it can go beyond the drill pipe in the well, and to choose the right equipment it is important to have a good understanding of this (Hall, 1992).

2.2 Taylor bubble and slug

The Taylor bubble is a large bubble where the height of the bubble is bigger than the size of the diameter of the bubble. This is the standard shape of the Taylor bubble. The front of the bubble is the surface, it is elongated and round, but the rest is like a cylindrical shape. In this thesis the Taylor bubble is addressed as a slug. That is because they are nearly the same and have a bit different from normal sphere-shaped bubbles. Small bubbles can be compared to Taylor bubbles or slugs with enough force and velocity between the fluid and bubbles in the system. A slug can also be a volume of another fluid in a pipe, but in this thesis, the slug is referred to as big Taylor bubble-shaped air bubbles (Bugg, 2002).

The velocity of Taylor bubbles is most known from Davies and Taylor in 1950 (R. M. Davies, 1949).

Bubble-flow: This flow regime occurs when the volume of the gas is relatively small in a liquid system. As more rate of gas is produced then more bubbles occur.

Slugs-flow: When the flow influx of gas increases even more the bubbles will combine and begin to take more of the whole area of the tube and become cylindrical. This is the slug flow and is still a stable flow with the high gas rate in the liquid tube.

Churn-flow: After the slug-flow increases in rate and velocity the flow will get unstable and the slug will rip apart and become churn-flow. The cylindrical shape of the slug will no longer occur and will look broken and turbulent.

Annular flow: This flow pattern will occur when the churn flow is broken down and even more rate and velocity of gas from the influx starts. The liquid will now just be on the well wall and the air will penetrate between (Ambrose, 2015).

Wispy-Annular-flow: This mostly occurs when there is more air influx rate, and the liquid is not still but has a rate in the opposite direction. The air has such high pressure and will combine and make small liquid bubbles or “wispy” shapes in the center of the tube.

As this thesis takes place in still fluid and with normal speed and rate, the bubble flow and slug flow will occur most of the time. All the flow patterns are illustrated in Figure 2.2.1.

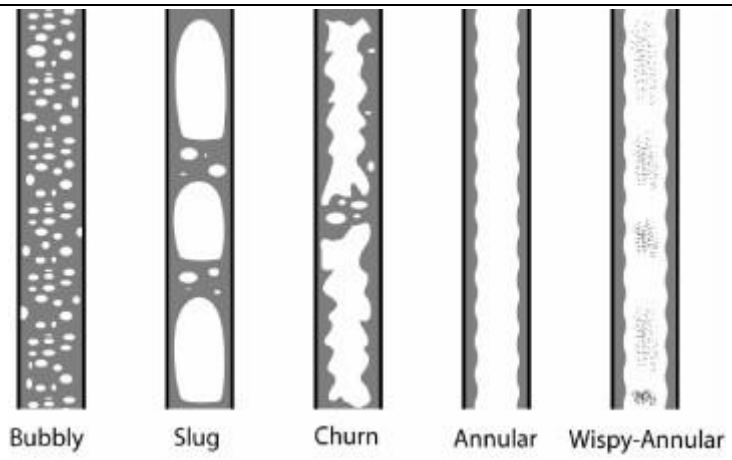

Figure 2.2.1: Flow patterns Figure gathered from (Ghajar, 2005)

Why are slugs spherical?

Slugs have a cylindrical shape with a spherical top. Big Bubbles, slugs, and Taylor bubbles have a spherical top shape because the surface condition must be satisfied as the pressure from the gravity pushes the sides inside. Bernoulli's equation applies the velocity on top of the slug should be net-zero so the surface condition will be illustrated as velocity with (R. M. Davies, 1949):

$$v^2 = 2 * g * h \qquad 1$$

Where:

- v = velocity, [m/s]
- g = gravity, [m/s^2]
- h = depth, [m]

2.3 Bubble rise velocity in a Newtonian fluid

Newtonian fluid follows Newton's law of viscosity and has a constant Shear stress/shear rate and starts from zero shear stress for zero shear rate. The bubbles are normally in an laminar steady flow and the biggest outcome of the velocity, is the diameter and the clearance of the tube filled with Newtonian fluid (Islam, 2020).

The Bubble will arise concerning the buoyancy law that explains that because of pressure difference going downward and upward on an object (or bubble) the object will rise or fall in a

liquid. In the bubble case in a Newtonian fluid, because of the low weight of the air bubble and its size, the upwards force will normally be greater than the downwards force (J. Tsamopoulos, 2008):

$$F_{buoyant} = F_{up} - F_{down} \quad (2)$$

Where:

- $F_{buoyant}$ = force of buoyancy, [N]
- F_{up} = force of pressure pointing upwards from the bottom of the object(bubble), [N]
- F_{down} = force of pressure pointing downwards from the top of the object(bubble), [N]

When there is talking about forces and pressure to the object, then this will relate to below (Gregersen, 2020):

$$P = \frac{F}{A} \quad (3)$$

Where:

- P = pressure, [Pa]
- F = force, [N]
- A = Area, [m^2]

The greater the force upward is relative to the force downward then the greater the velocity will be. As the formula says the greater the pressure and area are then the force will be bigger. For the pressure the formula can be written as below (Mobley, 2000):

$$P_{gauge} = \rho g h \quad (4)$$

Where:

- P = pressure, [Pa]
- ρ = density, [kg/m^3]
- g = gravity, [m/s^2]
- h = height (depth), [m]

As for the bubble velocity in a Newtonian fluid with constant viscosity, density, and steady flow, the more volume or area of the bubble will normally give more pressure difference and more upwards force and automatically give more velocity from bottom to top of a wellbore filled with Newtonian fluid.

To summarize the principle of the bubble forces in a Newtonian fluid can be understood from Archimedes' principle which looks at the volume in a fluid and the upwards force and connects those two for below (Mobley, 2000):

$$F_{buoyant} = \rho V_f g \quad (5)$$

Where:

- $F_{buoyant}$ = force of buoyancy, [N]
- g = gravity, [m/s^2]
- ρ = density, [kg/m^3]
- V_f = Volume of bubble(object), [m^3]

2.4 Bubble rise velocity in the non-Newtonian fluid

Non-Newtonian fluid is fluid that doesn't have the same pattern as Newtons' law of viscosity. To measure the velocity of the bubbles that rise in non-Newtonian fluid the viscosity and density are more included. As Aminia'a bubble rise experiment with small air bubbles in a solution with water and polymer to increase viscosity and change Newtonian fluid to non-Newtonian fluid, shown that the velocity was dependent on the power-law on the bubble volume. An increase in Xanthan or CMC and then the viscosity shows that the velocity rise decreased (Shahram Amirnia, 2013).

2.5 Materials description used in this thesis

Wellbore fluids are characterized by their Viscosity and Density. The well fluids are Water, Less and high viscous Polymeric fluids without solid additives, Water and polymeric fluid weighted by weighting agents.

2.5.1 CMC Polymer

CMC Is a naturally modified polymer. It is a cellulose product that is dispersed in water-based drilling mud. It reduces the filter loss and forms a thin, elastic filter cake with little permeability. The polymer is obtained from MISWACO (Skjeggestad, 1989).

2.5.2 Bentonite

Bentonite is used as an additive in drilling mud to give the liquid viscosity and filter loss control properties. Bentonite contains various minerals and the predominant is montmorillonite. In addition, there are 0-30% other non-clay minerals. When bentonite is added to freshwater, it will swell to several times its original volume (Skjeggestad, 1989; Stavanger, 2021).

2.5.3 Barite

Barite is a weight material that is used in drilling fluid, which has high specific density of 4.2 sg. The product is obtained from MI-SWACO. Barite is a naturally occurring mineral with the chemical formula BaSO4. It is commonly used as an additive in drilling fluids to increase density (Skjeggestad, 1989; Stavanger, 2021).

2.5.4 NaCl

NaCl or salt is used to increase density in the fluids in this thesis. Salt is also great for this experiment because of their colorless and see-through components so dynamics in the wellbore can be studied. Salt can be added to liquid before or after another polymer to improve the loose lights in the drilling fluid. Saltwater drilling fluid can be used to drill through salt formations (Schlumberger Oilfield, 2022).

2.5.5 Aluminum oxide nano

During the first phase on the project, Aluminum oxide was used to improve the performance of the conventional drilling fluid. Because of the experimental rig construction was successful, the project was shifted to the main kick dynamics. Due to the presence of the nanofluid based drilling fluid. We used the Al_2O_3 drilling fluid for the experiment.

2.5.6 Polymer -Xanthan gum

Xanthan, XG polymer is biopolymer that has been used in drilling mud to provide viscosity and control fluid loss. The XG polymer is obtained from MI-SWACO (Skjeggestad, 1989).

2.6 Fluid Characterization methods

This section presents the theory of rheological, hydraulic, and viscoelasticity. These will be used to model and simulate the experimental data to be measured in chapter 4.

2.6.1 Density measurements

A Baroid sludge weight is used to measure the density of the sludge. The weight is first calibrated by measuring the density of known water (1.00 SG). When the density of a liquid is measured, it is poured almost to the edge of the container and pressed on pressed with holes. If liquid comes out of the hole, the container is full. Liquid lying on the surface is wiped off before measurement. Then place the weight on the rocker. The weight is adjusted so that the weight is at rest and level. This is checked with a spirit level that is on the scales. Arrow on the arrow indicates where on the weight you read the density of.

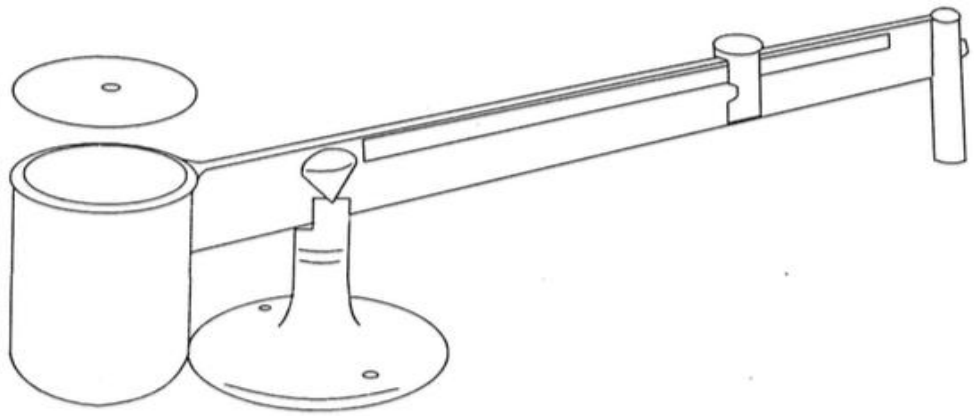

Figure 2.6.1: Baroid mud balance for measurements of fluid density, (Strand, 1998)

2.6.2 Viscosity measurements

The viscosity responses of the wellbore fluids were measured with An OFITE Model 800 8-Speed viscometer. The rheological properties of the fluids were then extracted using the measurement and the rheological models as shown in section 3.3. The viscometer has rotational speeds of 600, 300, 200, 100, 60, 30, 6 and 3 RPM. Figure 2.6.2 shows the photograph picture of OFITE Model 800 8-Speed viscometer.

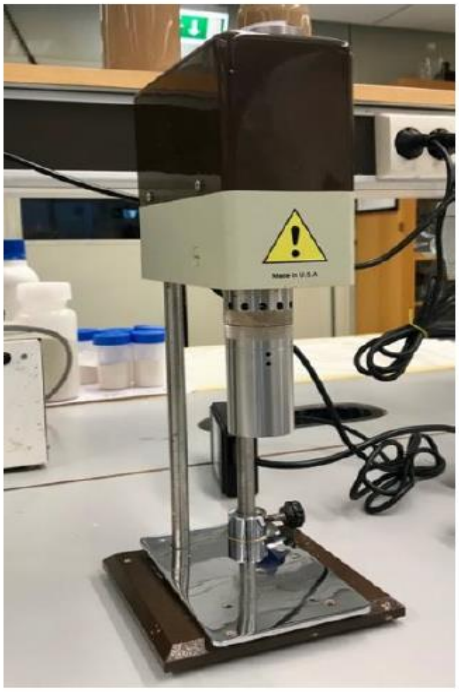

Figure 2.6.2: OFITE Model 800 8-Speed viscometer.

2.6.3 Rheometer measurements

The rheometer, Anton Paar MCR 302 model was used to measure the dynamic apparent viscosity. The fluid system is filled with in a cup in which the bob is rotated as a shear rate of 400 1/s. Since the annulus between the cup-bob is narrow, at higher rotational speed, it generates turbulence. Therefore, the reading was limited up to the expected rotational speed in a wellbore. However, for the evaluation of apparent viscosity with the kick dynamics, the apparent viscosity at a very low shear rate, which is almost like at static condition is considered. The main reason is that the kick dynamics experimental study is conducted at wellbore fluid at static condition when the wellbore is closed. Figure 2.6.3 shows the “cup and bob” setup of Anton Paar rheometer.

Figure 2.6.3: Anton Paar Rheometer

2.7 Fluid Rheology models

This section presents the Newtonian and non-Newtonian rheology models along with their prediction of the measured data. In this thesis both types of fluids are synthesized (3.3) and used for the experimental (3.1) and simulation (5.1) works. The rheological parameters of the fluids are extracted using the reviewed rheology models. The experimental gas bubbles speed is correlated with the rheological parameters.

2.7.1 Newtonian Fluid Rheology model

Fluids such as water, and oil are Newtonian fluids, which are described by below (Guo & Liu, 2011; Skjeggestad, 1989):

$$\tau = \mu\dot{\gamma} \qquad 6$$

Where:

- τ = Shear stress, [lbf/100ft^2]
- $\dot{\gamma}$ = Shear rate, [1/s]
- μ = Newtonian viscosity, [cP]

Figure 2.7.1 shows an illustration of the measured viscometer data and the predictions with the Newtonian model. Due to the significant deviations, the Newtonian model poorly describes the rheological properties of drilling fluids.

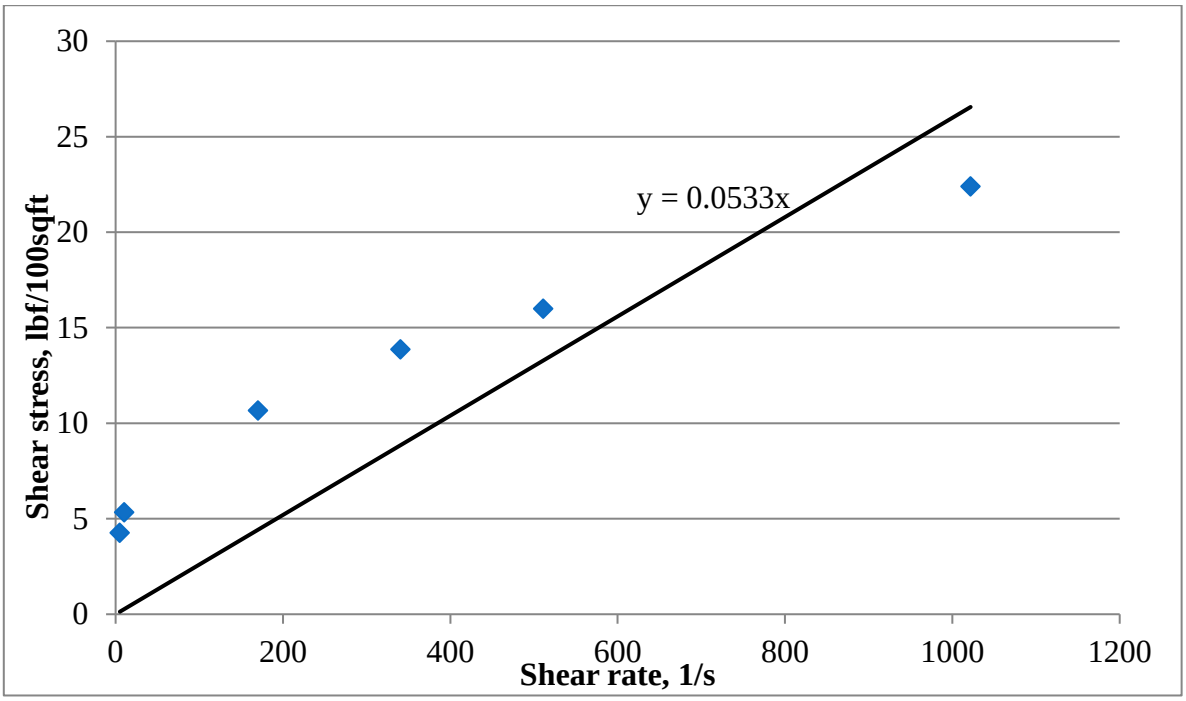

Figure 2.7.1: Newtonian fluid illustration

2.7.2 Non-Newtonian Rheological models

Non-Newtonian fluid behaviors are those that are not characterized by Newtonian fluids. Bingham, Power-law and Herschel-Bulkley were used to calculate the rheological properties of the drilling fluids tested in this thesis.

2.7.2.1 Bingham

The Bingham Plastic model is described by the yield stress and plastic viscosity parameters. The Bingham plastic fluid model is one of more models to characterize and describes mathematically non-Newtonian fluid. The shear stress-shear rate of the model is represented by the linear below(Skjeggestad, 1989):

$$\tau = YS + PV * \dot{\gamma} \qquad 7$$

Where:

- τ = Shear stress, [lbf/100 ft^2]
- YS = Yield stress, [lbf/ 100 ft^2]
- PV = Plastic viscosity, [cP]
- $\dot{\gamma}$ = Shear rate, [1/s]

Where PV is Plastic viscosity and YS Bingham yield stress. The parameters can be determined from the viscometer readings as:

$$PV[cP] = \theta_{600} - \theta_{300} \quad (8)$$

$$YS\left[\frac{lbf}{100sqft}\right] = \theta_{300} - PV = 2 * \theta_{300} - \theta_{600} \quad (9)$$

Where:

- PV = Plastic viscosity, [cP]
- $\theta_{300,\ 600}$ = Viscometer dial reading at 300, 600 RPM, [°]
- YS = Yield stress, [lbf/100 ft^2]

Figure 2.7.2 illustrates the comparison between the Bingham model prediction and the measured viscometer data, which shows a significant deviation. The viscosity according to the model is constant as the shear rate increases.

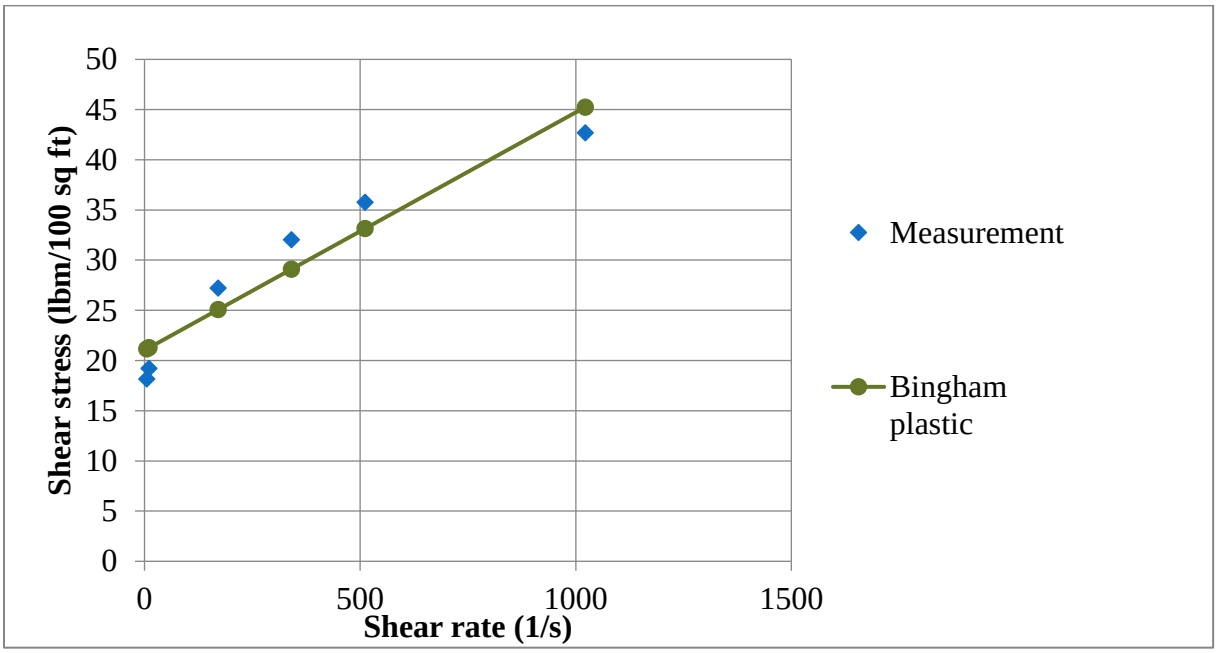

Figure 2.7.2: Bingham model that shows constant shear rate increase

2.7.2.2 Power law

Power law is an API model that represents shear-thinning fluids. The model is described by two parameters. As shown in below, at zero shear rate, the fluid flows without applying an external pressure. However, this is not the case for the non-Newtonian fluids. The model reads (Skjeggestad, 1989) :

$$\tau = K(\dot{\gamma})^n \tag{10}$$

Where:

- τ = shear stress, [lbf/ 100ft^2]
- n = flow index, []
- K = consistency index, [lbs/ 100 ft^2/s]
- $\dot{\gamma}$ = shear rate, [1/s]

Where n is the flow law index:

- When n =1, the fluid is Newtonian,
- When n < 1, shear-thinning.
- When n > 1, Shear thickening).

The parameters n and k can be calculated from the viscometer data as (Skjeggestad, 1989):

$$n = 3.32 \log\left(\frac{\theta_{600}}{\theta_{300}}\right) \tag{11}$$

$$K = \frac{\theta_{300}}{511^n} = \frac{\theta_{600}}{1022^n} \tag{12}$$

- Where, $\theta_{300,\,600}$ = Viscometer dial reading at 300, 600 RPM, [°]

Figure 2.7.3 displays the Power-law model prediction and the measure viscometer data, which shows shear thinning reducing the viscosity as the shear rate increases.

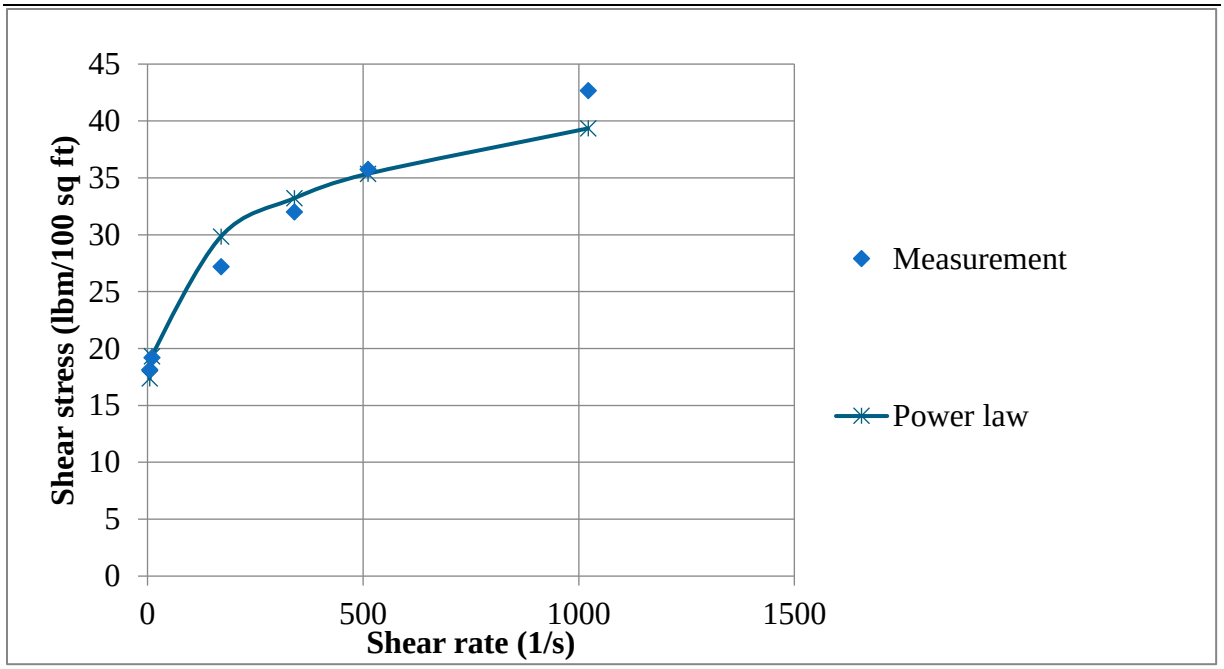

Figure 2.7.3: Model of the Power law in Shear stress/shear rate

2.7.2.3 Herschel-Bulkley model

The Herschel Buckley model is a modified and yielded Power-law model. Three parameters represent the model. The model describes the shear thinning features of drilling fluid as well as the yield stress at a low shear rate, which is more realistic. The Herschel-Bulkley model is defined as followed the below (Gucuyener, 1983):

$$\tau = \tau_y + K\dot{\gamma}^n \qquad 13$$

Where:

- τ_y = Herschel-Bulkley yield stress (YS), [lbf/ 100ft^2]
- n = flow index, []
- K = consistency index, [lbs/ 100 ft^2/s]
- $\dot{\gamma}$ = shear rate, [1/s]
- τ = shear stress, [lbf/ 100ft^2]

Both the flow and consistency index are estimated from the curve fitting between the measured data and the model. The Herschel-Bulkley yield stress (τ_y) is also called the lower shear yield stress (LSYS) can be estimated from lower RPM viscometer measurements as given in below as (M. Zamora, 1977):

$$\tau_y = (2 * \theta_3 - \theta_6) * 1.066 \quad (14)$$

Where:

- $\theta_{3,6}$ = Viscometer dial reading at 3, 6 RPM, [°]

Figure 2.7.4 shows the plot of H-B model prediction along with the measurement data. As shown, both the model's predictions are nearly the same and better than the Power law and Bingham Plastic models.

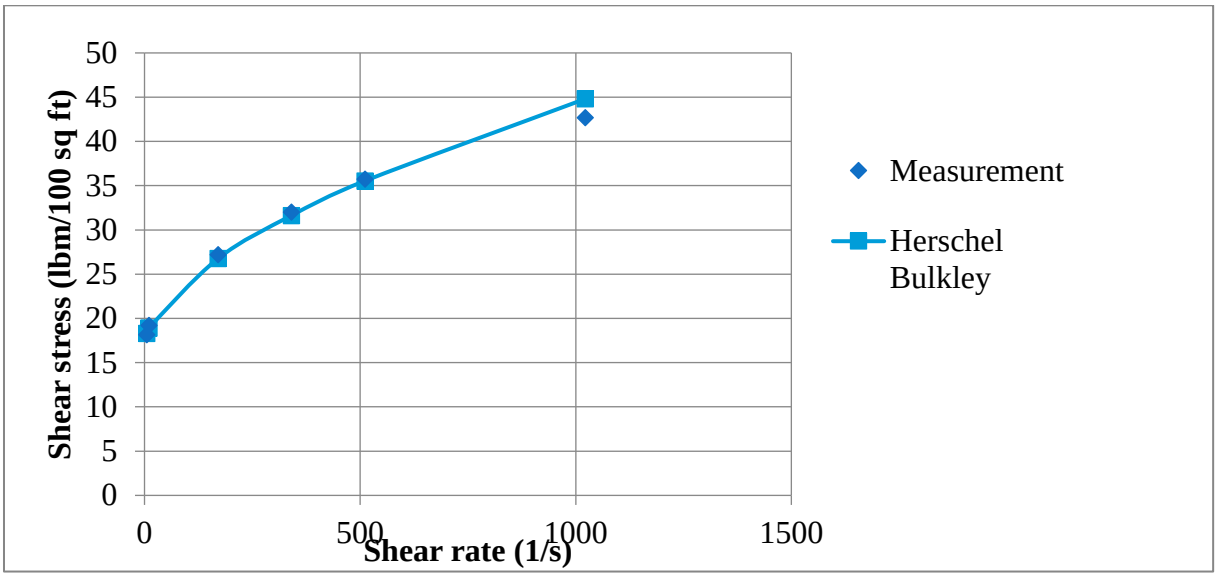

Figure 2.7.4: Model of Herschel-Bulkley law for Shear stress/Shear rate

2.7.3 Bubble velocity models

One of the primary purposes of this work is to test and modify the literature documented models used to calculate the speed of a kick and slugs/bubbles in a well. The models to be evaluated with measured data will be presented in sub chapter.

2.7.3.1 Wave analogy equation

Here is the viscous force of the regime that is dominant and the internal force equal to zero. Also, the Surface tension equals zero (Batchelor, 2012; Tomiyama, 2002).

$$V_T = \frac{\Delta \rho g d^2}{\mu_L} \quad (15)$$

Where:

- V_T = Terminal velocity of bubble, [m/s]
- $\Delta\rho$ = delta density, [kg/m^3]
- g = gravity, [m/s]
- d = diameter, [m]
- μ_L = Viscosity, [Pa·s]

2.7.3.2 Stokes or Hadamard-Rybczynski equation

Here is the surface tension force of the dominant regime and the viscous force is equal to zero (Tomiyama, 2002).

$$V_T = \sqrt{C_1 \frac{\sigma}{\rho_L d} + C_2 \frac{\Delta\rho g d}{\rho_L}} \qquad 16$$

Where:

- V_T = Terminal velocity of bubble, [m/s]
- σ = Surface tension, [N/m]
- ρ_L = density of liquid, [kg/m^3]
- $\Delta\rho$ = delta density, [kg/m^3]
- g = gravity, [m/s]
- d = diameter, [m]
- C_x = Correlation factor for x, []

The model will not be evaluated in this thesis. The main reason is that we didn't have equipment to measure the surface tension of the drilling fluids formulated in this thesis work.

2.7.3.3 Davies & Taylor equation

This can be used in an inertia dominant regime where viscous force is zero and surface force is zero. This is mostly used in the Newtonian flow regimes where viscous force is minimum (Tomiyama, 2002).

$$v_T = C\sqrt{\frac{\Delta\rho g d}{\rho_L}} \qquad 17$$

Where:

- v_T = Terminal velocity, [m/s]

- C = correlation factor, []
- $\Delta\rho$ = difference in density between liquid and object(bubbles/gas), [kg/m^3]
- g = gravity, [m/s^2]
- d = diameter, [m]
- ρ_L = density of liquid, [kg/m^3]

2.7.3.4 Li Zheng Model

For the bubble speed prediction of the measured data, an equation derived by (Li Zheng, 2000) was used. The authors derived bubble speed equation for buoyant of spherical and non-spherical bubbles/droplets as:

$$U_T = \frac{gd^2\Delta\rho}{18\mu} \tag{18}$$

Where:

- g = gravity, [m/s^2]
- d = diameter, [m]
- Δρ = Change in density between fluid and air, [kg/m^3]
- μ = apparent viscosity of the fluid, [pa·s]

The Li Zheng Model (above) is about 1/18 of the Wave analogy-based model (above)

2.7.3.5 Harmathy's equation

The Harmathy's model from 1960 gives a method of calculating the fluid or gas moving in liquid media. The interfacial tension is represented for the slip velocity. This equation is used in testing for suspension limits. Since the tension were not tested for fluids in this thesis, the only fluid conducted with this equation is the water-base-fluid and were set to 0,0772N/m (Harmaty, 1960; Thea Hang Ngoc Tat, 2021).

$$S = 1{,}53 \cdot \left(\frac{g \cdot (\rho_l - \rho_g) \cdot \sigma}{\rho_l^2}\right)^{0{,}25} \tag{19}$$

Where:

- S = gas migration velocity, [m/s]

- g = gravity, [m/s^2]
- ρ_l = density of liquid, [kg/m^3]
- ρ_g = density of gas, [kg/m^3]
- σ = interfacial tension, [N/m]

2.7.3.6 Slug flow gas migration regime

In this equation the model is adapted for slug flow where the gas migration velocity is represented. This is a Taylor rise bubble velocity equation suited annulus dimensions. This equation also consider clearance in the annulus (A. R. Hasan, 2007; Thea Hang Ngoc Tat, 2021).

$$S = 0{,}35\sqrt{\frac{g \cdot (\rho_l - \rho_g) \cdot d_{out}}{\rho_l}} \cdot \left(1 + \frac{0{,}29 d_{in}}{d_{out}}\right) \quad 20$$

Where:

- S = Gas migration velocity, [m/s]
- g = gravity, [m/s^2]
- ρ_l = density of liquid, [kg/m^3]
- ρ_g = density of gas, [kg/m^3]
- d_{out} = Outer diameter of the annulus, [m]
- d_{in} = Inner diameter of the annulus, [m]

2.7.4 Boyle's law

Boyle's law is the relationship between volume and pressure for gas substances at a constant temperature. It was Robert Boyle who first discovered this connection in that the given quantity of the volume of the gas, precisely the expansion, and compression, was related to the pressure in the gas. For isothermal state, the Boyle's law states that (Britannica, 2022):

$$pV = k \quad 21$$

Where:

- p = pressure, [Pa]
- V = volume, [m^3]
- *k* = constant, []

With a change of pressure or volume from start to finish will affect each other:

$$p_1 v_1 = p_2 v_2 \qquad 22$$

Where:

- p = pressure, [Pa]
- V = volume, [m^3]

So, if the same amount of gas expands to a bigger volume the pressure will decrease. And vise vista. The pressure and volume 1 will equal the pressure and volume 2 for constant temperature.

In the petroleum industry, the kick in a closed well will theoretically react in the same way. The condition for this is mainly that it is an ideal gas, the fluid is incompressible, the temperature is constant (unlikely) and the wellbore is closed.

As shown in Figure 2.7.5 the picture to the left there is a wellbore with a kick in annulus at the bottom of the well. To the right is the kick on the wellhead and the pressure and the volume are here the same.

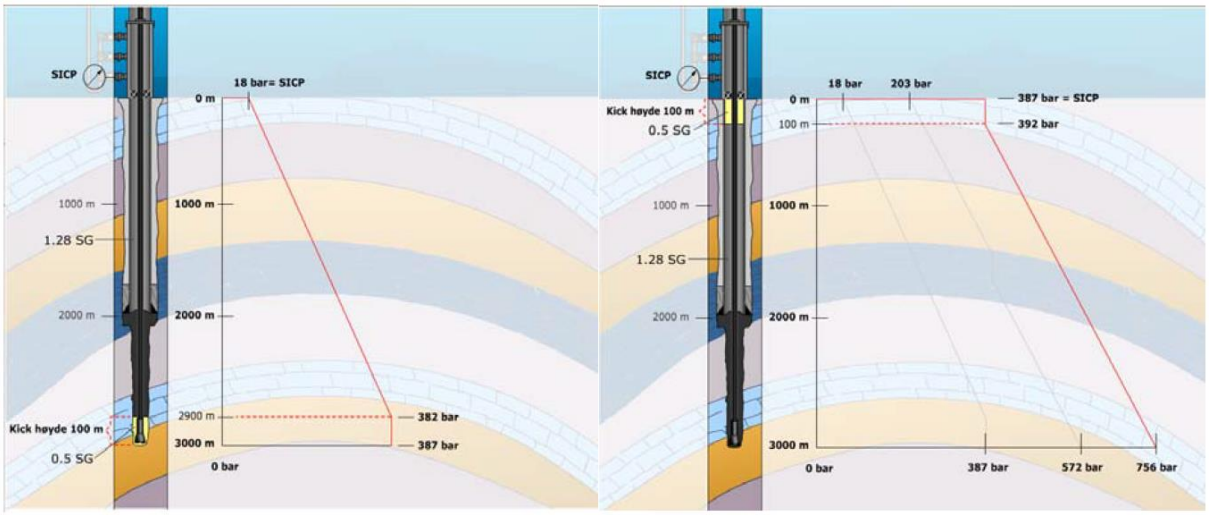

Figure 2.7.5: To the left the gas kick is at the bottom of the well, to the right the gas kick is at the top of the wellhead (Hamarhaug, 2011; Vikra).

3 Experimental works

3.1 Experimental Rig Construction

The gas kick phenomena have been investigated in closed and open wellbore conditions. The wellbore is smooth and hence the effect of friction on the wellbore is not considered. The gas bubble dynamics in the experimental wells were evaluated in different fluids' physical and rheological properties. In both the experimental rigs, the wellbore fluids are in stagnant condition.

3.1.1 Top open rig

The first experimental rig at is top of the well is open, through which the gas bubble dynamics were studied. A gas bubble is transported through different wellbore annular clearance. The length of the pipe is 2 m long and three annular clearance was considered for the experiment with 30mmx25mm, 50mmx25mm and 50mmx25mm. During testing, the air gas is injected at the bottom using a J-type injection pipe. The position of the gas front is measured at different times are recorded with an iPhone video camera. As shown the bubble in the experimental well is circled and magnified on one right side of the figures.

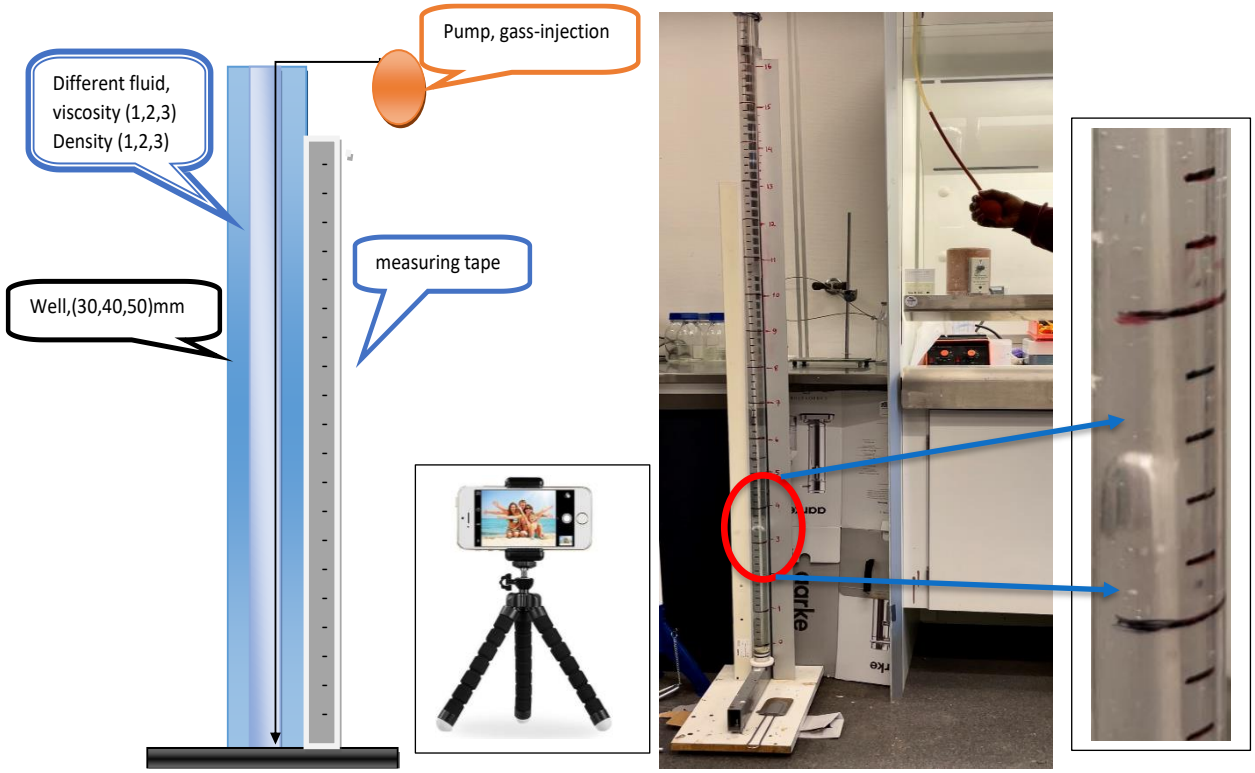

Figure 3.1.1: a. Open wellbore physical rig construction with measuring illustration and bubble/slug illustration of the open wellbore rig simulation, b: picture of the picture/filming set-up

In the gas migration this experimental setup, different fluid is filled in the well and the speed of the bubbles are studied. Figure 3.1.1 shows an illustration of the gas bubble (small and big bubbles) migration in the annular space. From the filmed video, the time required for the bubble front travel 3cm is peaked to calculate the bubble velocity and acceleration up the well. Both the small and large bubbles that travelled separately were analyzed. However, the small bubble trails behind the large slug are not considered since this bubble are sometimes colliding with the large bubble and recoiled back.

In most cases, the tail bubbles have seemed to be almost as fast as slugs following the way up to the surface. For the comparison purpose, the different dimensions of the well and different liquids, many samples are taken and compared with the same sizes of bubbles, then the average of all the sizes of the bubbles is also looked at to better compare parameters such as density, viscosity, and clearness in the annulus. The velocity for each front travel time is calculated as:

$$v\left(\frac{m}{s}\right) = \frac{3x10^{-2}m}{(t_{i+1} - t_i)} \qquad 23$$

Where:

- v = velocity of bubbles/slug, [m/s]
- t = time per step, [s]

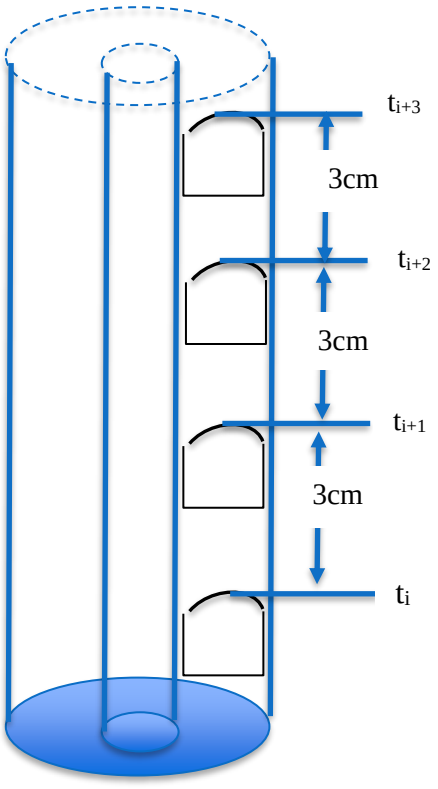

Figure 3.1.2: Slug/bubble illustration of measuring points and dynamic in the open wellbore rig, Illustration of bubble front and the corresponding time collection from the test

3.1.2 Top close rig

Figure 3.1.3 shows the experimental rig system. Fluids are filled in 1m length, and 50mm inner diameter well. The top of the well is closed and connected with the pressure sensor, which is further connected with the computer. The data is logged in LabVIEW. In this experimental setup, the wellhead pressure build-ups in different fluids are studied for the gas injected at bottomhole pressures (500, 1000, 1500, 2000, 2500 mbar).

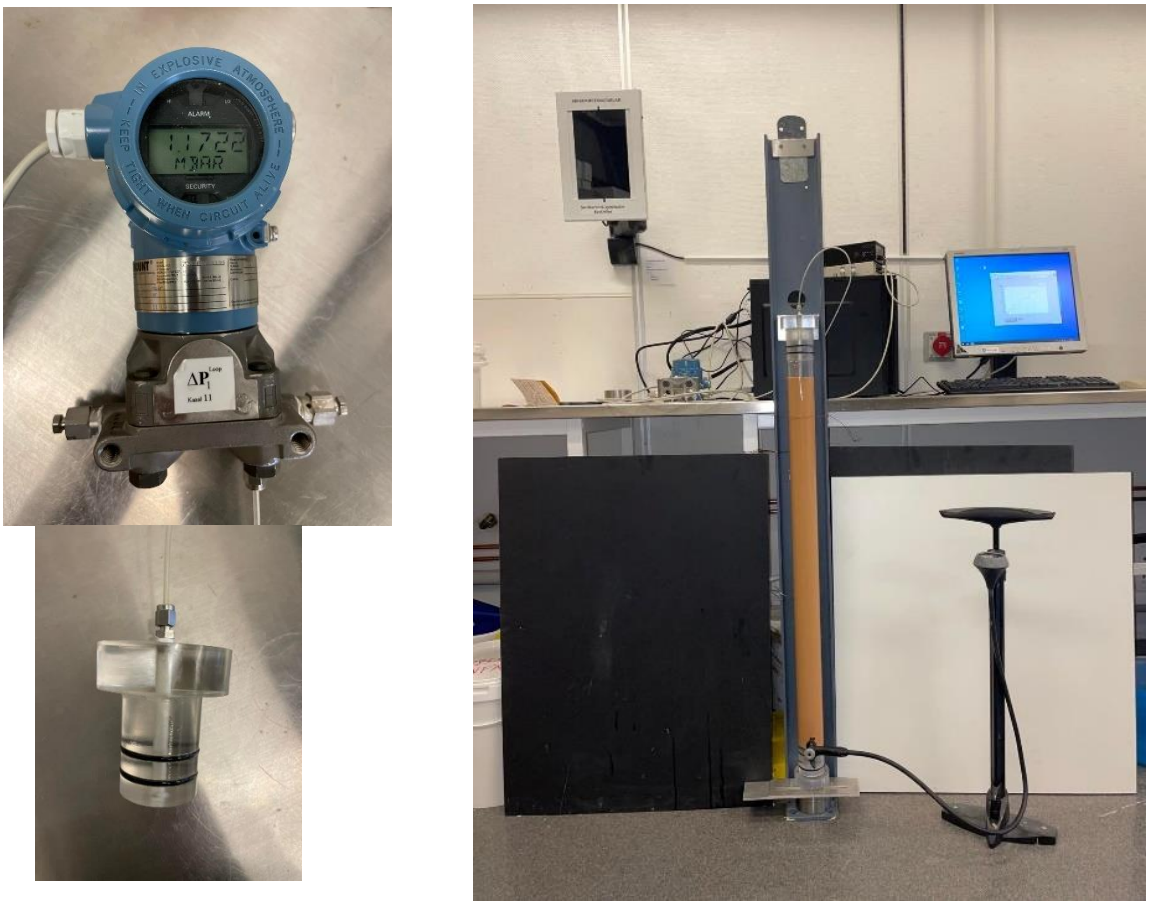

Figure 3.1.3: 1. Pressure sensor WHP, 2. top cover for tube, 3. Closed rig system setup, 4. Pump pressure BHP

3.2 Bubble Behaviors

The size of the bubble and slugs have an impact on the velocity. Normally the bigger bubbles migrates faster than the smaller one, which are commonly observed as trail of the bigger one. The biggest impact on the size is the diameter of the top of the bubble. A slug can have the same diameter and different sizes because the cylindrical shape and the length can variable from slug to slug. This size different from one length to another doesn't affect as much as the diameter of the slug dose. A bubble with 1cm diameter and a slug with 1 cm diameter has approximately the same velocity. Two slugs with same length but different diameter have a more different velocity. There the biggest diameter has normally the fastest velocity if all other condition is the same.

3.2.1 Slugs and Trails

Slugs can have tails of small bubbles on the bottom of the slug. These small bubbles behave in a whole different way than other normal small bubbles alone. The "trail" bubbles follow the velocity speed of the slug that normally the slug has a much higher velocity then the small bubbles. Normally when gas is injected into the bottom of the tube/wellbore like an influx, the bubbles combine themselves into a slug if enough gas rate. The small bubbles that don't have enough velocity to combine with the slug or are too small to force themselves to combine, these are the bubbles that can be "trails". A shown on Figure 3.2.1 under the start of the influx combines bigger bubbles and slugs. Some middle big bubbles combine with the slug on the way to the top. Smaller bubbles struggle to combine but use the slug like a bulldozer up the liquid and follows right behind to the top. Other small bubbles, at the same size, fall off and use much longer time to come to the top. To measure small bubbles velocity in the liquid it is important to see if the bubbles are alone or behind bigger bubbles or slugs. Without this information the calculation can be misunderstood and difficult.

Because of the almost same velocity of the slug and small bubble tails the calculation for the tail and slug can be calculated with the diameter of the slug and not the diameter of the small bubbles. For small bubbles alone in the tube, the diameter of the small bubbles can be used.

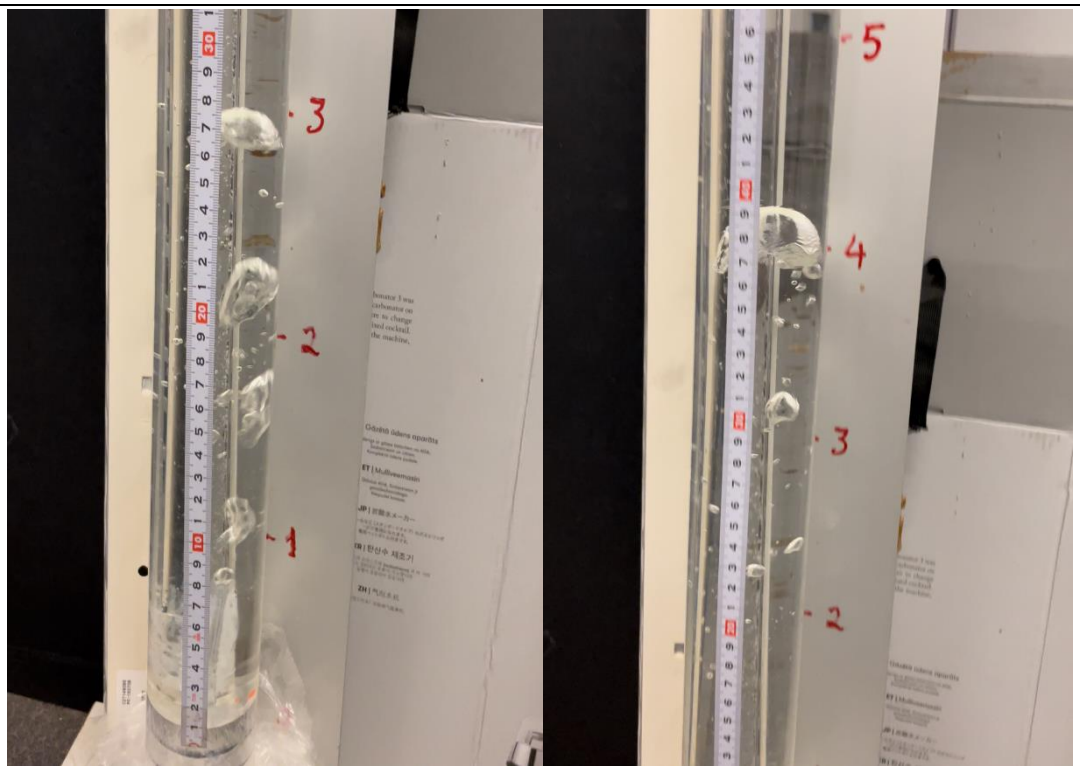

Figure 3.2.1: picture 1: bubble/slug dynamics from 1-3 measurements points, Picture 2: Slug combining point from 2-5 measurements points.

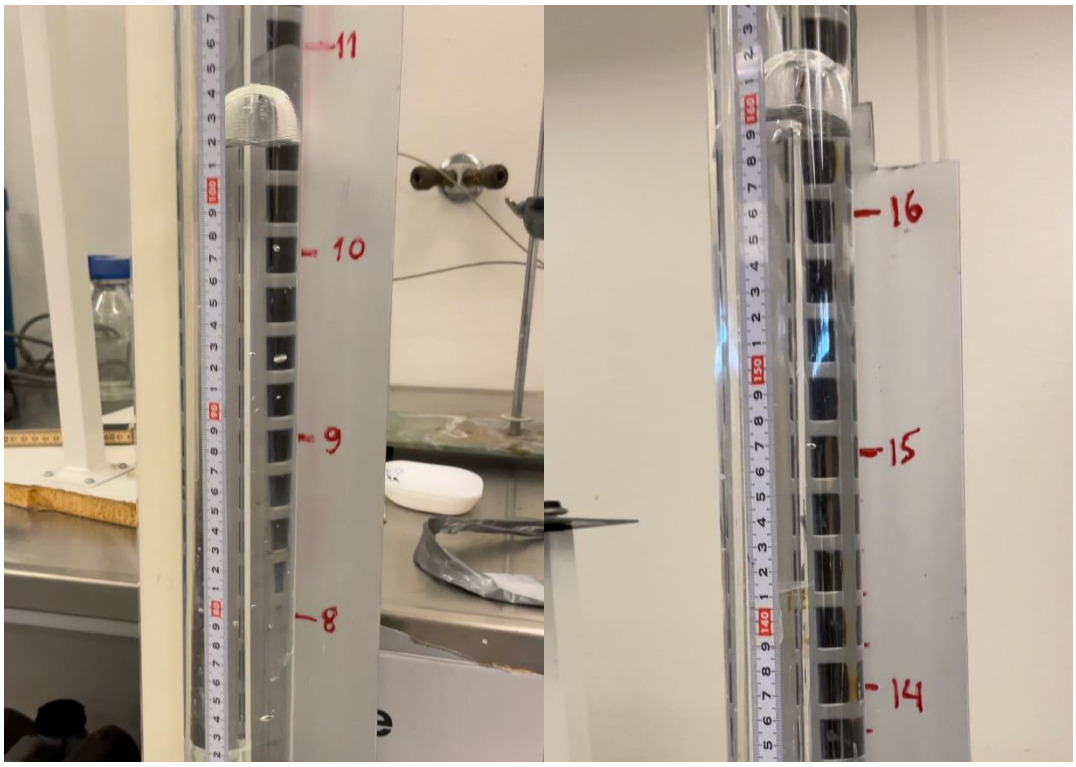

Figure 3.2.2: picture 3: bubble/slug dynamics from 8-11 measurements points, Picture 2: Slug ending point from 14-16 measurements points.

3.2.2 Collision between bubbles

The collision of particles and bubbles is studied from(Pavlina Basarova, 2014). They studied different collision parameters that have effect of gravity, interception mechanism and inertia. The density also is an important parameter to reflect because if the density different between the air-bubble and the fluid is big then the bubble will lower the velocity and the interception mechanism will be less effective. The gravity collision parameters use different velocity of the fluid and gas to be calculated.

The collision efficiency is here given by: Gravity, buoyancy effect and intersection. The gravity and buoyancy factor react with velocity different between fluid and gas-bubble. The interception efficiently reacts with the size of the big and small bubble. On Figure 3.2.1 the smaller bubbles below the bigger bubbles, as migrating on the top, experimental show that the smaller bubbles were accelerating and colliding with higher bubble ahead of them (Pavlina Basarova, 2014).

3.2.3 Bubble break with bentonite fluid

In bentonite fluid the bubbles can interact in a different way than normal water-fluid with viscosity polymer or salt. The bubble dynamics tended to break up. In 2.1.2 bubbles behavior the different flow behavior was considered. From bubbly to wispy annular flow were considered. The pattern from one flow to another were the flow rate velocity of the gas-influx. In Bentonite fluid the bubbles tend to break and tear up without any different in influx-rate.

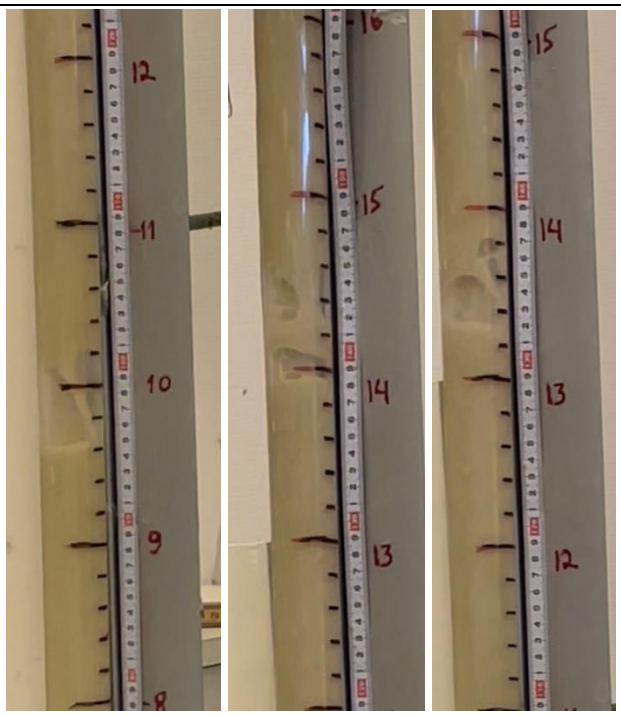

Figure 3.2.3: Slug thru 40/25 mm tube with bentonite fluid nr 2.

Figure 3.2.4: Big slug 30/25 struggle thru top of the wellbore

3.3 Experimental Fluid Synthesis and Characterization

A total of 13 fluids having different densities, and viscosities were formulated to study the gas bubble dynamics behaviors with respect to the fluid properties. In the following, the fluid formulation the calculated rheological parameters will be presented. Later, these parameters will be correlated with the measured gas bubble speed. The fluids properties dataset is also used as input for literature model to calculate the bubble speed. All the rheological and the rheometer data are measured at room temperature.

3.3.1 Fluid 1-Water

In this system, tap water was used without any additive. This will be used as base fluid with which viscosified and densified fluids to be compared with.

Figure 3.3.1 shows rheology measurements of tap water and Figure 3.3.2 shows measured rheometer data for Fluid 1. Table 3.3.2 shows the calculated Bingham and Power-law model rheological parameters as well as density and the smallest viscoelastic data conducted form the tests. The reason because the smallest viscoelastic data is conducted is because of the fluid is tested in a steady (still) wellbore and not a rotational test.

Table 3.3.1: Fluid 1 mixing recipe

Fluid 1	
Water, tap, [g]	4000

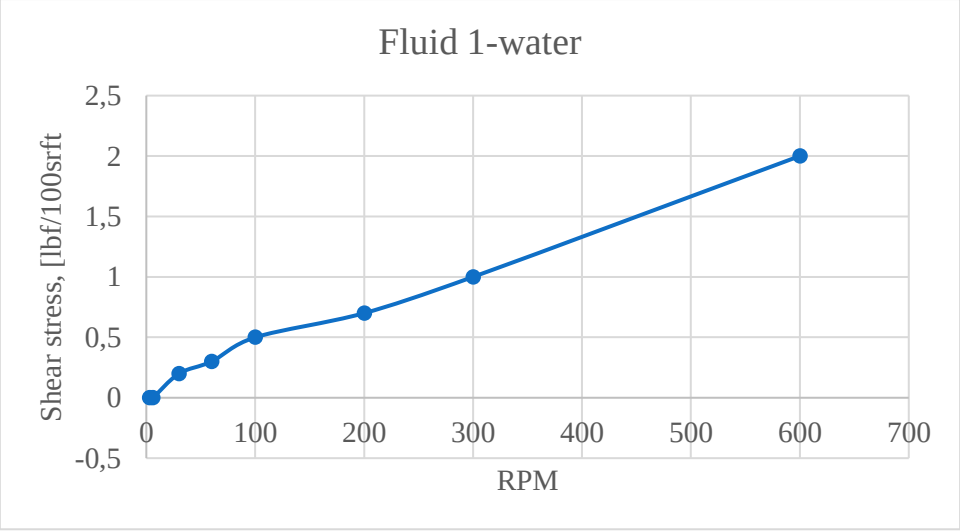

Figure 3.3.1: Viscometer data at 22°C for Water

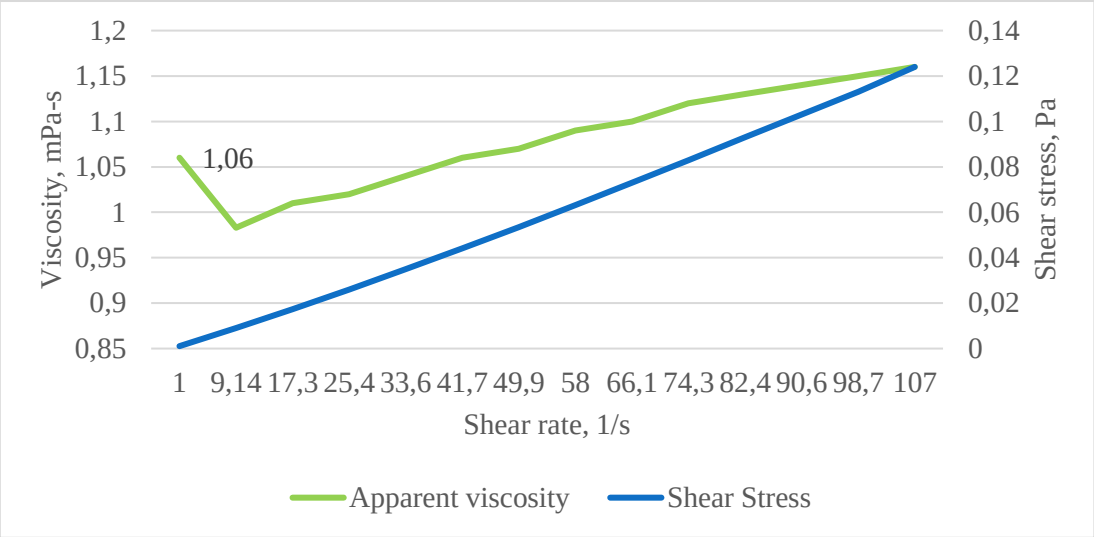

Figure 3.3.2: Viscoelastic data from at 22°C for Water

Table 3.3.2: Rheology Parameter data at 22°C for Water

Rheology parameters	Values
PV [cP]	1,00
YS [lbs/100sqft]	0,00
LSYS [lbs/100sqft]	0,00
n [-]	1,00
K [lbf-s^n/100sqft]	1,00
Density [sg]	1,00
Apparent Viscosity, [mPa/s]	1,06

3.3.2 Fluid 2-Viscous Fluid

The design objective of viscous fluid synthesis (Fluid 2) was to study the effect of viscosity on the bubble dynamics by comparing with fluid 1 (Tap water only). Fluid 2 is formulated by mixing 2,5 g Carbopol (CP) and 2 g Xanthan (XG) with 4000 ml water. Both polymers were added in water to obtain a higher viscous without increasing the density og the fluid significantly. The polymeric solution is relatively transparent or nearly colorless to get a better visualization of the dynamics of the bubble in the experimental rig.

2.5 g CP and 2 g XG mixed with 4000 ml water. The mixed additives were mixed for several hours with high-speed mechanical mixers. Both polymers added were added for increasing the fluids viscosity without increasing the density of the fluid especially. Both polymers are also to an extent transparent or colorless to get a better view of the dynamics of the bubble in further physically testing.

Table 3.3.3 shows the chemical recipe. Figure 3.3.3 shows rheology measurements and Figure 3.3.4 shows rheometer data for Fluid 2. Table 3.3.4 shows the calculated Bingham and Power-law model rheological parameters, density and apparent viscosity data obtained from the rheometer test.

Table 3.3.3: Fluid 2 chemical compositions.

Fluid 2	
Water, [g]	4000
Carbopol, [g]	2,5
Xanthan, [g]	2

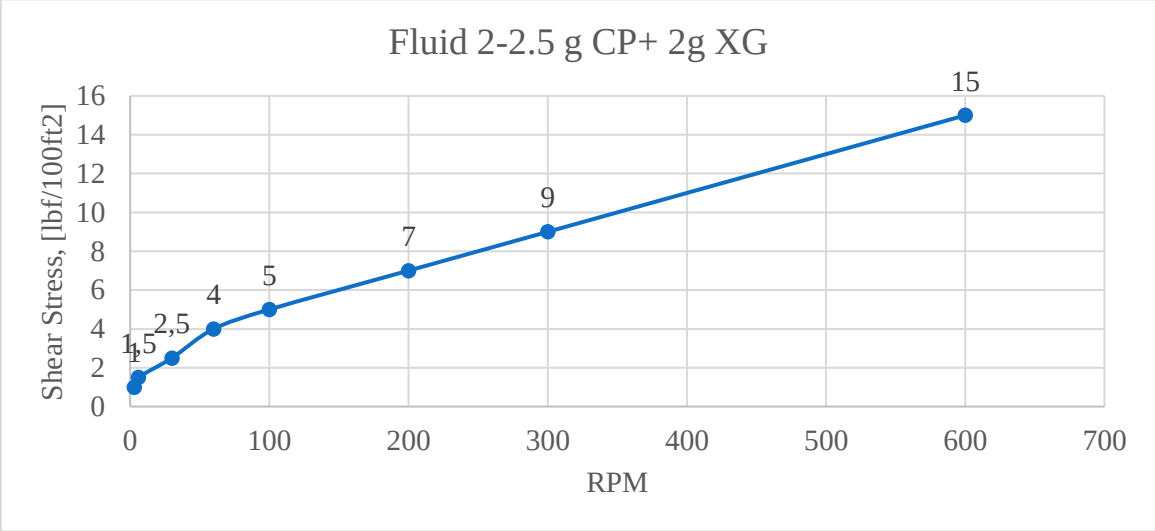

Figure 3.3.3: Viscometer data at 22°C for Viscous Fluid

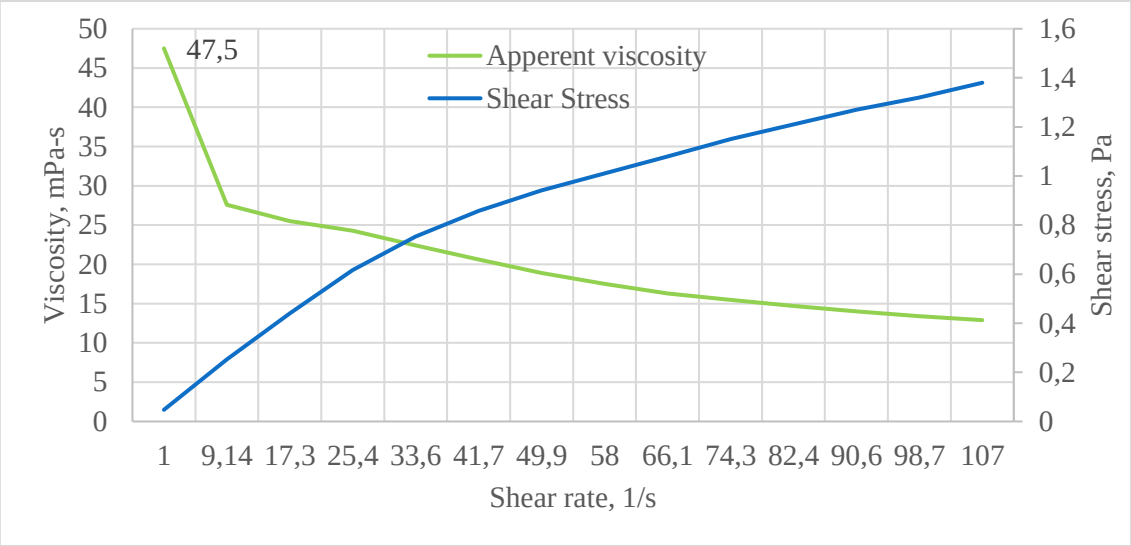

Figure 3.3.4: Fluid 2-Rheometer measured apparent viscosity and shear stress

Table 3.3.4: Rheological and density parameter of Fluid 2

Rheology parameters	Values
PV [cP]	6
YS [lbs/100sqft]	3
LSYS [lbf/100sqft]	0.5
n [-]	0.737
K [lbf-s^n/100sqft]	0.091
Density [sg]	1,00
Apparent Viscosity, [mPa/s]	47,5

3.3.3 Fluid 3-High Viscous

As shown in the fluid 2 design, the Bingham Plastic viscosity and the Herschel-Bulkley parameters are still low. To study the effect of very high viscous fluid on the bubble dynamics, Fluid 3 is designed. For this, the concentration of CP was increased to 30 g while maintain the concentration of Xanthan as it was.

Table 3.3.5 shows the fluids recipe. Figure 3.3.5 shows viscometer measurements and Figure 3.3.6 shows rheometer data of Fluid 3. Table 3.3.6 shows the calculated Bingham and Power-law model rheological parameters, density, and apparent viscosity of the fluid. As shown, comparing with Fluid 2, the rheological properties of the fluid 3 recoded relatively

higher values. Specially, the apparent viscosity for Fluid 3 is almost 11 times higher than the fluid 2.

Table 3.3.5: Fluid 3 mixing recipe in mixing order

Fluid 3	
Water, [g]	4000
Carbopol, [g]	30
Xanthan, [g]	2

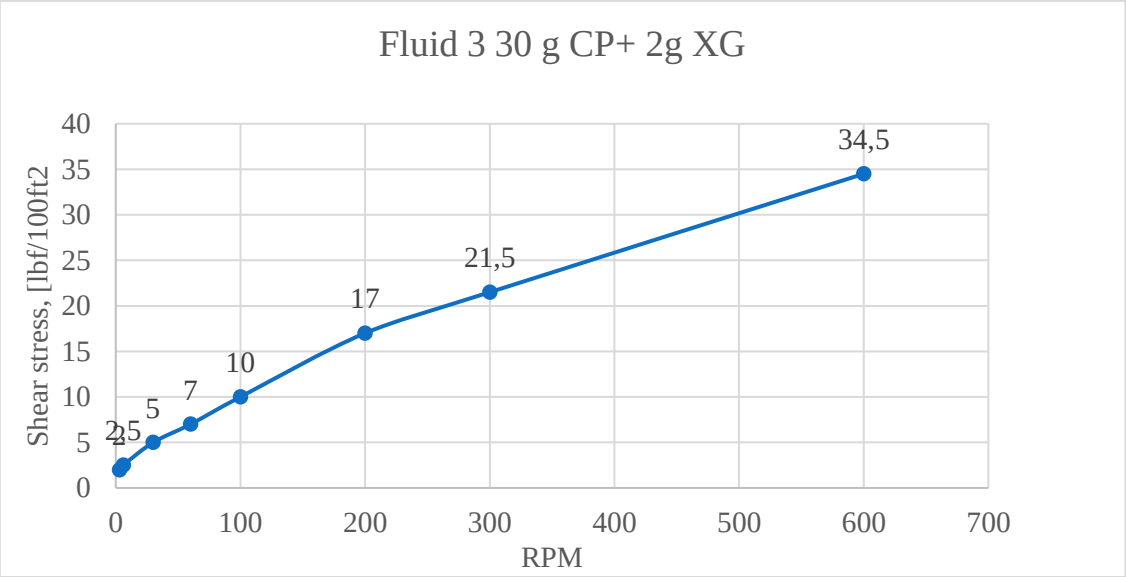

Figure 3.3.5: Viscometer data at 22°C for High Viscous Fluid

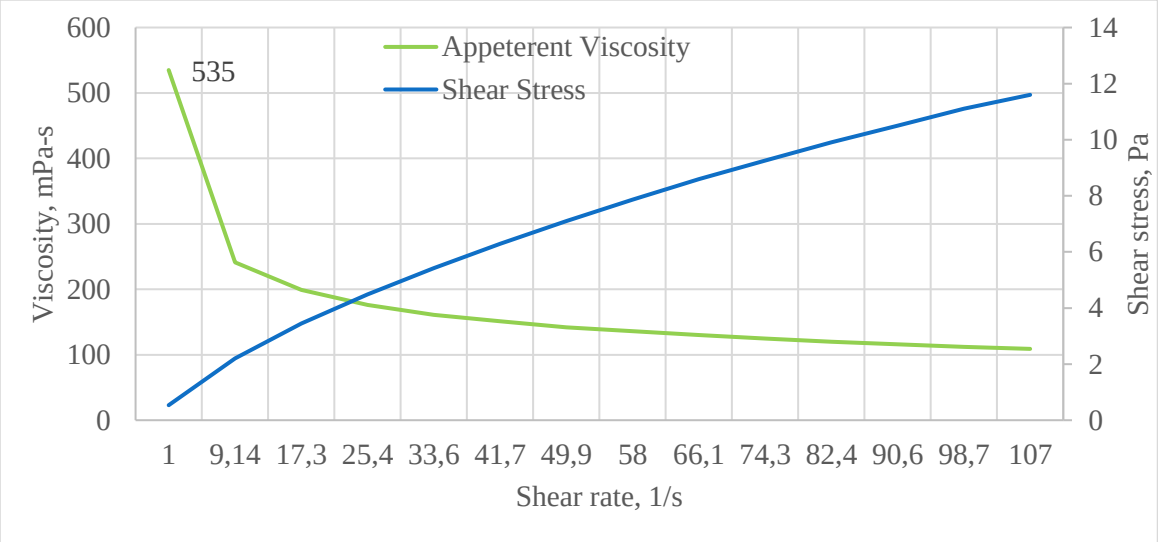

Figure 3.3.6: Viscoelastic data at 22°C for High Viscous Fluid

Table 3.3.6: Rheology Parameter data at 22°C for High Viscous Fluid

Rheology parameters	Values
PV [cP]	13
YS [lbs/100sqft]	8.5
LSYS [lbs/100sqft]	1.5
n [-]	0.682
K [lbf-s^n/100sqft]	0.306
Density [sg]	1,00
Apparent Viscosity, [mPa/s]	535

3.3.4 Fluid 4-Brine

In the previous designs, an attempt was made to maintain the fluid density nearly constant and vary the viscosities. Here, the fluid 4 design objective was to investigate the effect of density on the bubble migration speed while maintaining the viscosity as closer to water or the less viscous fluid as possible. For this, Fluid 4 was formulated by blending 1000-gram salt mixed with 4000-gram water. The brine mixture yielded 1.17 sg, which is a little bit higher than the previous water and polymeric fluids.

Table 3.3.7 shows the fluid compositions. Figure 3.3.7 shows rheology measurements and Figure 3.3.8 shows viscoelastic data for Fluid 4. Table 3.3.8 shows the calculated Bingham and Power-law model rheological parameters, density, and rheometer data of the brine solution.

From the rheological parameters we can observe the Bingham plastic parameters are a little bit higher than water fluid system, but not very significant. The apparent viscosity of the brine is higher than that of water by about 0.47 cP.

Table 3.3.7: Fluid 4 mixing recipe in mixing order

Fluid 4	
Water, [g]	4000
Salt, NaCl, [g]	1000

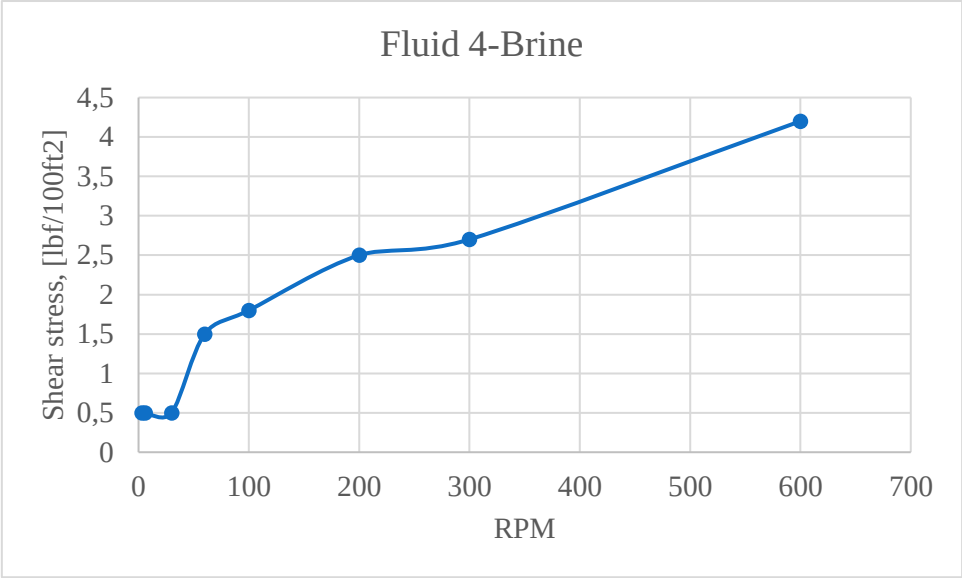

Figure 3.3.7: Viscometer responses of Brine

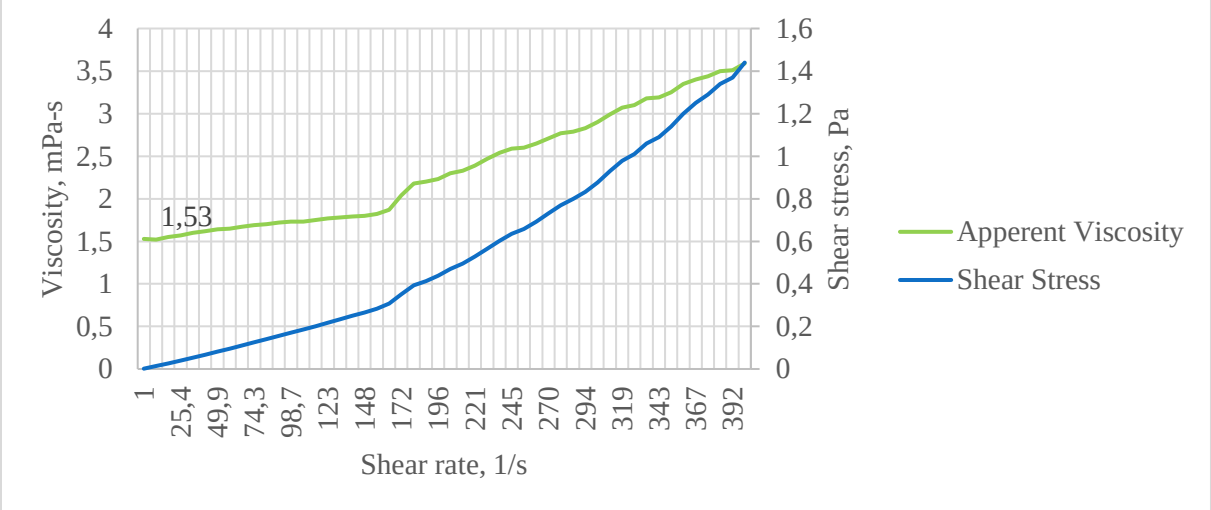

Figure 3.3.8: Rheometer measured shear stress and apparent viscosity of Brine

Table 3.3.8: Rheological and density parameter of Brine

Rheology parameters	Values
PV [cP]	1,5
YS [lbs/100sqft]	1,2
LSYS [lbs/100sqft]	0,5
n [-]	0,637059947
K [lbf-s^n/100sqft]	0,050808607

Density [sg]	1,17
Apparent Viscosity, []	1,53

3.3.5 Fluid 5-High Viscous with density modifier

To investigate the combined effect of density and viscosity, Fluid 5 was designed. At first the fluid 3, which was formulated by 30 g CP with 4000g water, was blended by 1000-gram salt. The density increased to 1,18 sg. However, the added salt, create a repulsive force between the polymers and polymers becomes designated. As a result, salt reduced the viscosity of the salt free polymeric fluid. In order to improve the viscosity of fluid 5, 20 g more Carbopol, 6 g xanthan, and 1 g CMC were added. The additives were added successively by controlling the viscosity improvement.

Table 3.3.9 shows the fluid 5 chemical composition. Figure 3.3.9 shows viscometer measurements and Figure 3.3.10 shows rheometer measured data. Table 3.3.10 shows the calculated Bingham and Power-law model rheological parameters, density and viscoelastic data conducted form the tests.

Comparing with fluid 3, the high polymer and brine treated system exhibited nearly closer the Bingham plastic and Herschel-Bulkley yield stress. On the other hand, the Bigham Plastic value of the brine blended system (Fluid 5) reduced by about 58% as compared with the salt free system (Fluid 3). However, the apparent viscosity and the density of fluid 5 are higher than the fluid 3 by 72% and 18% respectively.

Table 3.3.9: Fluid 5 mixing recipe in mixing order

Fluid 5	
Water, [g]	4000
Salt, NaCl, [g]	1000
Carbopol, [g]	50
Xanthan, [g]	6
CMC, [g]	1

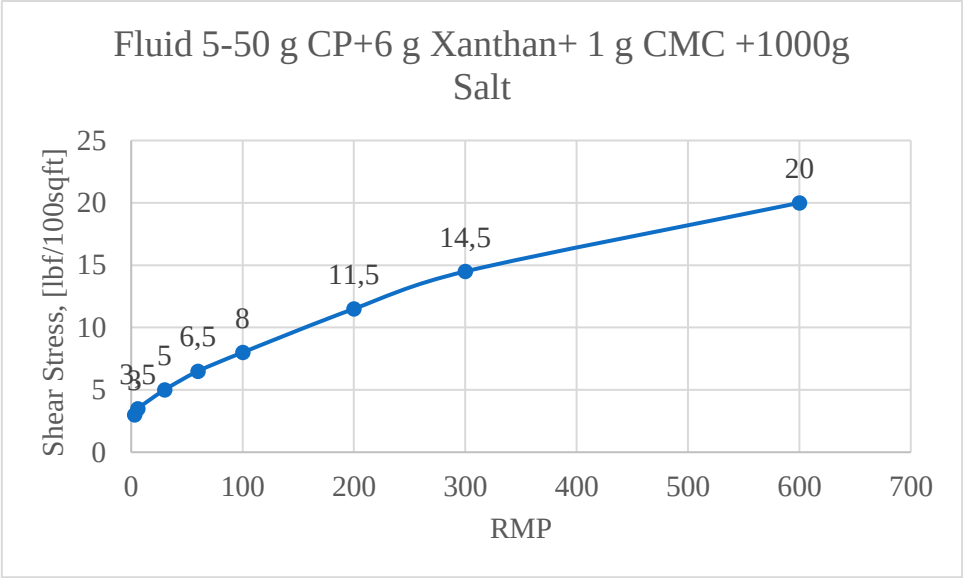

Figure 3.3.9: Viscometer data of Fluid 5

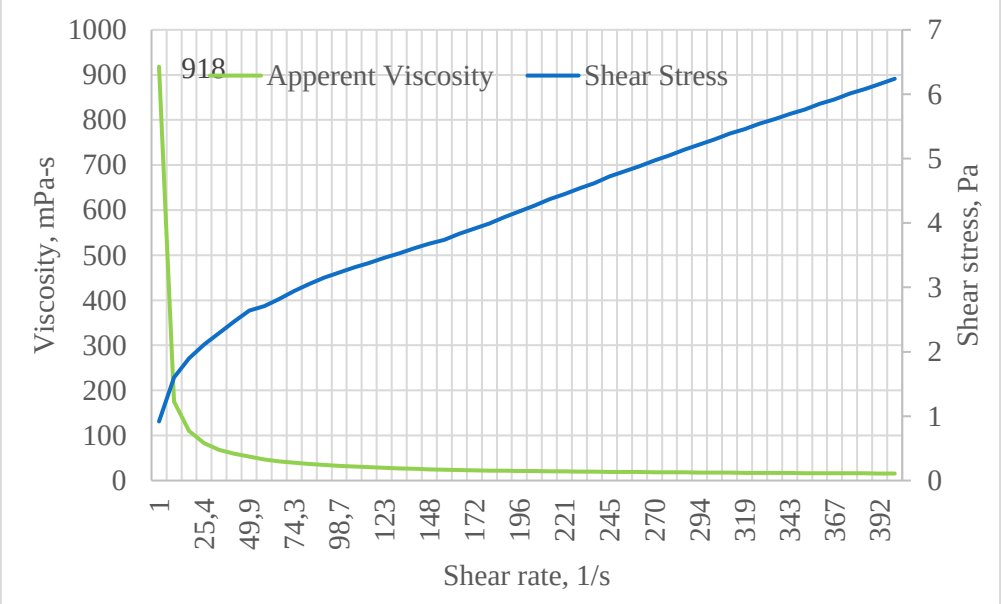

Figure 3.3.10: Rheometer measurement of apparent viscosity and shear stress of fluid 5

Table 3.3.10: Rheology Parameter data at 22°C for High Viscous Fluid with density modifier

Rheology parameters	Values
PV [cP]	5,5
YS [lbs/100sqft]	9
LSYS [lbs/100sqft]	2,5
n [-]	0,46367782
K [lbf-s^n/100sqft]	0,80451345

Density [sg]	1,18
Apparent Viscosity, [mPa/s]	918

3.3.6 Fluid 6-Bentonite

Since the brine didn't provide a higher density, we thought to use Barite as weight control additive. For this, barite should be blended with Bentonite, which is commonly used as viscosity control additive in drilling fluid. At first, we synthesized barite free and bentonite fluid by mixing 57 g bentonite with 4000g water.

Table 3.3.11 shows the fluids recipe Figure 3.3.11 shows rheology measurements and Figure 3.3.12 shows viscoelastic data for Fluid 6. Table 3.3.12 shows the calculated Bingham and Power-law model rheological parameters, density, and apparent viscosity of the fluid.

Fluid characterization results show that Bentonite does enot increase the density so much since it is not a weight material, but increases the gel strength and some viscosity, and some LSYS. However, the bentonite drilling fluid exhibited a very higher apparent viscosity (i.e 1060 cP) as compared with the fluids 1-5. For comparison purpose, before modifying the bentonite fluid with Barite, we decided to test the gas bubble dynamics in the barite free, bentonite fluid system (Fluid 6).

Table 3.3.11: Fluid 6 mixing recipe in mixing order

Fluid 6	
Water, [g]	2000
Bentonite, [g]	57

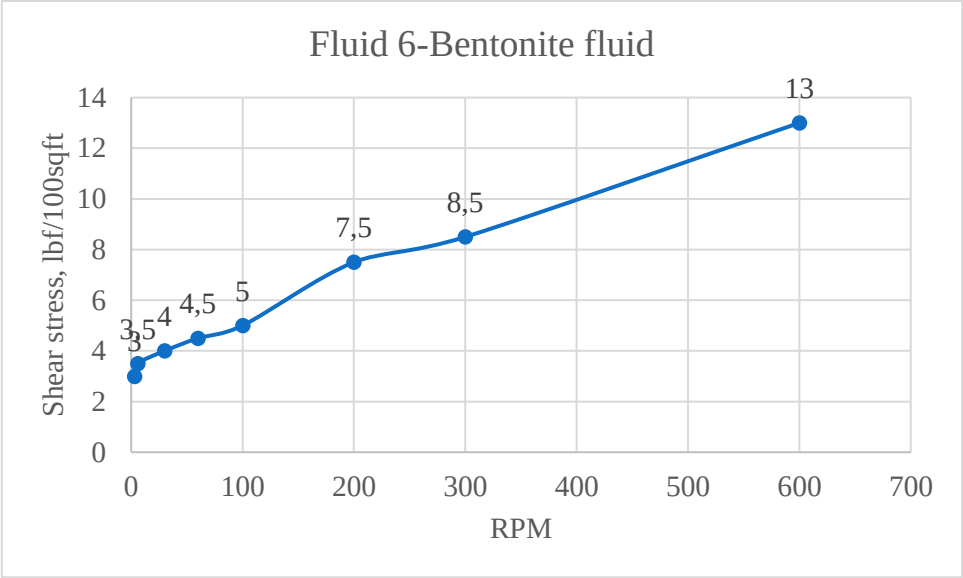

Figure 3.3.11: Viscometer respnonces of the Bentonite Fluid

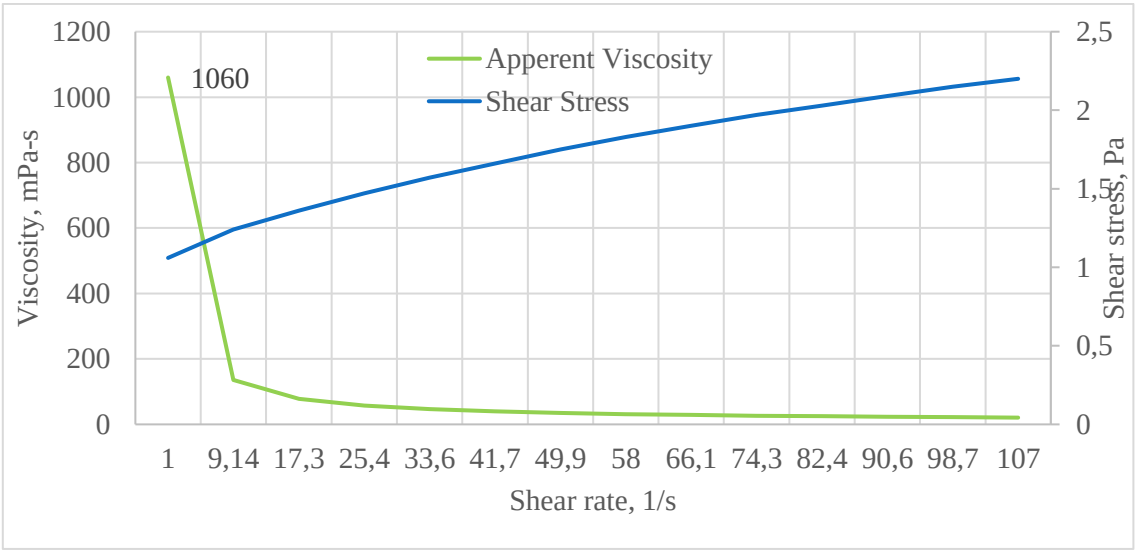

Figure 3.3.12: Apparent viscosity and shear stress data of Bentonite fluid

Table 3.3.12: Rheology Parameter data at 22°C for Bentonite Fluid

Rheology parameters	Values
PV [cP]	4.5
YS [lbs/100sqft]	4
LSYS [lbs/100sqft]	2.5
n [-]	0.6126211
K [lbf-s^n/100sqft]	0.18628726
Density [sg]	1,02

Apparent Viscosity, [mPa/s]	1060

3.3.7 Fluid 7-Bentonite #2

In terms of chemical additives, the Fluid 7 composition is the same as fluid 6. Here, the fluid and bentonite amount were doubled to test in higher annular clearance. The comparison of the viscometer responses of fluid 7 with fluid 6 show that the fluid 7 responses a little bit lower since the measurement were conducted right after mixing without aging for 24 hr. until the bentonite swell as has been done for fluid 6. The reason we called the fluid as bentonite #2 is due its viscometer measurement, which is done after mixing and bubble dynamics we conducted right after mixing. The reason for the bentonite #2 fluid was not aged for 24 hrs was due to the thesis work delay while constructing the rig. However, comparing with fluid 6, the rheological parameters difference is not so significant.

Table 3.3.13 shows the fluid's composition. Figure 3.3.13 shows viscometer measurements data of Fluid 7. Table 3.3.14 shows the calculated Bingham and Power-law model rheological parameters and density of the fluid.

Table 3.3.13: Fluid 7 composition.

Fluid 7	
Water, [g]	4000
Bentonite, [g]	114

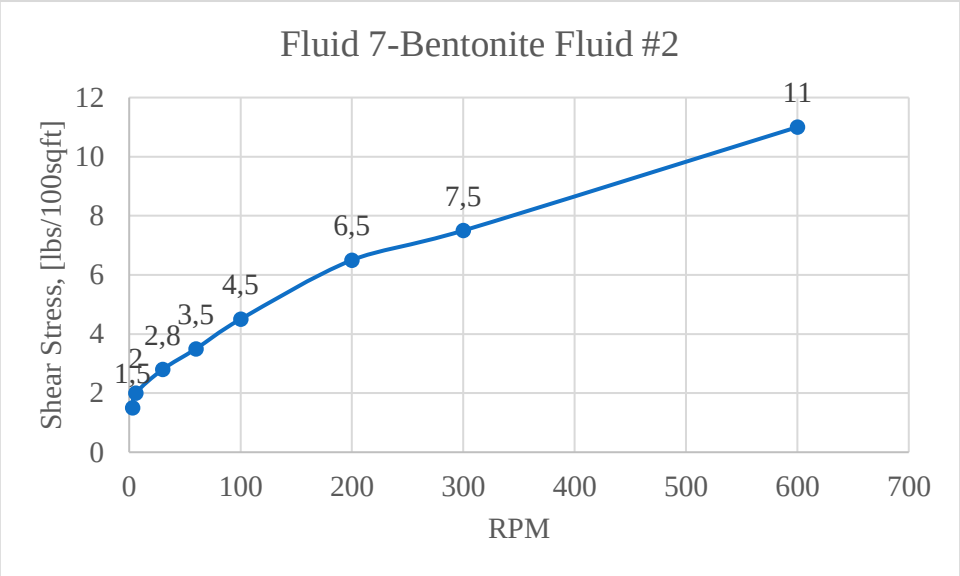

Figure 3.3.13: Viscometer response of Bentonite Fluid # 2

Table 3.3.14: Rheology Parameter data at 22°C for Bentonite Fluid # 2

Rheology parameters	Values
PV [cP]	3.5
YS [lbs/100sqft]	4
LSYS [lbs/100sqft]	1
n [-]	0,55222032
K [lbf-s^n/100sqft]	0,239561049
Density	1,02

3.3.8 Fluid 8-Ref Without Nano

Fluids 8 9 and 10 were originally designed as a backup plan for this thesis work if in case the equipment and constructing of the experimental rig for Plan A will not be in place. Since these fluids were synthesized and characterized, they were used for pressure build up phenomenon and kick dynamics in computer simulations well. The well is built in a well-known simulator called Drillbench. The results obtained from the computer simulation will be used to verify the results obtained from the small scale based experimental data.

Fluid 8 is nanoparticle free drilling fluid synthesized based on the thermal stable fluid of Lene (Fattnes, 2020) by replacing Xanthan gum polymer by CMC. In this fluid system, the concentration of barite was 150 g and resulting in the density the drilling fluid as 1.33sg.

Table 3.3.23 shows the fluids chemical compositions. Figure 3.3.18 shows viscometer measurements data. Table 3.3.24 shows the calculated Bingham and Power-law model rheological parameters and density of the fluid.

Table 3.3.15: Fluid 10 mixing recipe in mixing order

Fluid 8	
Chemical additives	Amount
Water, [g]	350
Soda ash, [g]	3,2
CMC, [g]	0,6
Carbopol, [g]	0,05
Bentonite, [g]	10
Barite, [g]	150

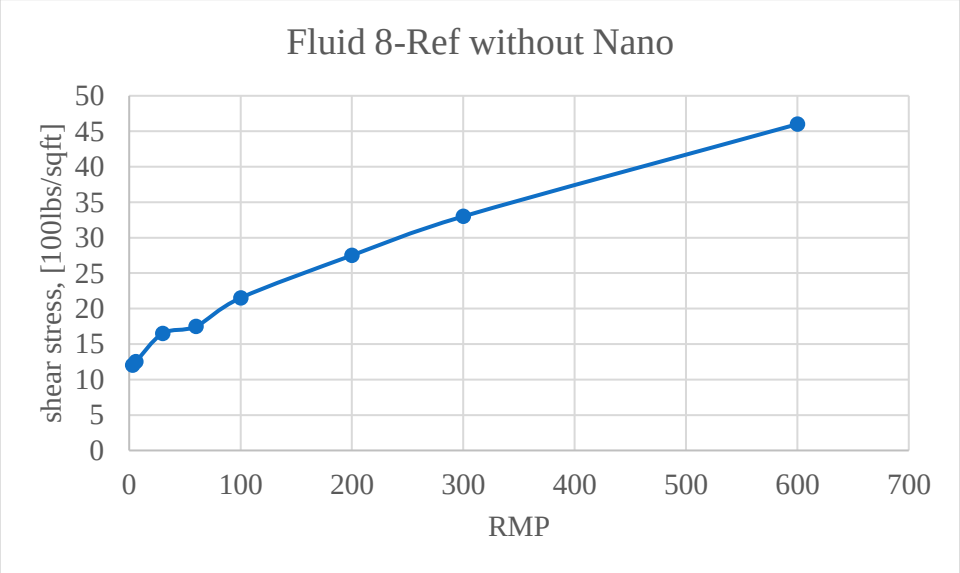

Figure 3.3.14: Viscometer data at 22°C for Ref without Nano

Table 3.3.16: Rheology Parameter data at 22°C for Ref without Nano

Rheology parameters	Values
PV [cP]	13
YS [lbs/100sqft]	20
LSYS [lbs/100sqft]	11,5
n [-]	0,478889721

K [lbf-s^n/100sqft]	1,665248347
Density [sg]	1,33

3.3.9 Fluid 9-Ref + 0,2 Nano

Fluid 9 were formulated by treating base drilling fluid with 0.2g Al2O3 (Aluminum oxide) nanoparticles. The density of Fluid 9 is the same as that of fluid 8, which is 1.33sg. However, the nanoparticle additive in fluid 8 reduced the Bingham and Herschel-Bulkley rheological parameters. This could be due to the fact that the nanoparticle additive might have created a repulsive force in the fluid systems and hence reduced the gel strength.

Table 3.3.21 shows the fluids recipe Figure 3.3.17 shows viscometer response measurements. Table 3.3.22 shows the calculated Bingham and Power-law model rheological parameters and density of this fluid.

Table 3.3.17: Fluid 9 mixing recipe in mixing order

Fluid 9	
Chemical additives	Amount
Water, [g]	350
Al2O3 (nano), [g]	0,2
Soda ash, [g]	3,2
CMC, [g]	0,6
Carbopol, [g]	0,05
Bentonite, [g]	10
Barite, [g]	150

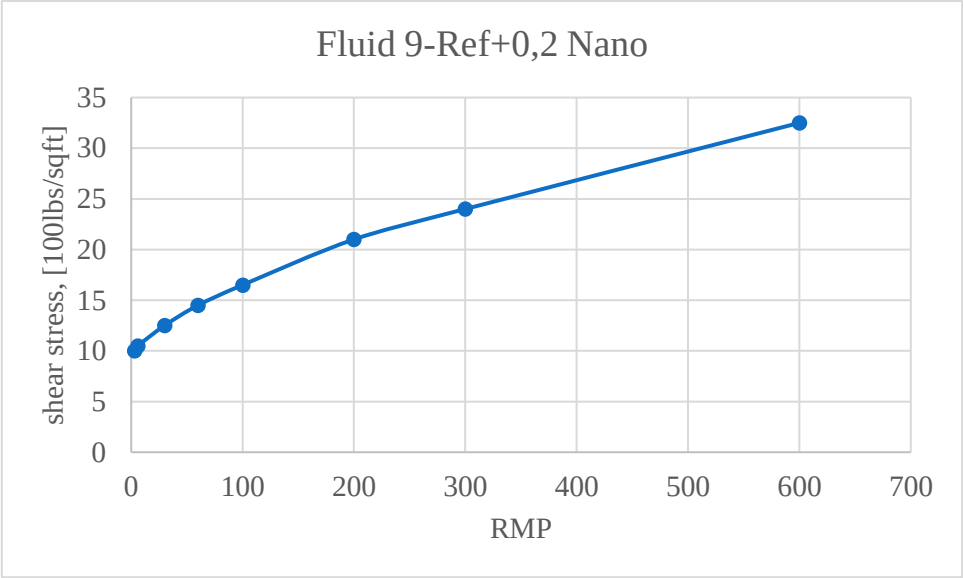

Figure 3.3.15: Viscometer data at 22°C for Ref+0,02 Nano

Table 3.3.18: Rheology Parameter data at 22°C for Ref+0,2 Nano

Rheology parameters	Values
PV [cP]	8,5
YS [lbs/100sqft]	15,5
LSYS [lbs/100sqft]	9,5
n [-]	0,437151436
K [lbf-s^n/100sqft]	1,571162685
Density [sg]	1,33

3.3.10 Fluid 10-Modified fluid

In order to investigate the effect of higher density, Fluid 10 was designed by adding 250 g more Barite in Fluid 8 and 9. The additive resulted in the drilling fluid density as 1.7 sg.

Table 3.3.19 shows the fluids recipe Figure 3.3.16 shows viscometer measurements data for Fluid 10. Table 3.3.20 shows the calculated Bingham and Power-law model rheological parameters and density of the drilling fluid.

Comparing with fluid 8, the added barite also increased the Bingham Plastic and Herschel-Bulkley rheological parameters as well.

Table 3.3.19: Fluid 8 mixing recipe in mixing order

Fluid 8	
Chemical additives	Amount
Water, [g]	350
Al2O3 (nano), [g]	0,2
Soda ash, [g]	3,2
CMC, [g]	0,6
Carbopol, [g]	0,05
Bentonite, [g]	10
Barite, [g]	150+250++

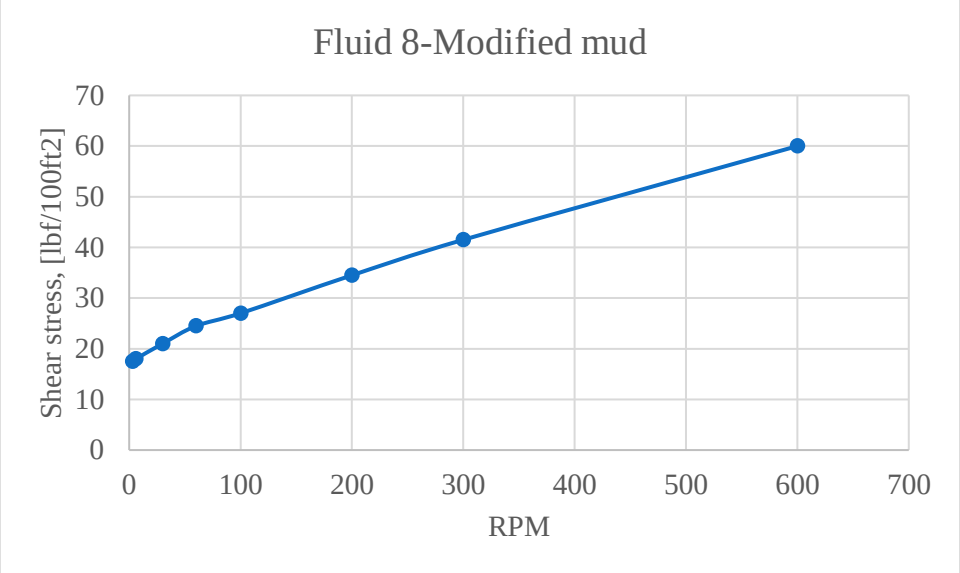

Figure 3.3.16: Viscometer data at 22°C for Modified Fluid

Table 3.3.20: Rheology Parameter data at 22°C for Modified Fluid

Rheology parameters	Values
PV [cP]	18,5
YS [lbs/100sqft]	23
LSYS [lbs/100sqft]	17
n [-]	0,53154247
K [lbf-s^n/100sqft]	1,508020902
Density [sg]	1,70

3.3.11Fluid 9-Ref + 0,2 Nano

Fluid 9 were conducted to compared fluid with and without nanoparticles (for Plan B). This fluid is added Al2O3 (Aluminum oxide) nanoparticles. Different from fluid 8 is that this fluid is not conducted with more barite when the originally recipe.

Table 3.3.21 shows the fluids recipe Figure 3.3.17 shows rheology measurements data for Fluid 9. Table 3.3.22 shows the calculated Bingham and Power-law model rheological parameters and density conducted form the tests.

Table 3.3.21: Fluid 9 mixing recipe in mixing order

Fluid 9	
Water, [g]	350
Al2O3 (nano), [g]	0,2
Soda ash, [g]	3,2
CMC, [g]	0,6
Carbopol, [g]	0,05
Bentonite, [g]	10
Barite, [g]	150

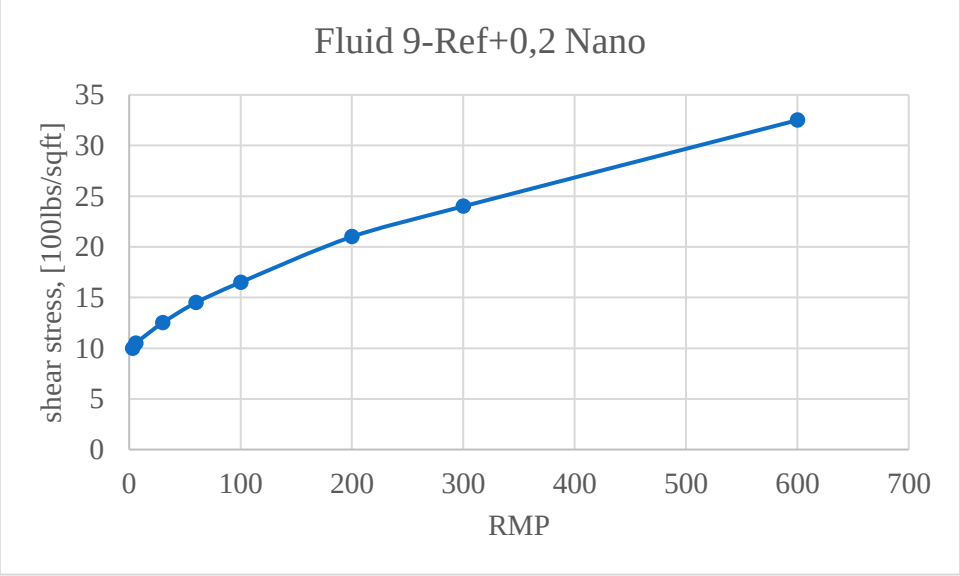

Figure 3.3.17: Viscometer data at 22°C for Ref+0,02 Nano

Table 3.3.22: Rheology Parameter data at 22°C for Ref+0,2 Nano

Rheology parameters	Values

PV [cP]	8,5
YS [lbs/100sqft]	15,5
LSYS [lbs/100sqft]	9,5
n [-]	0,437151436
K [lbf-s^n/100sqft]	1,571162685
Density [sg]	1,33

3.3.12 Fluid 10-Ref Without Nano

Fluid 10 were mixed with the same recipe and mixing order like Fluid 8 and Fluid 9 but is not added with nanoparticle and had the originally amount of barite. The comparison between nanofluid and non-nanofluid was given lower priority when the Plan A begun. Table 3.3.23 shows the fluids recipe Figure 3.3.18 shows rheology measurements data for Fluid 10. Table 3.3.24 shows the calculated Bingham and Power-law model rheological parameters and density conducted form the tests.

Table 3.3.23: Fluid 10 mixing recipe in mixing order

Fluid 8	
Water, [g]	350
Soda ash, [g]	3,2
CMC, [g]	0,6
Carbopol, [g]	0,05
Bentonite, [g]	10
Barite, [g]	150

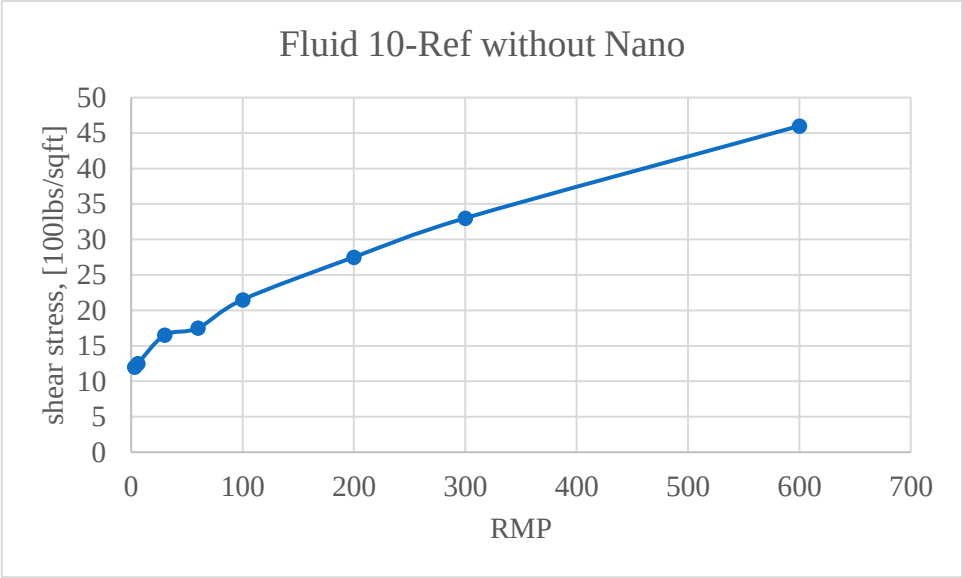

Figure 3.3.18: Viscometer data at 22°C for Ref without Nano

Table 3.3.24: Rheology Parameter data at 22°C for Ref without Nano

Rheology parameters	Values
PV [cP]	13
YS [lbs/100sqft]	20
LSYS [lbs/100sqft]	11,5
n [-]	0,478889721
K [lbf-s^n/100sqft]	1,665248347
Density [sg]	1,33

3.3.13 Fluid 11-Bentonite and Barite

Fluid 11 was tested in the physical open well rig. The reason barite was added was to get a heavier mud and higher the density. This fluid unfortunately became too heavy and could not pass the test to use in the open wellbore. The fluid is a modified fluid from fluid 6 and then added barite to get a higher value for density. It was first added 600g barite and then added more and more so the density become 2 sg.

Table 3.3.25 shows the fluids recipe Figure 3.3.19 shows rheology measurements data for Fluid 11. Table 3.3.26 shows the calculated Bingham and Power-law model rheological parameters and density conducted form the tests.

Table 3.3.25: Fluid 11 mixing recipe in mixing order

Fluid 11	
Water, [g]	2000
Bentonite, [g]	57
Barite, [g]	600+

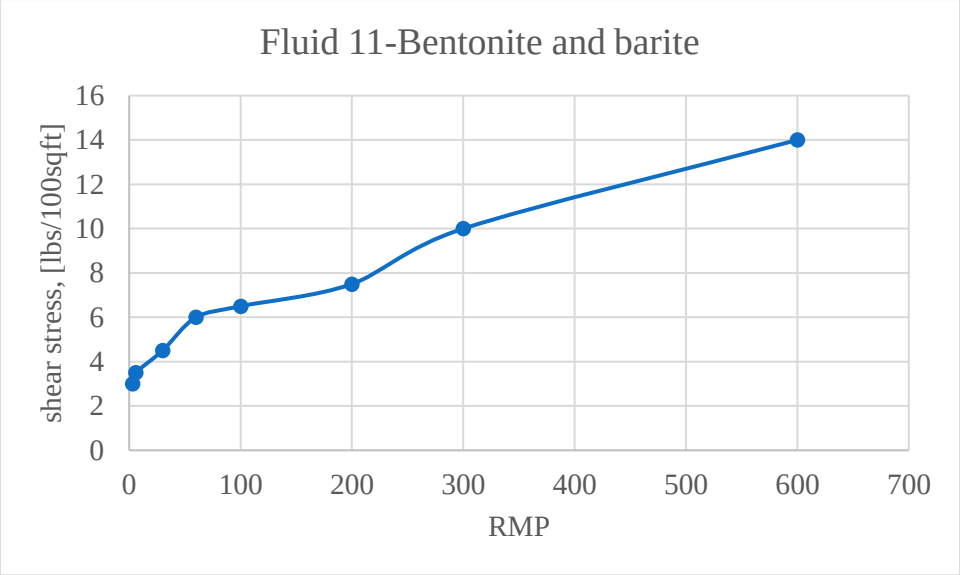

Figure 3.3.19: Viscometer data at 22°C for Bentonite and Barite

Table 3.3.26: Rheology Parameter data at 22°C for Bentonite and Barite

Rheology parameters	Values
PV [cP]	4,0
YS [lbs/100sqft]	6,0
LSYS [lbs/100sqft]	2,5
n [-]	0,485145078
K [lbf-s^n/100sqft]	0,485314123
Density [sg]	2,00

3.3.14 30 g cp with 500 g salt

Fluid 12 is a modified fluid of fluid 3. The purpose of adding salt in this mix is to make a heavier mud and still have a high viscous fluid. The salt dissolves the bonds that made the liquid viscous, and the liquid therefore became less viscous, but the density increased. This fluid was used for the closed drill rig construction. Table 3.3.27 shows the fluids recipe Figure 3.3.20

shows rheology measurements data for Fluid 12. Table 3.3.28 shows the calculated Bingham and Power-law model rheological parameters and density conducted form the tests.

Table 3.3.27: Fluid 12 mixing recipe in mixing order

Fluid 12	
Water, [g]	4000
Salt (NaCl), [g]	500
Carbopol, [g]	30
Xanthan, [g]	2

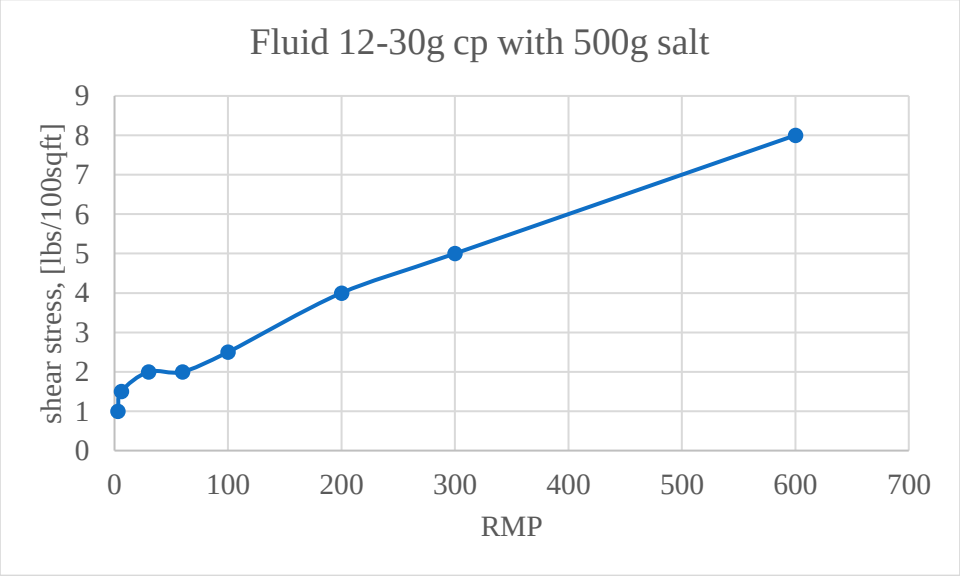

Figure 3.3.20: Viscometer data at 22°C for Fluid 12

Table 3.3.28: Rheology Parameter data at 22°C for Fluid 12

Rheology parameters	Values
PV [cP]	3,00
YS [lbs/100sqft]	2,00
LSYS [lbs/100sqft]	0,50
n [-]	0,6777
K [lbf-s^n/100sqft]	0,073
Density [sg]	1,09

3.3.15 Bentonite and barite #2

Fluid 13 were made for use in the closed physical rig construction. The reason to make this fluid was to make a higher density fluid to test and try to see a trend compared to lighter liquids. There were first added 500g barite and then more and more scoops of barite to get both higher density and higher viscosity. Table 3.3.29 shows the fluids recipe Figure 3.3.21 shows rheology measurements data for Fluid 13. Table 3.3.30 shows the calculated Bingham and Power-law model rheological parameters and density conducted form the tests.

Table 3.3.29: Fluid 13 mixing recipe in mixing order

Fluid 13	
Water, [g]	4000
Bentonite, [g]	114
Barite, [g]	500+

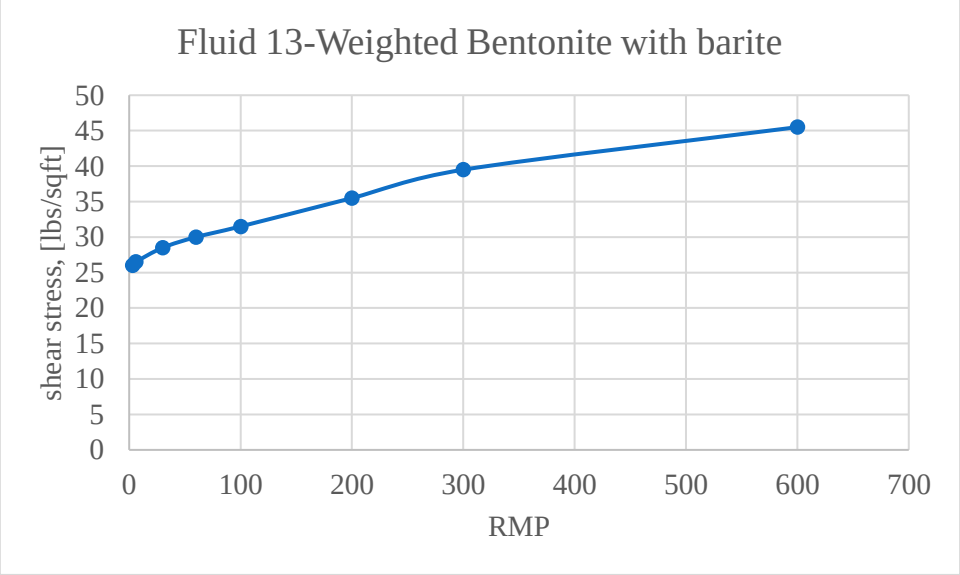

Figure 3.3.21: Viscometer data at 22°C for Fluid 13

Table 3.3.30: Rheology Parameter data at 22°C for Fluid 13

Rheology parameters	Values
PV [cP]	6,00

YS [lbs/100sqft]	33,50
LSYS [lbs/100sqft]	25,50
n [-]	0,204
K [lbf-s^n/100sqft]	11,075
Density [sg]	1,28

3.3.16 Nanofluid based drilling fluid

Based on the thermal stable fluid synthesized by Lene (Fattnes, 2020), in this thesis work, the fluid system was reformulated by replacing Xanthan gum polymer by CMC. The nanofluid system was synthesized during the first phase of the project. However, after the rig construction become successful the thesis work primarily focused on the main tasks, which are kick dynamics and wellhead pressure build up. For this experimental work, we took the opportunity of using the nano-based drilling fluid in the experimental well. Table 3.3.31 provides the fluid chemical compositions with and without nanoparticle.

Table 3.3.31: Mix composition for reference mud with and without nanoparticle with modified mud

	Mud 4	Mud ref	M4+250
Addtivies			
Water [g]	350	350	350
Al2O3	0,2	0	0,2
Soda ash [g]	3,2	3,2	3,2
CMC [g]	0,6	0,6	0,6
Bentonite [g]	10	10	10
Barite [g]	150	150	150+250
Anti-foam [AR]	0	0	0
Carbopol Polynomer [g]	0,05	0,05	0,05
Density [sg]	1,33	1,33	1,33

4 Results

The bubble dynamics and the pressure build-up phenomenon were investigated in the open and closed well experimental wells. The wells have been filled with the fluids synthesized and characterized in Experimental Fluid Synthesis and Characterization.

In open hole, gas bubble speed was studied in an annulus between 25mm inner tubes and three wells (i.e., 30mm, 40mm and 50mm). These results annular clearance of 2.5mm, 7,5mm and 12,5mm. The length of the well is 2m, but 1.6 m of the well is filled with the well fluid.

In closed well, the wellhead pressure build-up studied in 1m length and 50mm experimental rig. The results obtained from the open and closed rigs are presented in Top close rig.

4.1 Open system

The results from the physical rig construction test had the three parameters (density, viscosity, Clearance) to be compared with velocity. The dynamic in the test and the errors were also studied and documented. To easy show trends and result two to three fluids were compared with each other.

4.1.1 Effect of density of the fluid and annular clearance

The first experiment is to study the effect of density on the bubble speed. Barite is commonly weight control additive in drilling fluid. However, due to its brownish color, it was difficult to observe the bubble migration in the wellbore. Because of this reason, we used 1000g salt blended with 4000g water. The brine solution gives density of 1.17sg. To make the rheological parameters nearly the same, but density variation, brine fluid is compared with tap water. The rheological parameters and the rheometer apparent viscosity properties are shown in section 3.3.1. The brine system increase is not Newtonian like water, but comparing with water, the salt additives increased the rheological parameters PV, YS and LSYS by 0.5cP, 0.2lbf/100sqft, and 0.5lbf/100sqft, respectively. The rheometer apparent viscosity of brine system is 1.53cp and that of water is 1.05 cp.

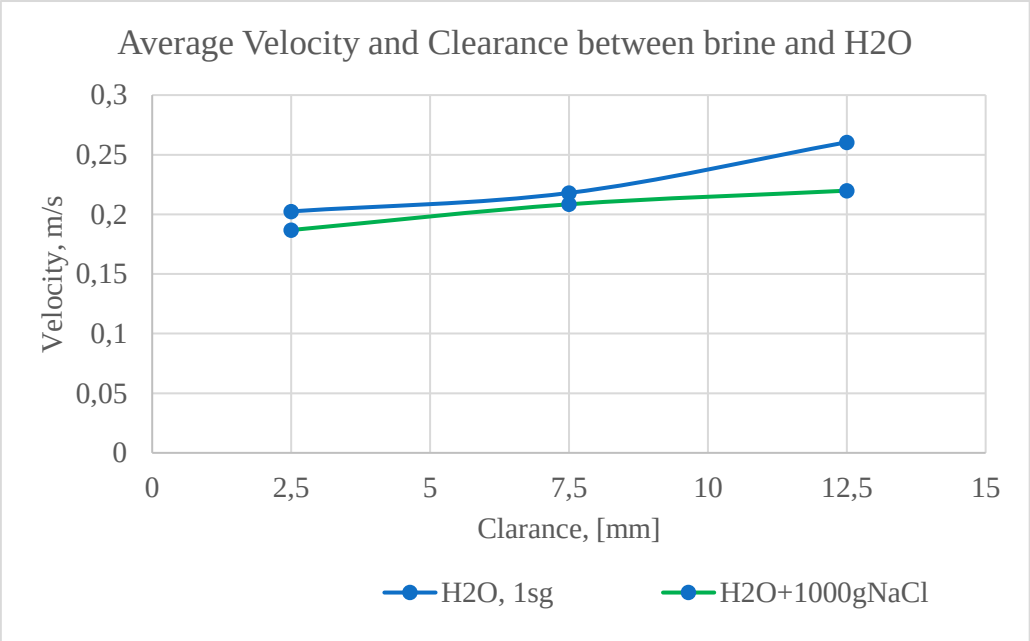

Figure 4.1.1: Average velocity between small and big bubbles in H2O vs in Brine.

4.1.2 Effect of plastic viscosity and annular clearance

Here is the effect of Plastic viscosity concerning annular clearance. Here the liquids are represented: H2O, Viscous liquid, and High viscous liquid (Fluid 1, Fluid 2 and Fluid 3). The plastic viscosity sees a gas connection in increased plastic viscosity and lower speed in the bubble/slug together.

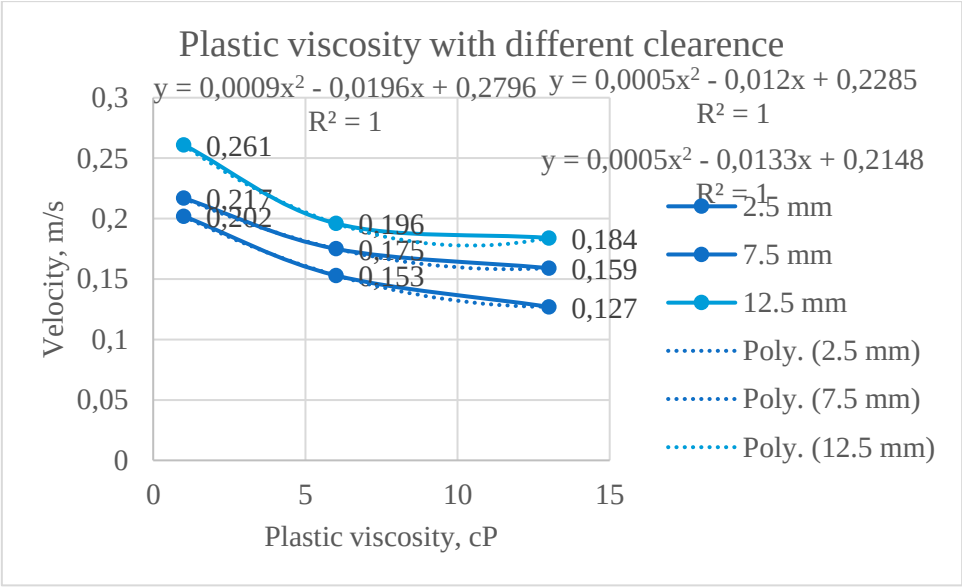

Figure 4.1.2: Plastic Viscosity and Velocity of water(1cp), Fluid 2(6cp) and Fluid 3(13cp) with different clearance

4.1.3 Effect of YIELD stress and LSYS and annular clearance

Here is the effect of LSYS on annular clearance. Here the liquids are represented: H2O, Viscous liquid, and High viscous liquid. The LSYS sees a good connection between increased LSYS and lower speed in the bubble/slug together.

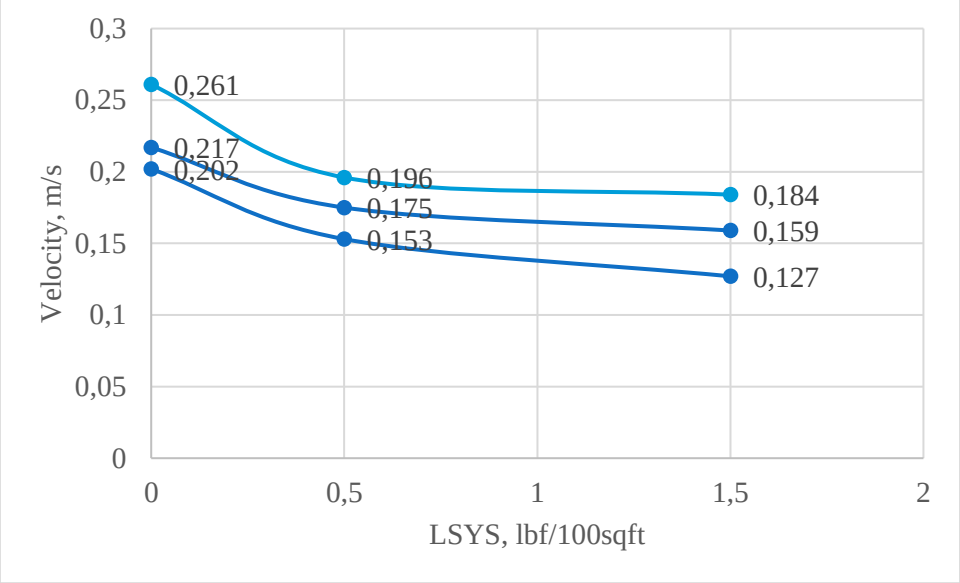

Figure 4.1.3: Low shear yield stress and Velocity of water(0cp), Fluid 2(0,5cp) and Fluid 3(1,5cp) with different clearance

Here is the effect of Yield Strength concerning annular clearance. Here the liquids are represented: H2O, Viscous liquid, and High viscous liquid. The Yield Strength sees a good connection in increased Yield Strength and lower speed in the bubble/slug together at least between 0 and 2 Yield Stress.

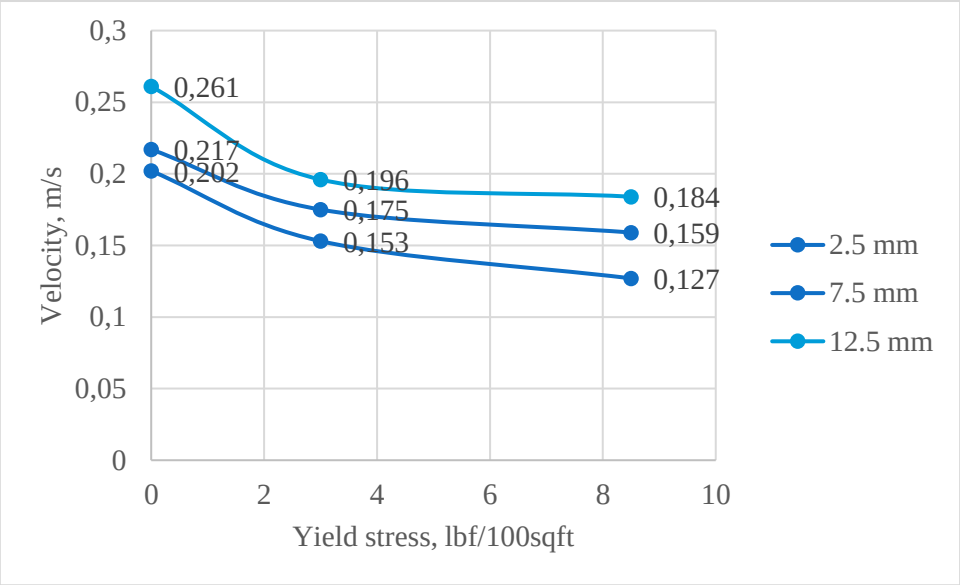

Figure 4.1.4: Yield stress and Velocity of water(0cp), Fluid 2(3cp) and Fluid 3(8,5cp) with different clearance

4.1.4 Effect of flow index parameter and annular clearance

Here is the effect of flow index n, on annular clearance. Here the liquids are represented: H2O, Viscous liquid, and High viscous liquid. The flow index sees a good connection between increased flow index and increase speed in the bubble/slug together at least between to second and third points.

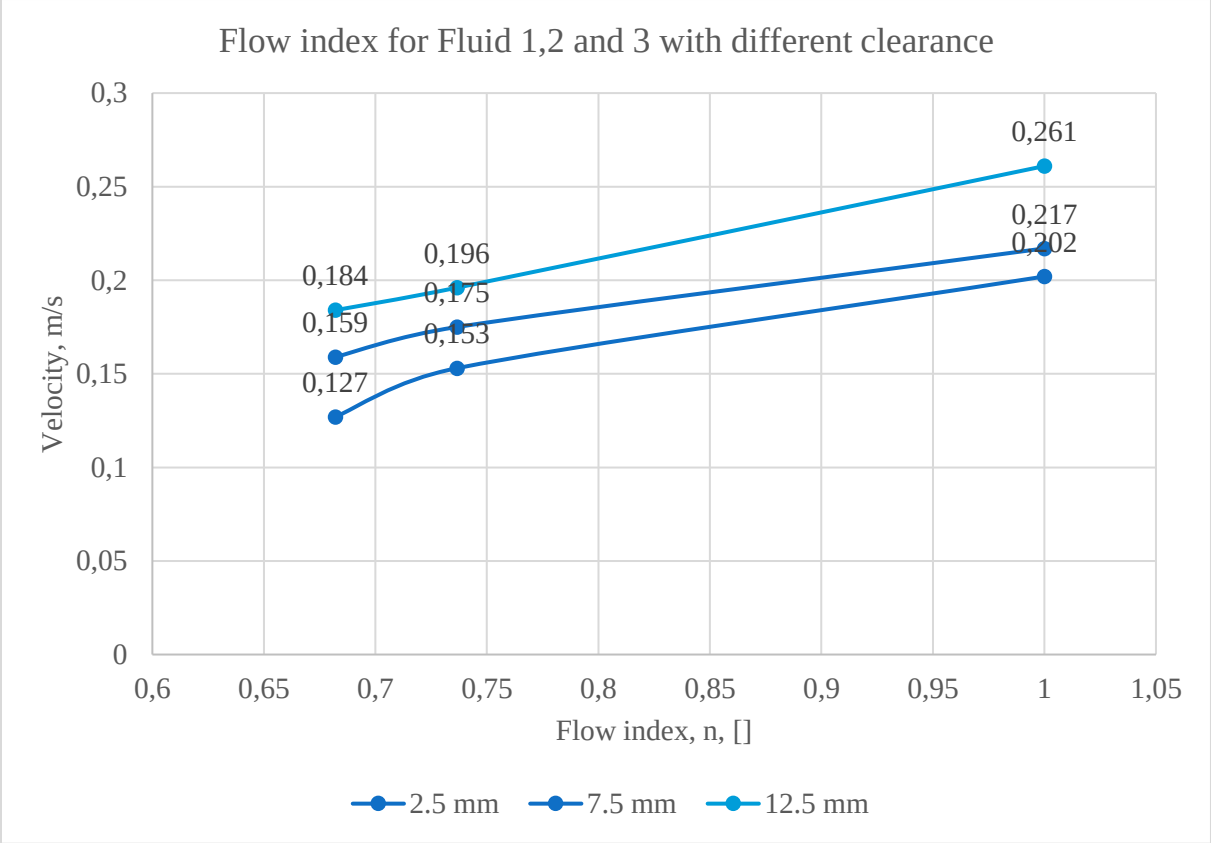

Figure 4.1.5: Flow index and Velocity of (form right to left) water (0), Fluid 2(0,73) and Fluid 3(0,68) with different clearance

4.1.5 Effect of LSYS effects in 2.5 mm clearance

Here compares the bentonite fluid with the 2.5 g CP + 2g XG, 30 g cp+ 2 g XG and the bentonite fluid. For the bentonite fluid, the small bubbles were difficult to analyze so this comparison is for the slugs in all fluids.

Here you can see a good connection between LSYS and the speed. The higher the LSYS, the lower the speed of the Slug or the bubble. It is a 2.5 g CP fluid that has the lowest LSYS and comes with s 30 cp fluid and then Bentonite fluid the with highest LSYS and lowest speed.

This test is from 2.5 mm clarence and equal length of wellbore size.

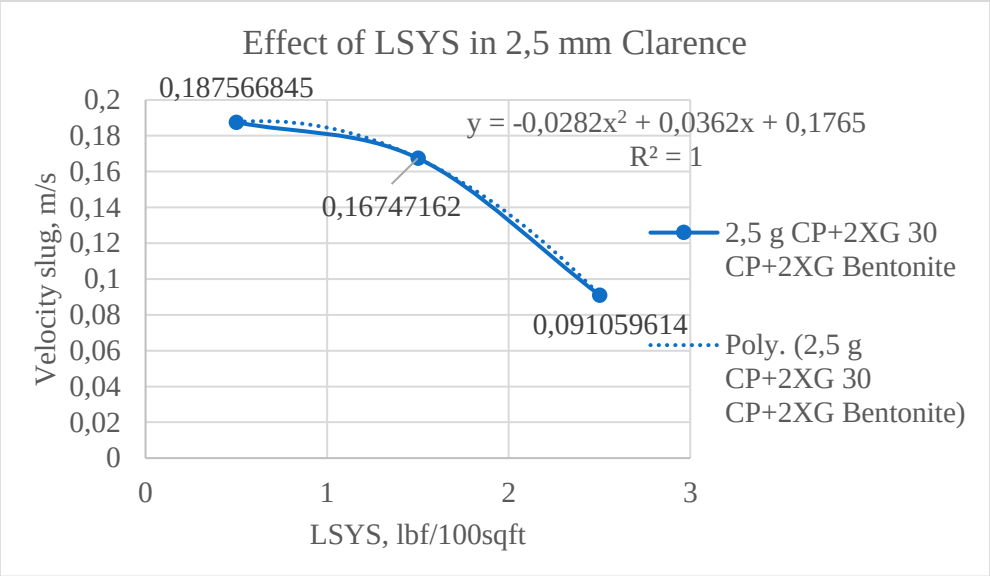

Figure 4.1.6: LSYS and Velocity of Fluid 2(0,5cp) and Fluid 3(1,5) and Fluid 7(2,5cp) with the same clearance

4.1.6 Effect of H2O in Annular Clearance

For most liquids tested, viscosity increased density and vice versa. It is therefore difficult to see what affects the speed. With increased clearance, it is the same liquid that is measured, and it is therefore easier to see a clear trend that affects the speed. In all attempts, we saw an increasing speed of slugs and bubbles at greater clearance. With an increase in clearance, the speed of both bubbles and slugs also increased. Most of all was the increase in slug. This can be explained by the larger surface volume of the slug compared to the bubbles.

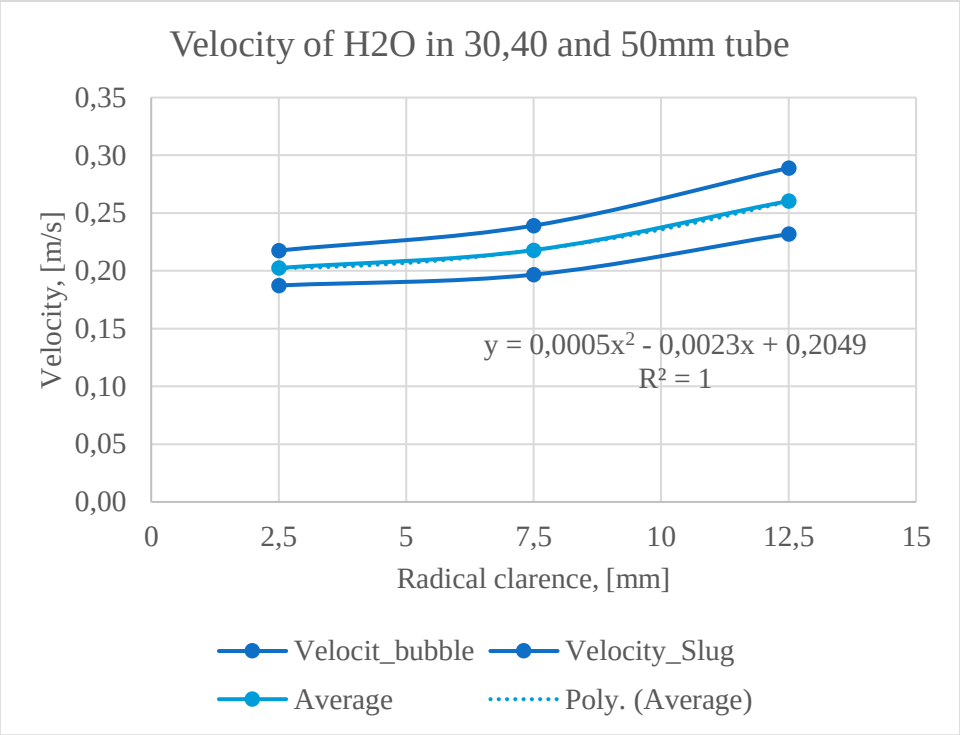

Figure 4.1.7: Velocity of bubbles, Slugs and their average together in different clearance.

4.1.7 Effect of density and viscosity and annular clearance

Here is brine and water in different clearance represented. In the first glance the higher density will decrease the bubble/slug velocity in the fluid. On the other hand, the brine has a higher viscosity then water. The brine doesn't have high viscosity measurements, but it has a big effect on the graph and data conducted and will lower the speed significantly.

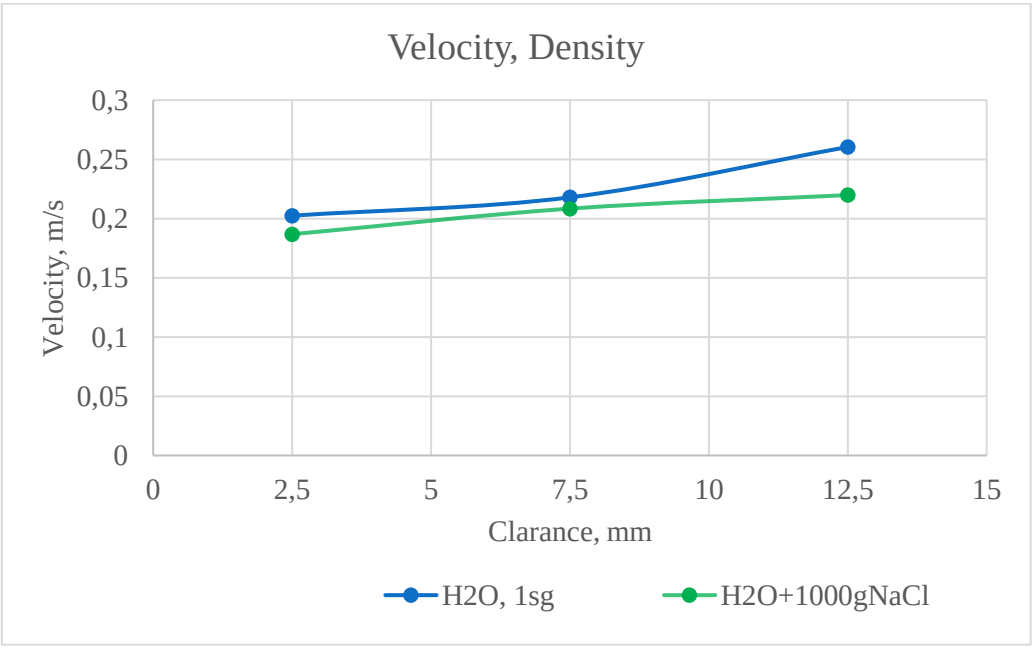

Figure 4.1.8: Velocity compared high- and low-density fluid (Water and brine) with different clearance

Here use the high viscous with salt, and the 2.5 CP /2XG and 50cP

To take this example further the Fluid 7 with the third lowest viscosity measurement (Water and brine were lower) vs brine with the same condition as over shown at Figure 4.1.9:

The bentonite fluid that is represented had also a low viscosity, same as brine, but since brine had a much higher density, the velocity increased with higher density fluid. The water has still higher velocity then the brine, but the viscosity triumphs the higher density in this exercise.

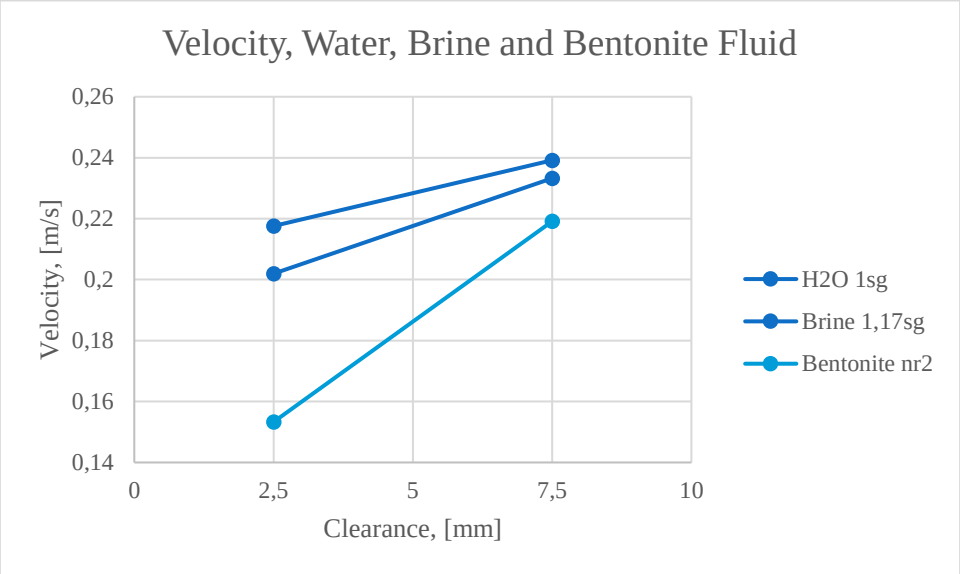

Figure 4.1.9: Velocity vs clearance for water, brine and bentonite fluid

4.2 Closed system

In the physical closed system, the WHP were measured compared with BHP with different injection rate and fluids.

4.2.1 Well Head pressure under different injection rate

It has long been believed that the pressure at the bottom of the well is carried by gas to the surface without being changed. This according to Boyles law is interpreted as the volume of the kick is the same and the well fluid is incompressible (Britannica, 2022). From an

experiment from Louisiana State University, they investigated this (Otto L. A Santos, 2021). In their experiment it was tried in a 5000 meter well, while in this experiment it was only tried in a 1 meter long well as like compression, pressure difference was uncertain that one could imagine. The main goal was therefore to investigate the wellhead pressure dynamics in different fluid rheological properties. During experimental work, different rate of injection and method of injection were employed. This are low rate and high rate for each bottomhole pressure. The third type is that the injection pressures were applied continuously. The results obtained from these injection rates are compared.

Figure 4.2.1 shown an illustration of the WHP build up phenomenon obtained from the 1m experimental rig and 5000ft (full scale) experimental rig (Otto L. A Santos, 2021). Regardless degree of wellhead pressure reduction difference, in terms of trend wise, one can observe a similar behavior.

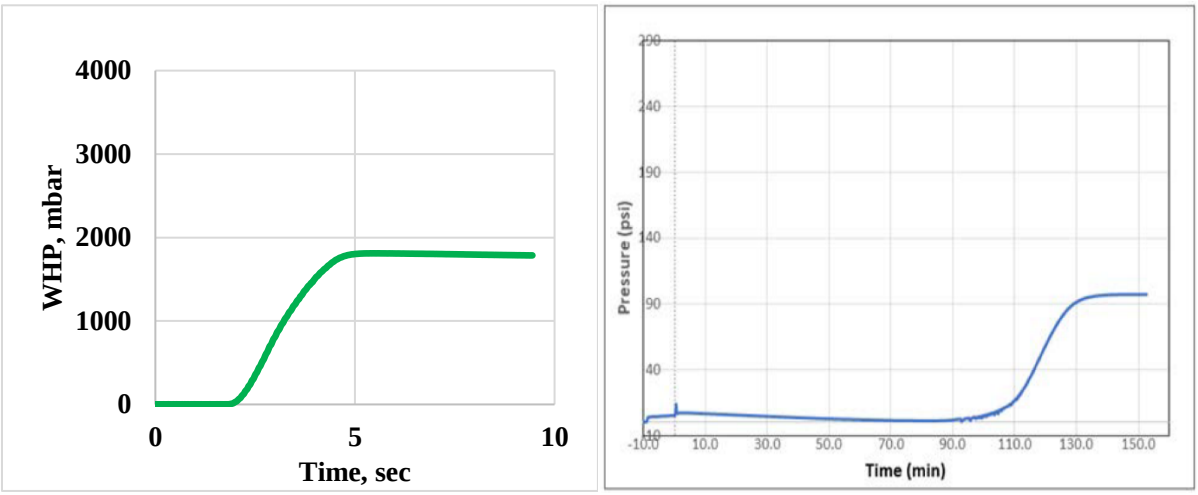

Figure 4.2.1: 1. WHP build-up in 1m rig, 2. Pressure build-up in full scale well, (Otto L. A Santos, 2021)

4.2.1.1 Low injection rate

In the low pump injection rate, it is pumped individually at low speed for each measuring point. For each measuring point, the pressure in the well was reset and a new injection of gas was performed with another BHP. An advantage of this measurement method was that at a low measurement rate it becomes easier to get the exact BHP that is added to the well.

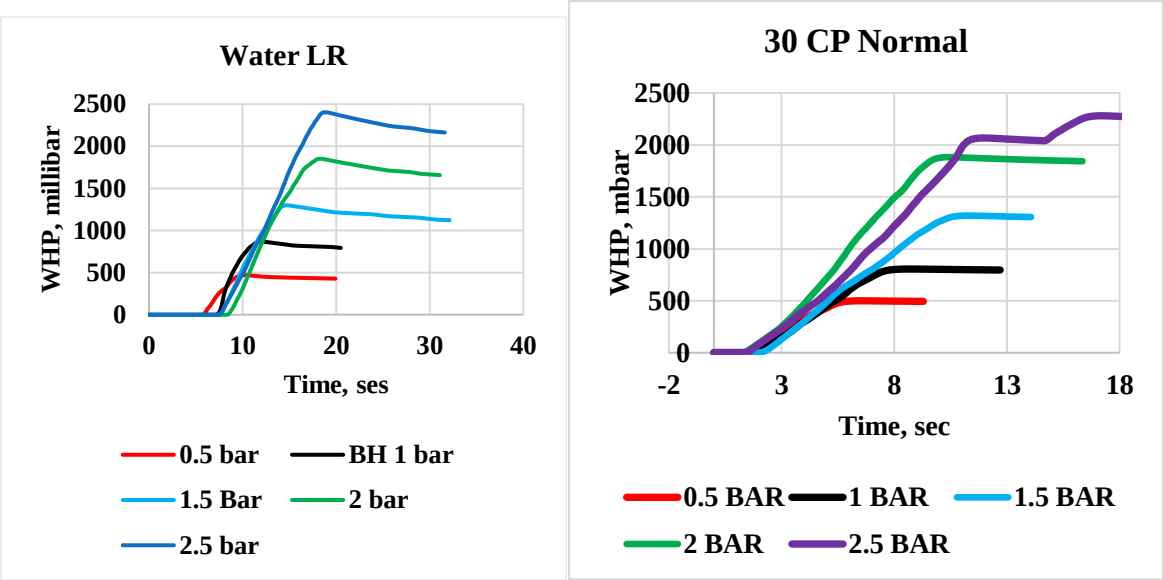

Figure 4.2.2: Fluid 1 and 12 Pressure dynamics with same low-rate injection and BHP

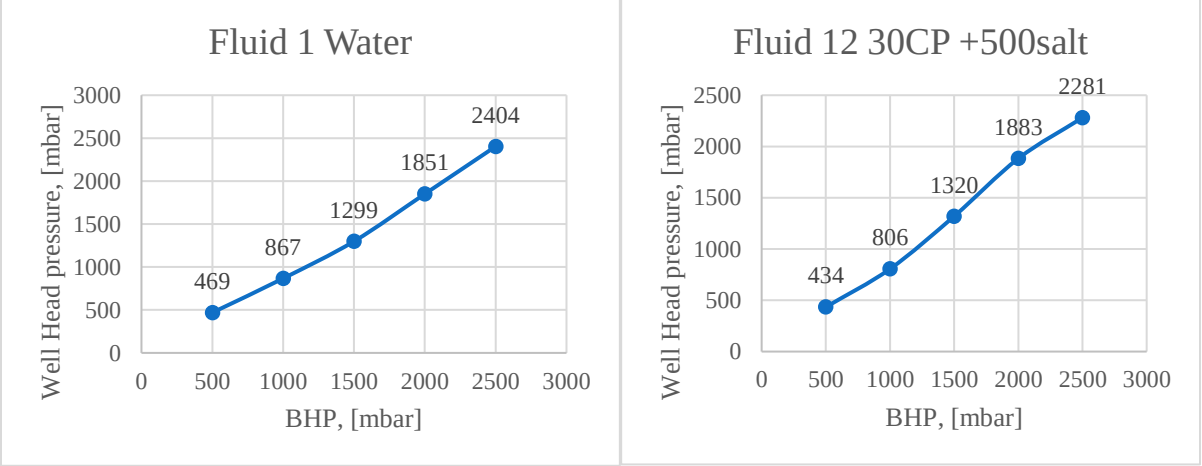

Figure 4.2.3: Fluid 1 and Fluid 12 WHP with same low-rate injection and BHP

This rig construction is a great simulation to figure out if there is difference in BHP gas injection and WHP but is not very advanced compared to other physical simulation in the industry. There is simulation there is 5000 feet long (Otto L. A Santos, 2021)and there is this simulation of 1 meter. Because of the big difference in size and only 2 pressure sensors to conduct measurements compared with more than hundreds of sensors all the way from BHP to WHP the results are also more exact.

With limit time and limit resources we still conducted to get great trends and good research, found the dynamics, which was the main task. Another thing we wanted to investigate was whether the pressure had a difference in viscosity, density, and concentration of liquid with different polymer (which is used in the real drilling operation) had a degree of influence on this

pressure developed. What we found with this exercise was thus that with this self-developed physical closed rig, we do not find a real connection between these parameters. One cannot say with this that there is no connection just because no connection was found with this exercise. But if you go in depth and look at other exercises that have been tried in others' work, you can conclude that you should have a larger volume and length in the well to get a better result. to find a good connection, we have also used these fluids in the simulation program drillbench which simulates much larger drilling wells and the dimension thus becomes to a much greater extent.

4.2.1.2 High injection rate

In the high injection rate, it is pumped at a higher pump rate than at a low pump rate. In this measuring frequency, it is also measured individually and the pressure in the well is reset for each experiment. An advantage of this measurement method is that the trend in the injection phase becomes more correct when in a real well you get a kick or are injected with gas, BHP increases rapidly.

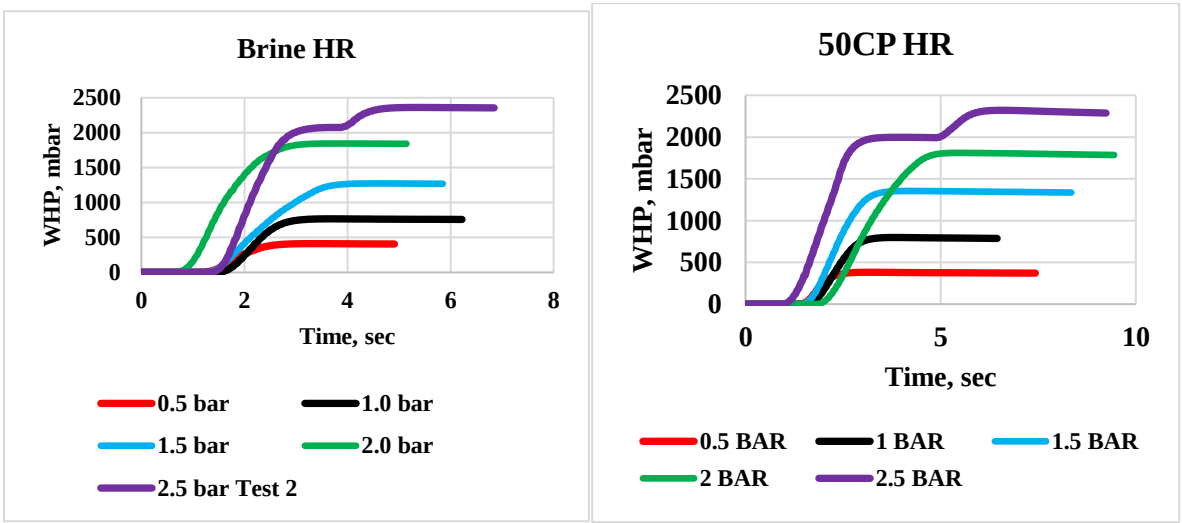

Figure 4.2.4: Fluid 4 and 5 pressure dynamics with same high-rate injection and BHP

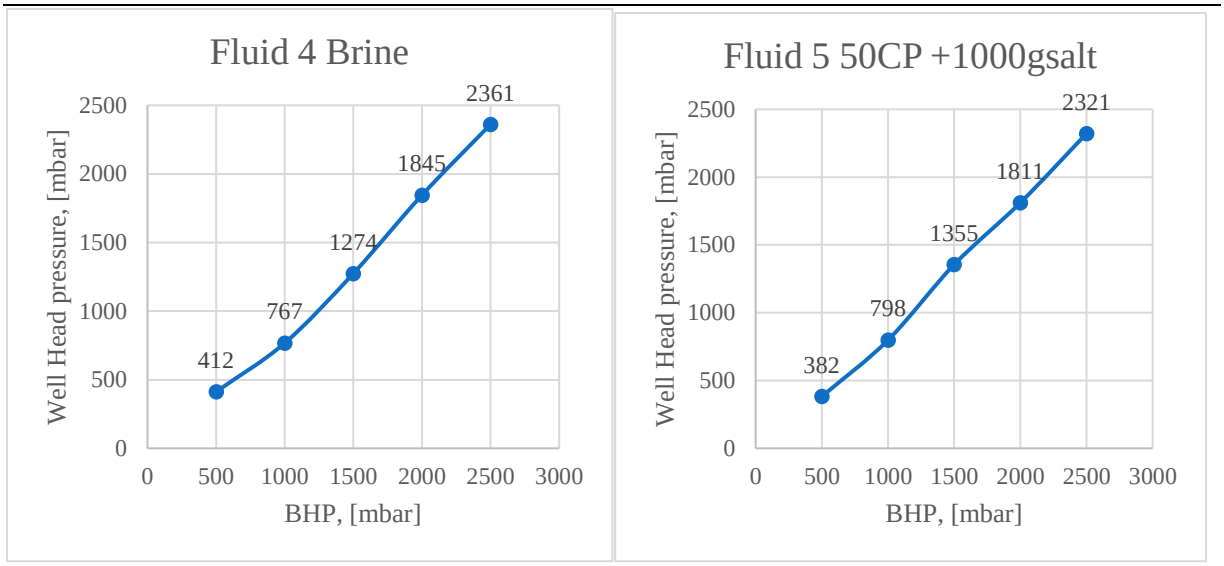

Figure 4.2.5: Fluid 4 and Fluid 5 with same high-rate injection and BHP

4.2.1.3 Continuous -average injection rate

In the continuous injection rate, the gas was injected continuously step by step for each measuring point from 500-2500mbar. The pressure in the well is also not reset for each experiment but is reset from each individual liquid in the well. It is also a good indication of how the different liquids gradually react with higher and higher pressures.

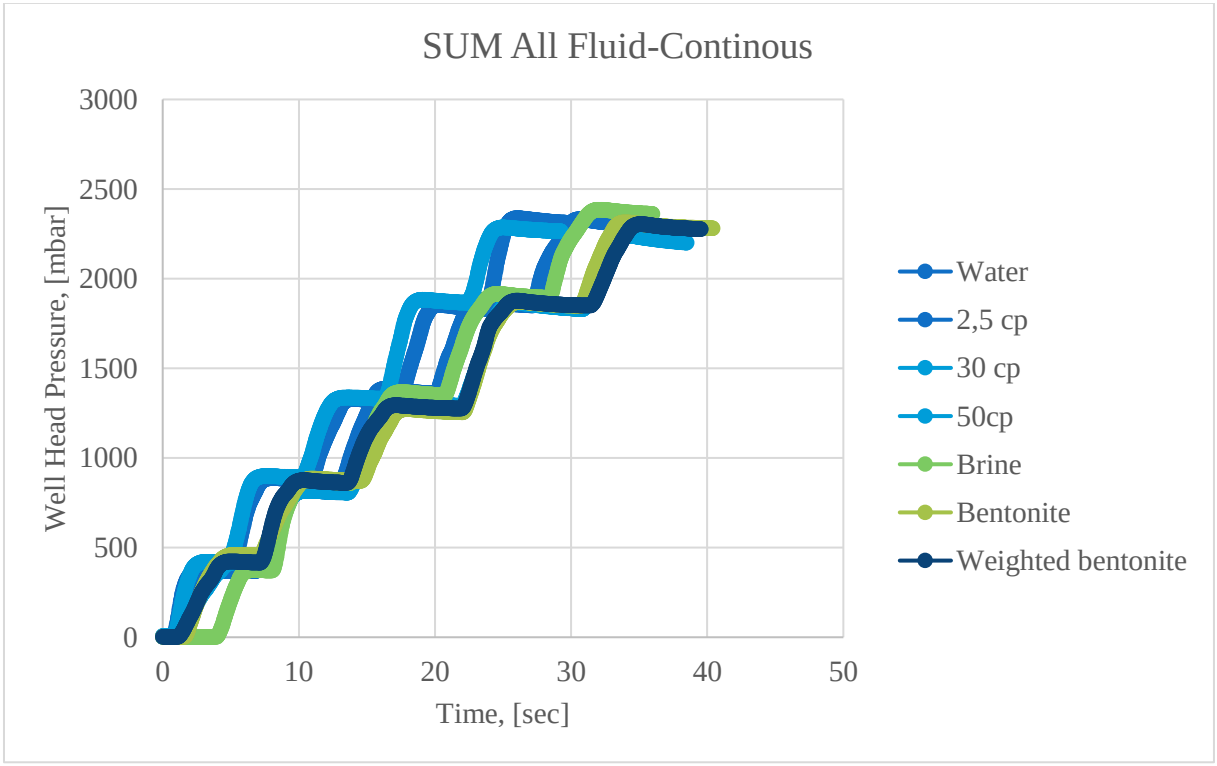

Figure 4.2.6: All fluids (use in closed rig physical simulation) in continuous injection rate

4.2.1.4 Comparisons between BHP and Well head pressure under different injection rate

The physical close rig construction is only 1 meter (85cm filled with fluid) and shows indication for compression for the fluid because of different BHP/WHP and the trend shows 8-10% reduction of pressure from BHP to WHP. Under is a comparison between all three injection rates and from Figure 4.2.11 the average BHP and WHP from all fluids were shown. Some fluids indicated more compression then the other, but the most important observation is that the trend that is conducted at all fluid had a compression from 8-10% pressure reduction.

Figure 4.2.7: Water as fluid in the wellbore with BHP vs WHP, b, 2,5 CP as fluid in the wellbore with BHP vs WHP

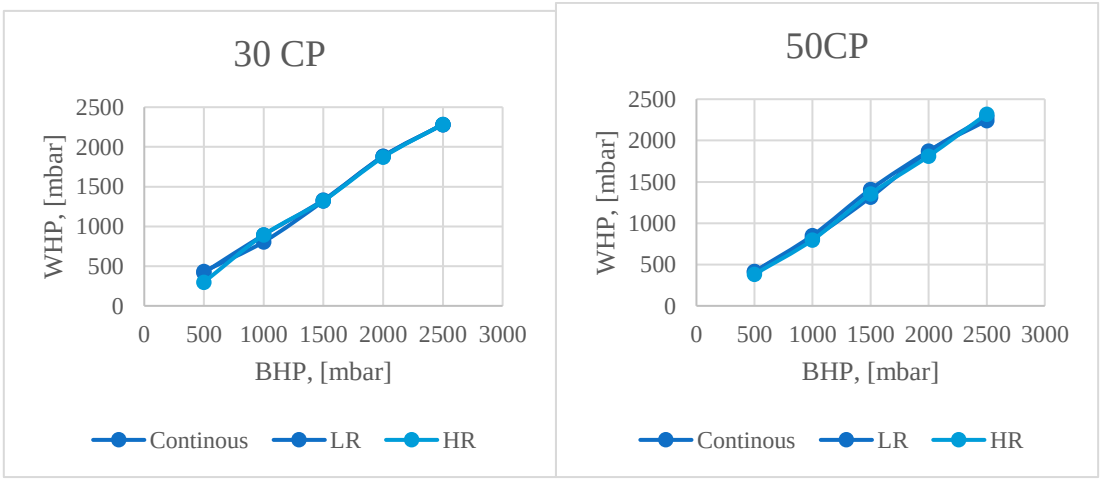

Figure 4.2.8: Fluid 12 in the wellbore with BHP vs WHP, b, Fluid 5 in the wellbore with BHP vs WHP

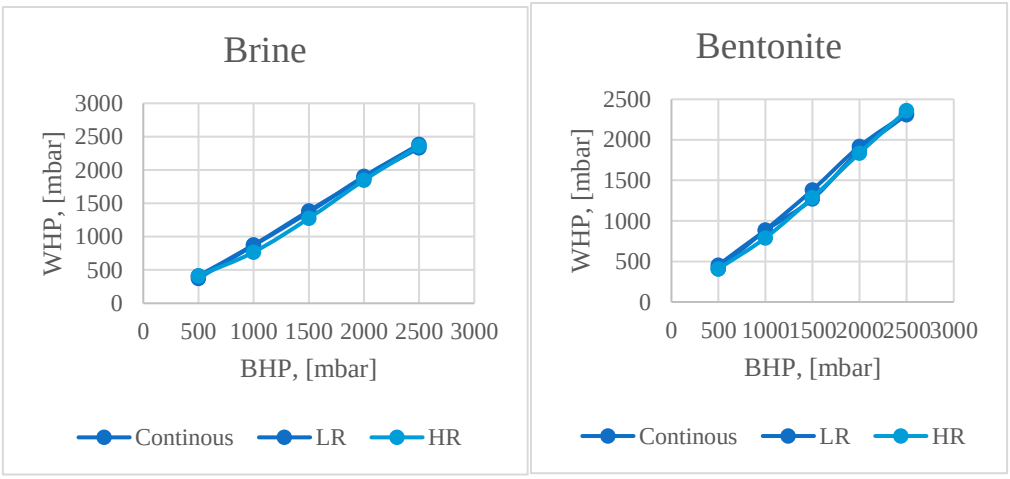

Figure 4.2.9: Brine in the wellbore with BHP vs WHP, b, Bentonite fluid in the wellbore with BHP vs WHP

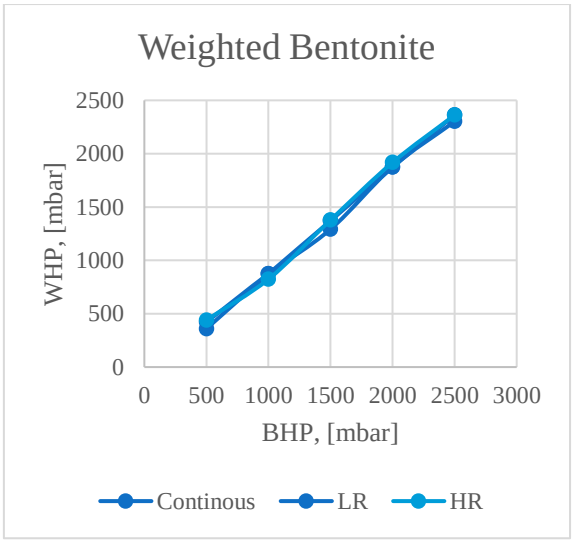

Figure 4.2.10: Weighted Bentonite in the wellbore with BHP vs WHP

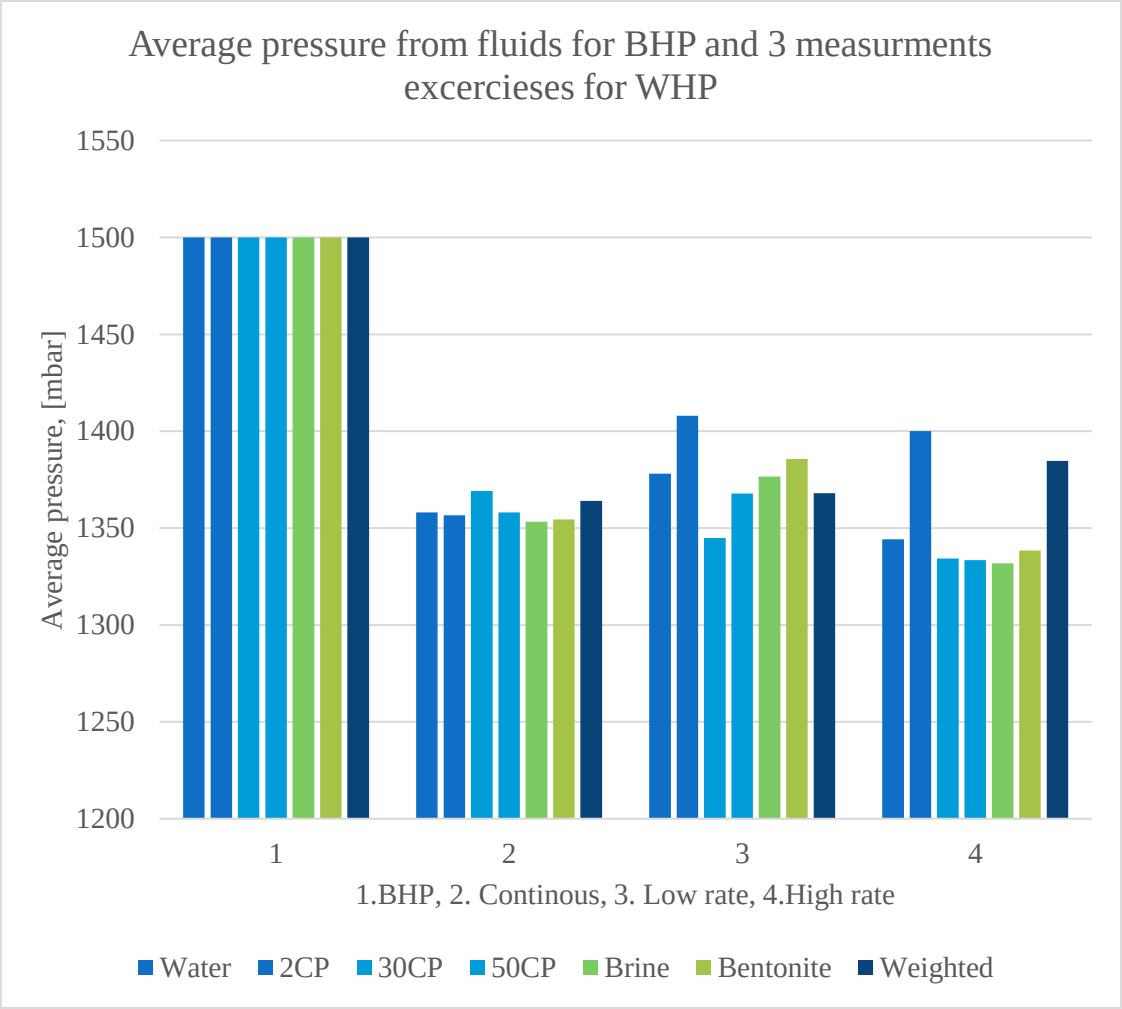

Figure 4.2.11: The average measurements from BHP and WHP in continuous, low rate and high rate of gas injection.

4.2.2 Effect of length of wellbore for WHP

All previous test for closed rig were 1 meter. One last test was conducted with the same clearance, but different wellbore length. This test was 2 meter in length and shows how the same injection pressure compared to 1 meter is.

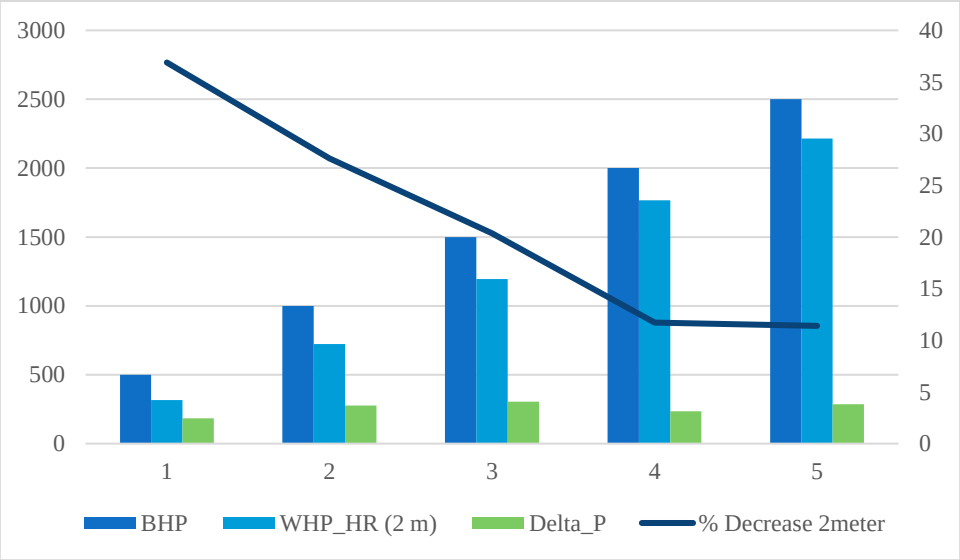

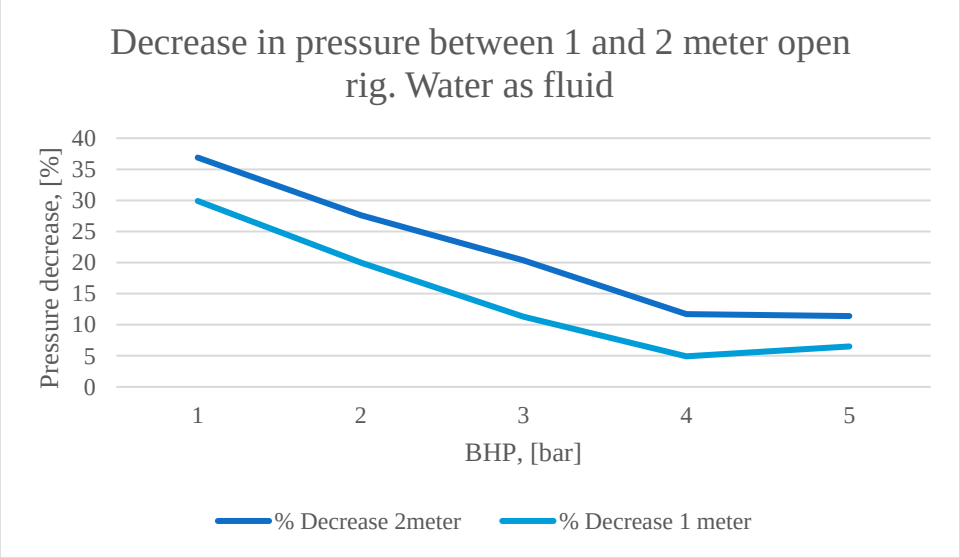

5 Gas bubble dynamics in closed well Computer Simulation

Drillbench is a simulation program for drilling wells. Drillbech is developed by Scanpower Petroleum Technology Group and Schlumberger (Software, 2022).

The experimental setup presented in section “Top close rig” are based on 1m long and 50mm wellbore. The experimental results in the considered setup showed that the wellhead pressure reductions in the different fluid systems are within the range of 8-11%. This result is valid for the small-scale experiments. However, to investigate the effect of wellbore length and

clearance, Drillbench is used to build and simulate the kick dynamics in realistic wellbore geometry. The wellhead pressures build up phenomenon in the fluid systems that are used for the small-scale experiment were investigated in different annulus scale using different influxes (Air, and Methane). The main reason is to study the trends observed in the experimental setup

5.1 Simulation set up

An offshore well is built in Drillbench, where the wellhead is located at subsea and 21'' riser connected surface with the wellhead. The detail of the well construction specification is provided in Figure 5.1.3 and Figure 5.1.4. The OD of the drillstring at the normal set-up were 5,875" and the inner diameter of the wellbore were 11,875".

The simulation is tested with all fluids from the thesis with normal and realistic drillstring, drillcollar, riser and casing. It was also tested simulation with big clearance for comparing physical measurements and big scale simulation. In this simulation it is not realistic drilling set up because of it is to big wellbore vs drillstring. The purpose of this simulation is to see the dynamics in the wellbore and the pressure build up. The Drillstring where 2 3/8" and Casing 20".

Table xx Well construction components

Data: Big and normal Clearance from drillbench:

Normal Clearance

Casing:

Casing program				
Name	Hanger depth [m]	Setting depth [m]	Inner diameter [cm]	Outer diameter [cm]
36"	2601,00	2686,00	88,9	91,4
26"	2601,00	3000,00	63,5	66
22"	2601,00	3330,00	50,8	55,9
14.00"	2601,00	3920,00	32,3	35,6
11 7/8"	3820,00	4250,00	27,4	29,8

Figure 5.1.1: Simulation set up for casing for normal clearance

STRING

Component section				
Component	Type	Section length [m]	Inner diameter [cm]	Outer diameter [cm]
Stabilizer	DrillCollar	2,81	8,9	20,3
XOver	DrillCollar	0,57	4,9	20,3
LWD	DrillCollar	3,71	5	20,3
LWD	DrillCollar	4,25	4,9	20,3
Xover	DrillCollar	0,57	8,3	20,3
LWD	DrillCollar	4,97	6	20,3
LWD	DrillCollar	5,34	6	20,3
Xover	DrillCollar	0,57	8,3	20,3
LWD	DrillCollar	6,21	4,8	20,3
MWD	Mwd	4,81	10,2	20,7
Stabilizer	DrillCollar	1,57	7,3	20,3
VCP	DrillCollar	0,69	7,3	20,3
Drill Collar	DrillCollar	63,98	7,1	20,3
Jar	DrillCollar	6,61	7	20,6
Drill Collar	DrillCollar	18,28	7,1	20,3
Xover	DrillCollar	0,66	7,1	20,3
HWDP	Drillpipe	227,00	10,2	14,9
DP 5-7/8" S	Drillpipe	4068,00	13,1	14,9

Figure 5.1.2: Simulation set up for Drillstring for normal clearance

Riser

Name	Length (m)	Inner diameter (cm)	Outer diameter (cm)	Properties
21" Riser	2601,0	48,3	53,3	

Casing / Liner

Depths are measured depth with reference to RI

Name	Hanger depth (m)	Hanger vertical depth (m)	Setting depth (m)	Setting vertical depth (m)	Inner diameter (cm)	Outer diameter (cm)
36"	2601,0	2601,0	2686,0	2686,0	88,9	91,4
26"	2601,0	2601,0	3000,0	3000,0	63,5	66
22"	2601,0	2601,0	3330,0	3330,0	50,8	55,9
14.00"	2601,0	2601,0	3920,0	3920,0	32,3	35,6
11 7/8"	3820,0	3820,0	4250,0	4250,0	27,4	29,8

Figure 5.1.3: Simulation set up for riser and casing for normal clearance

Drillstring:

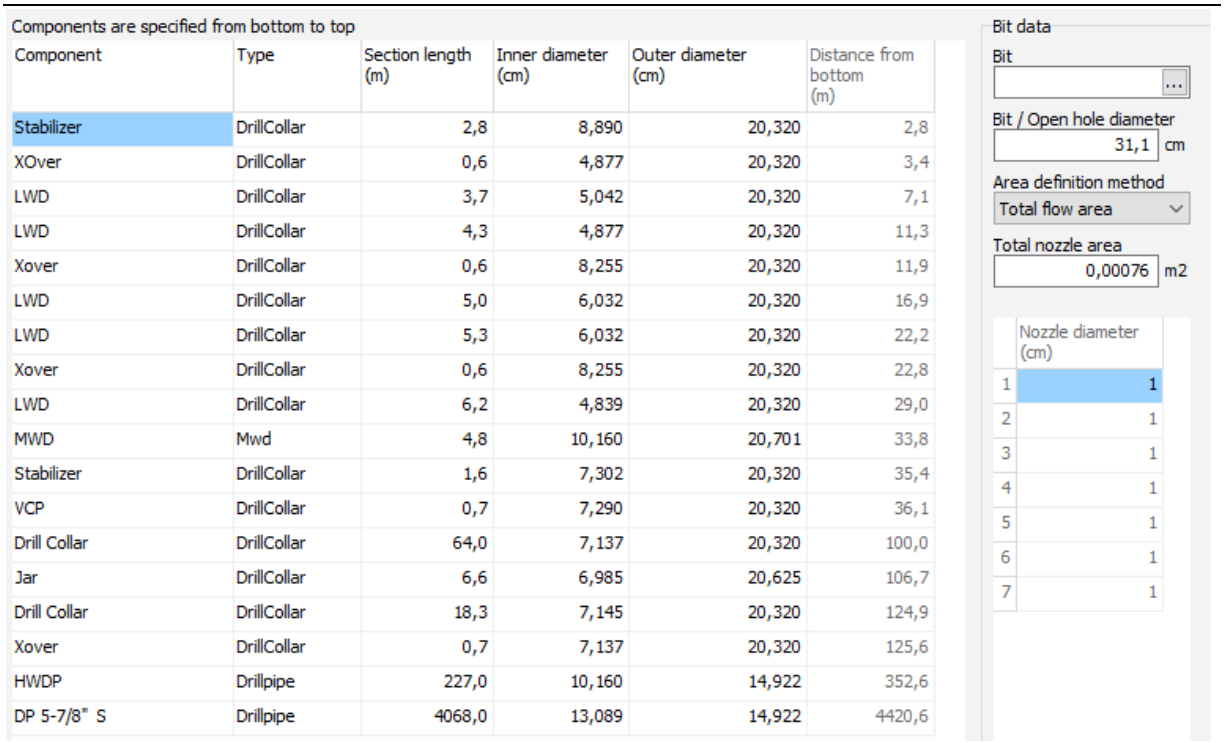

Components are specified from bottom to top

Component	Type	Section length (m)	Inner diameter (cm)	Outer diameter (cm)	Distance from bottom (m)
Stabilizer	DrillCollar	2,8	8,890	20,320	2,8
XOver	DrillCollar	0,6	4,877	20,320	3,4
LWD	DrillCollar	3,7	5,042	20,320	7,1
LWD	DrillCollar	4,3	4,877	20,320	11,3
Xover	DrillCollar	0,6	8,255	20,320	11,9
LWD	DrillCollar	5,0	6,032	20,320	16,9
LWD	DrillCollar	5,3	6,032	20,320	22,2
Xover	DrillCollar	0,6	8,255	20,320	22,8
LWD	DrillCollar	6,2	4,839	20,320	29,0
MWD	Mwd	4,8	10,160	20,701	33,8
Stabilizer	DrillCollar	1,6	7,302	20,320	35,4
VCP	DrillCollar	0,7	7,290	20,320	36,1
Drill Collar	DrillCollar	64,0	7,137	20,320	100,0
Jar	DrillCollar	6,6	6,985	20,625	106,7
Drill Collar	DrillCollar	18,3	7,145	20,320	124,9
Xover	DrillCollar	0,7	7,137	20,320	125,6
HWDP	Drillpipe	227,0	10,160	14,922	352,6
DP 5-7/8" S	Drillpipe	4068,0	13,089	14,922	4420,6

Figure 5.1.4: Simulation set up for Drillstring for normal clearance

Table 5.1.1: Drillbench simulation set-up

Simulation set-up	OD	ID	Clearance
Normal set-up	5,875”	11,875”	6”
Big Clearance set-up	2,375”	20”	17,625”

Figure 5.1.5 shows the well schematics in which gas (in yellow color) is migrating in a closed well from bottom through the annulus on the way to the wellhead. The yellow color code bar on the right side indicates the speed of the gas kick as it migrates in the well.

Wellbore fluids

- ✓ The well is filled with the fluids synthesized and characterized in section above.

Kick influx.

- ✓ In the physical experiments presented in section “Top close rig”, an air was used as a kick that was injected by pump. However, in this computer simulation well, both dry air and methane ware used as influx.

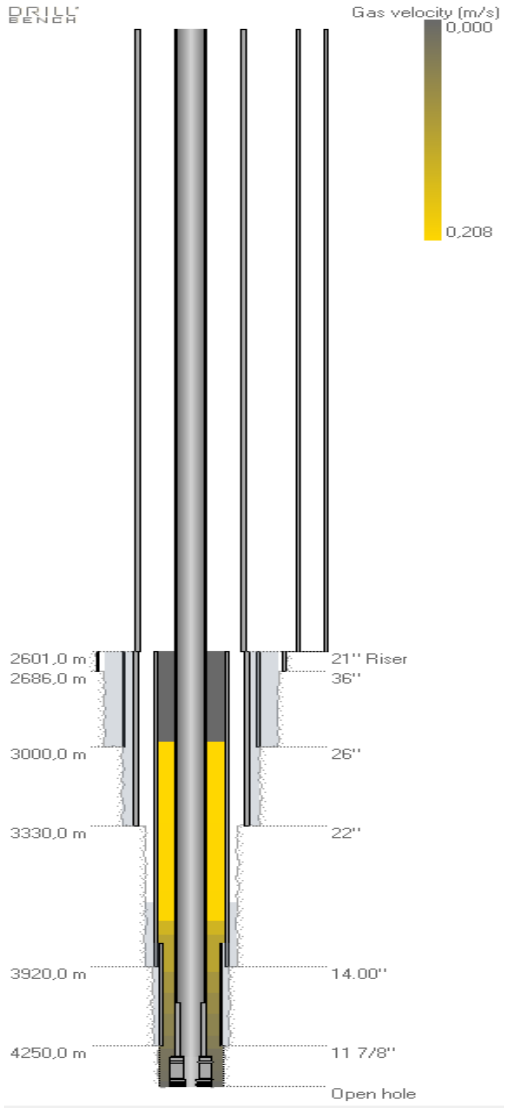

Figure 5.1.5: Simulation well schematics

5.2 Simulation results

The main target here is to study the wellhead build up phenomena, where the well is filled with the fluids systems formulated in section above and dry air/methane influxes. The simulation is conducted for various kick influx intensity and clearance, where $3m^3$ influx is received in the wellbore.

5.2.1 Effect of kick intensity and kick types on wellhead pressure

In this simulation, the kick intensity was varied in the range of 0.02- 0.10 sg. The magnitude of these values is due the difference between the reservoir pressure and the well pressure. The

higher the kick intensity is due to the higher-pressure difference. For this simulation, Fluid 11 is filled in the wellbore and Dry gas and Methane gas are influxes. Figure 5.2.1 shows the comparison results. As shown the well head pressure in methane influx wellbore is higher than in dry gas influx wellbore. The difference ranges from 11.3 to 2.5 bar.

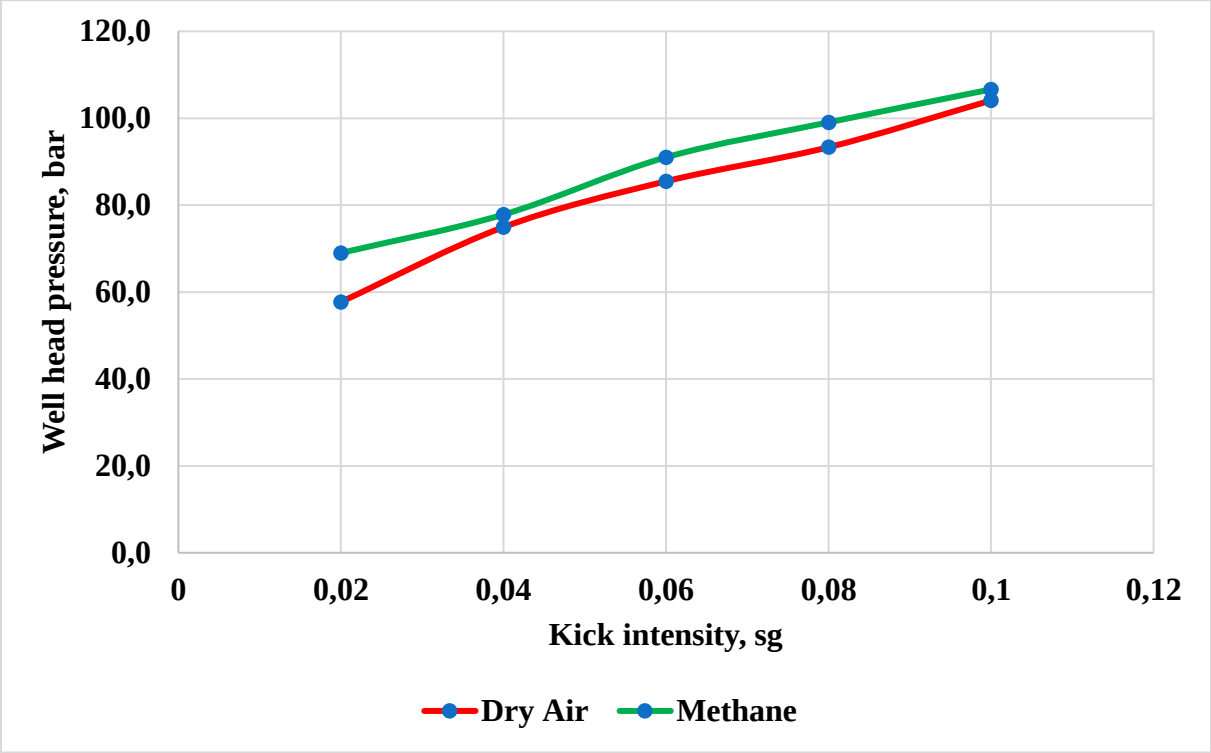

Figure 5.2.1: Fluid 11 Dynamics with Dry air and Methane as kick influx gas with different kick intensity

5.2.2 Effect of annular Clearance

The effect of annular clearance is studied by filling a well with Fluid 3. The first wellbore annular spacing is 5.875" OD x 11,875" ID Well ax, and the second wellbore annulus is 2.375" OD x 20"ID Well. In these two annular clearances, dry air was used as gas influx.

There is used wellbore size and drillstring size in the normal wellbore size that is realistic to offshore operations. In the big clearance wellbore operation, it is used unrealistic big clearance dimensions to demonstrate how kick dynamics react with bigger clearance and to compare to our physical exercise.

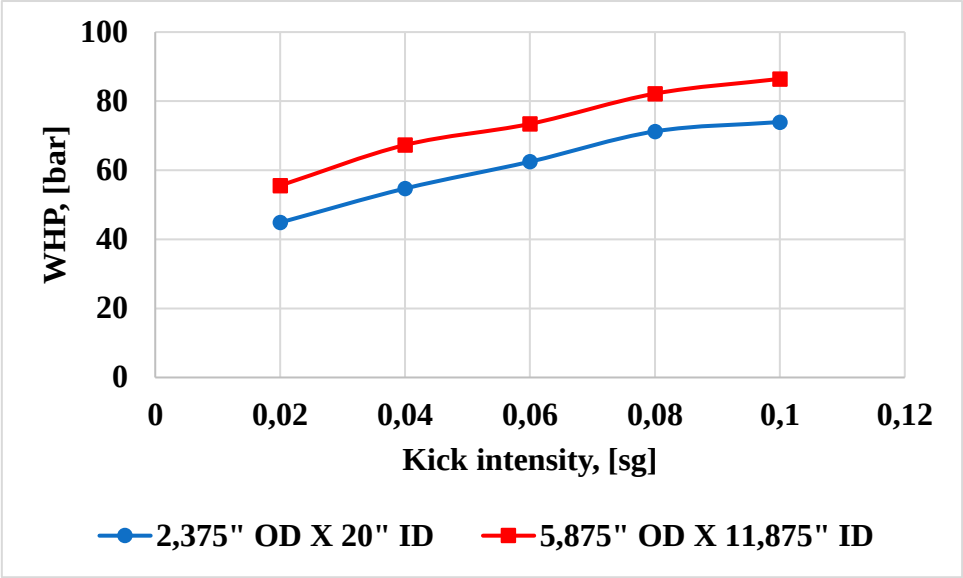

Figure 5.2.2: Well head pressure with different kick intensity for fluid 3 in regular clearance in annulus.

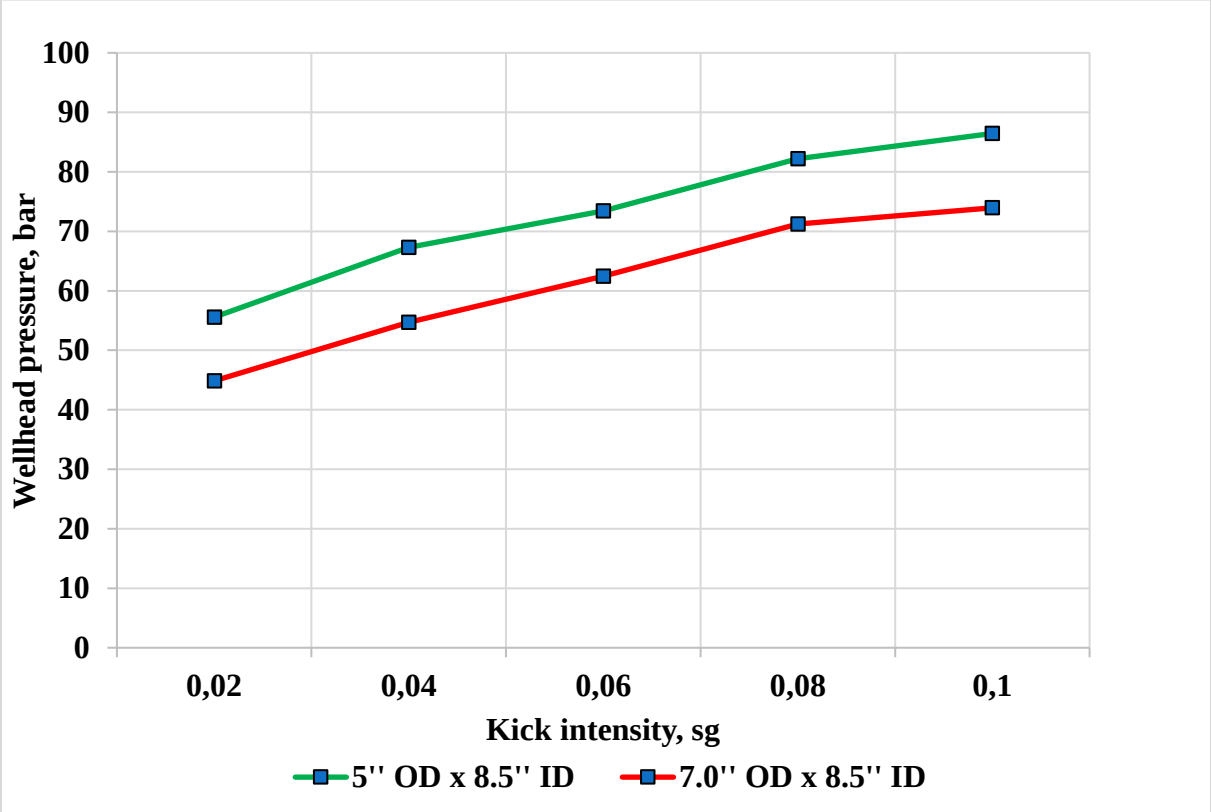

Figure 5.2.3: Well head pressure with different kick intensity for fluid 3 in regular clearance in annulus.

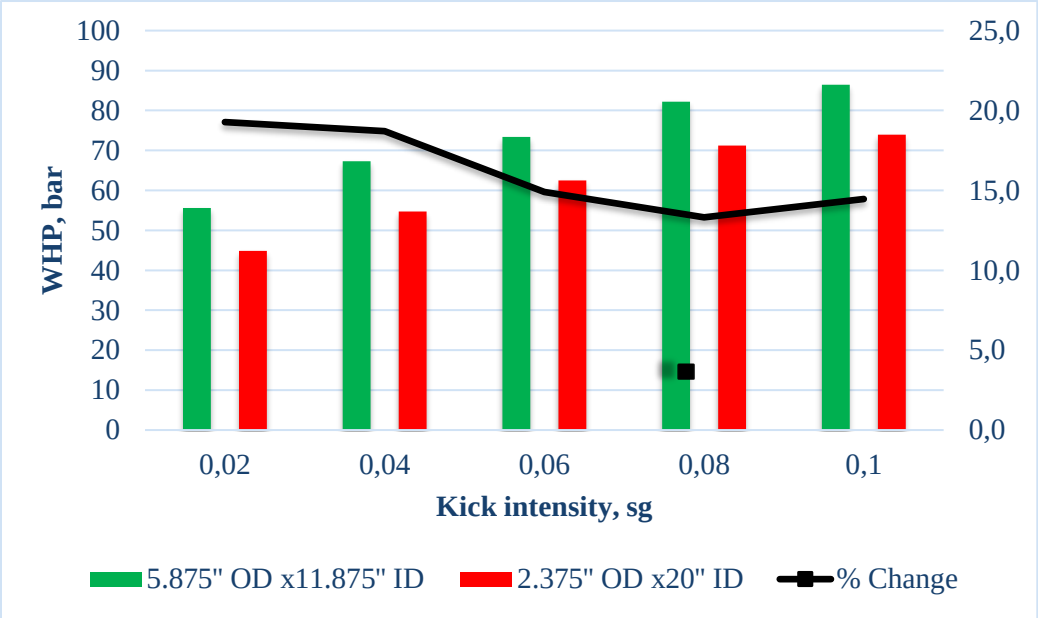

Figure 5.2.4: Fluid 3 with normal and big clearance

5.2.3 Effect of Methane vs Dry gas

Several methods for modification were examined in this thesis in Bubble velocity models. The density difference of the liquids and gas-kick has been taken into consideration in most formulas. Where many is conducted with density difference between fluid and gas. To studied how they really work the gas kick is tested with both dry air and methane gas. Due to a lack of data, there was no kick that reached the well head. Well head pressure was detected, but not when the kick landed on the well head.

Why wasn't it recorded?

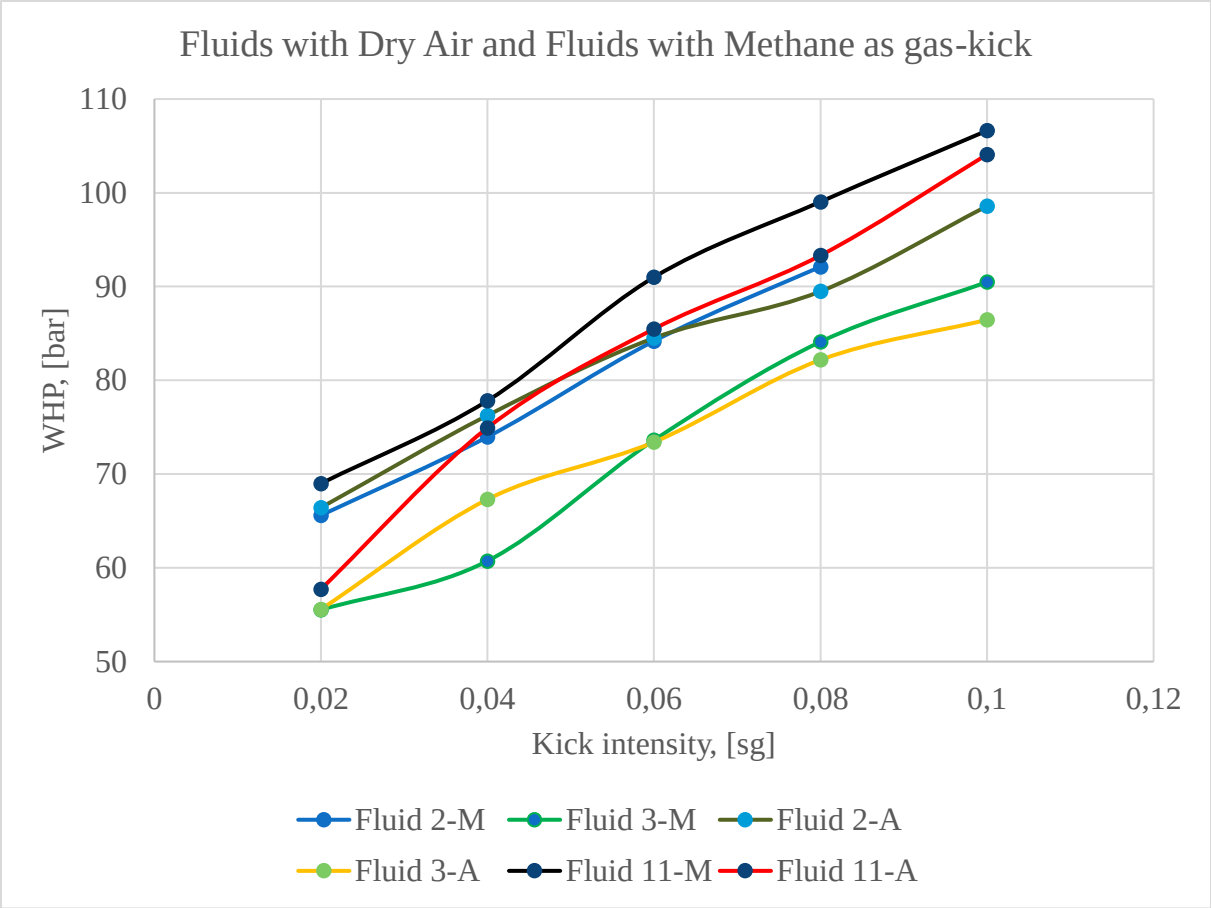

Figure 5.2.5: Compered Dry air and Methane gas with different kick intensity for fluid 2, 3, 8 and 11

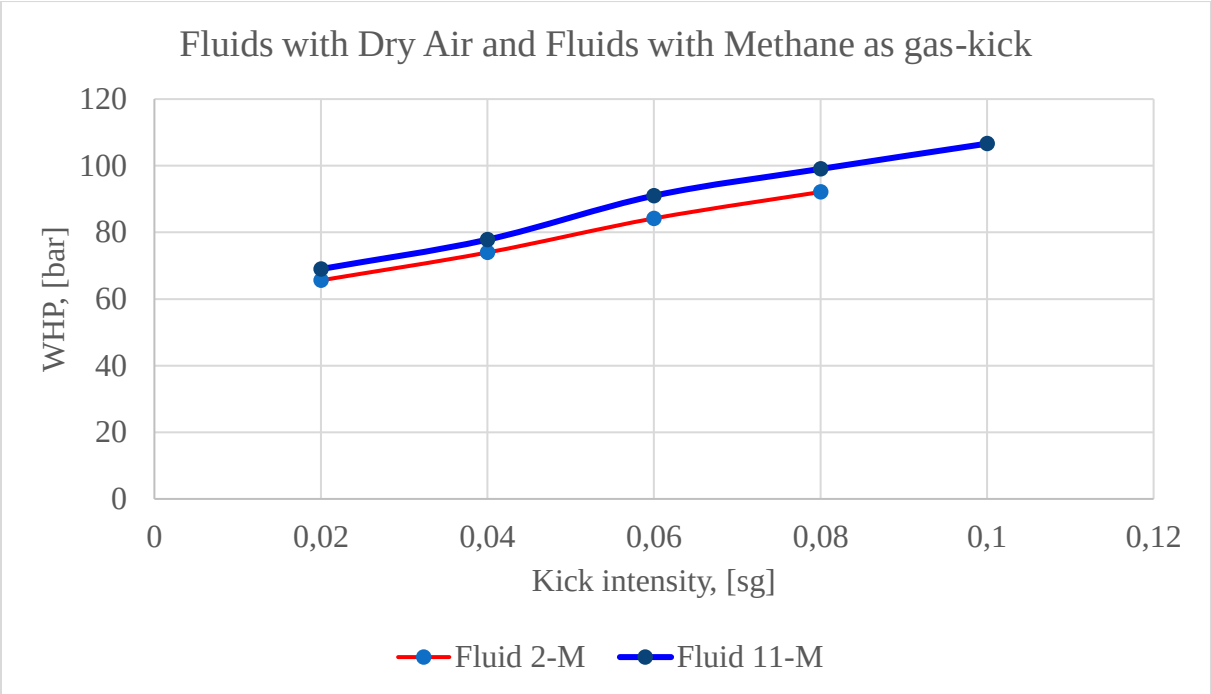

Figure 5.2.6: Compared Fluid 2 and Fluid 11 with Methane gas as injection

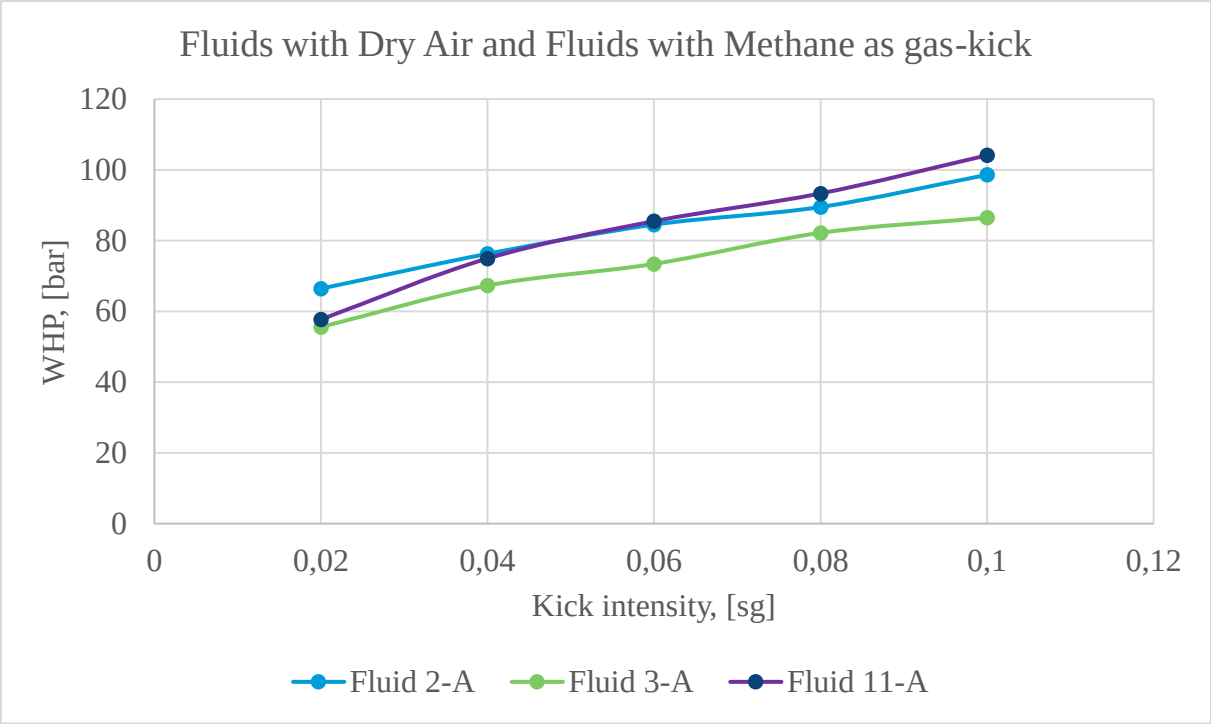

Figure 5.2.7: Compered Fluid 2,3 and 11 with dry gas as gas injection

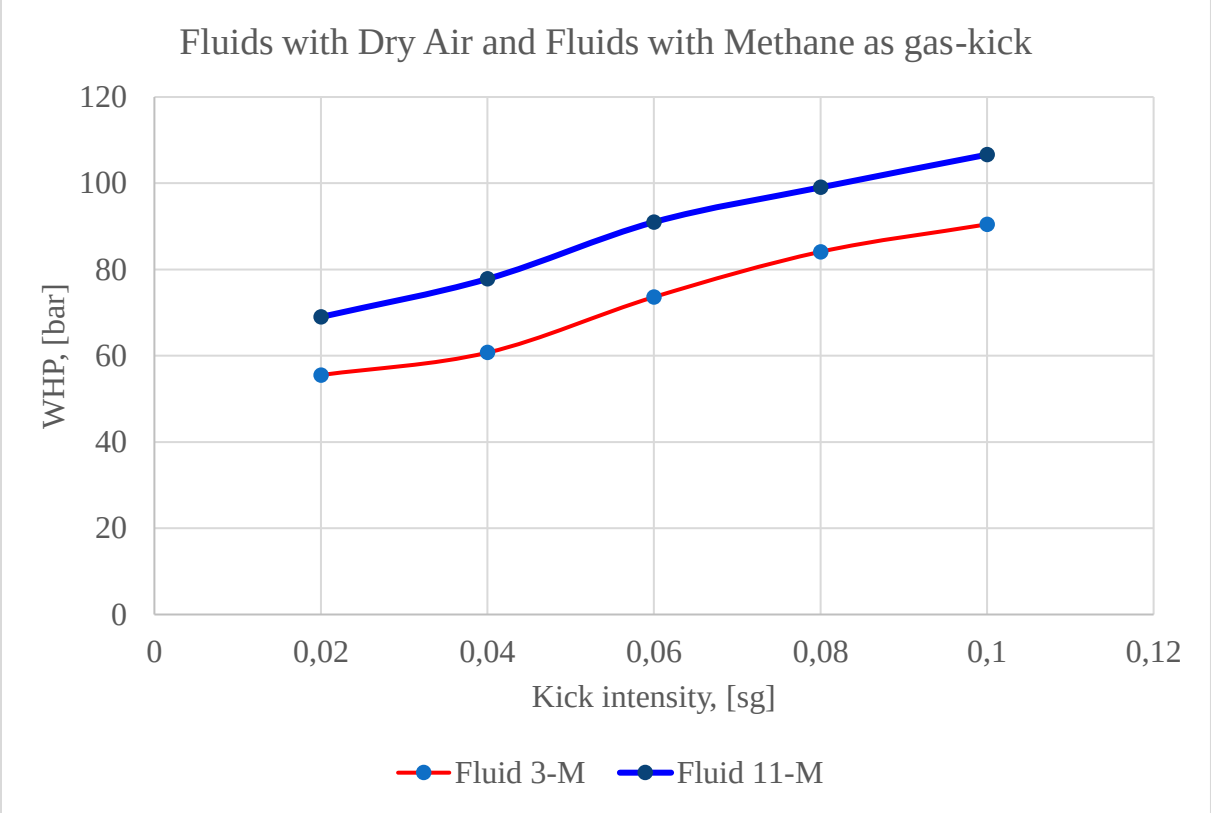

Figure 5.2.8: Compered Fluid 3 and 11 with Methane gas as gas injection

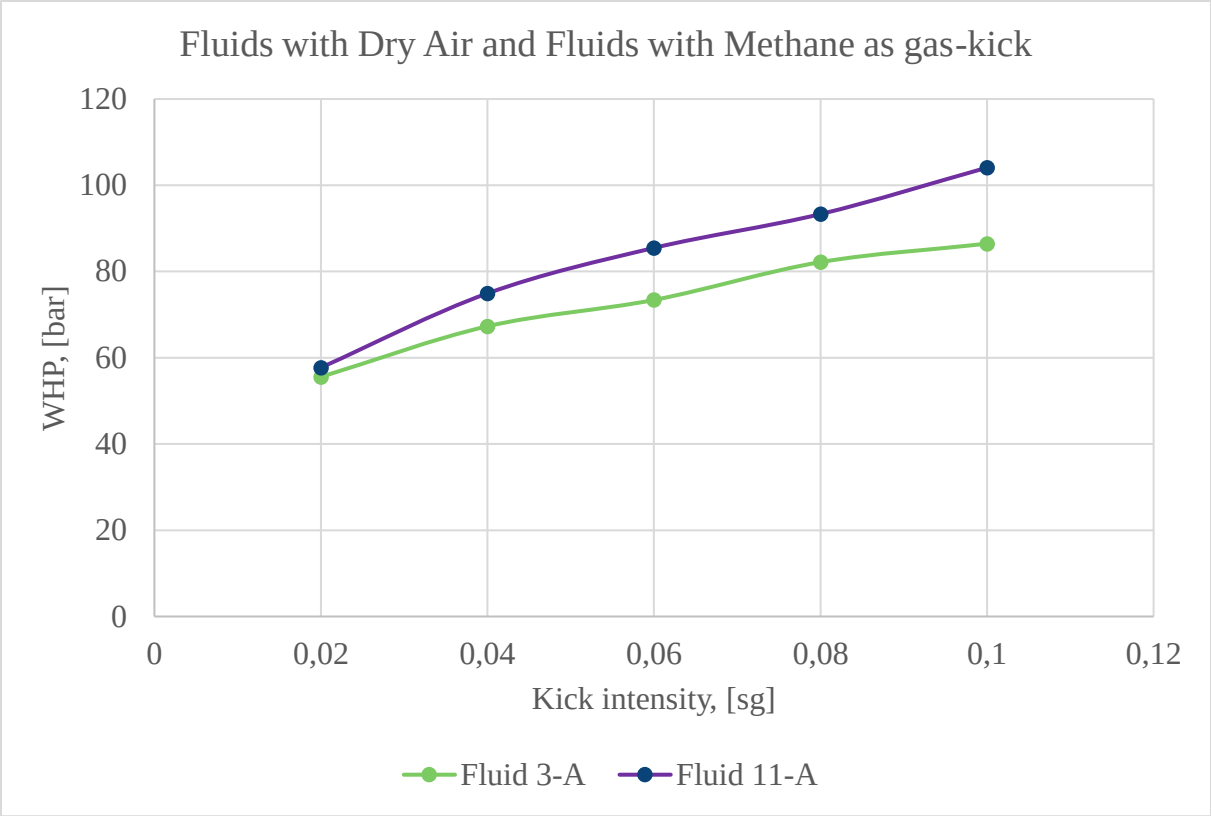

Figure 5.2.9: Compered Fluid 3 and 11 with Dry air as gas injection

From (Thea Hang Ngoc Tat, 2021) the effect of different suspension limits were conducted and studied. This studied show that when a gas volume percentage is lower than the limit of suspension, then the gas can be trapped in the fluid in the wellbore. For fluid 2 with methane as kick gas injection the kick were trapped in the well and the kick didn't go thru all the way up to the top of the well head.

From the other fluids with methane and dry gas as kick injection the WHP gets affected. The methane gas and dry air have different suspension reaction to the fluid and then the WHP will be different.

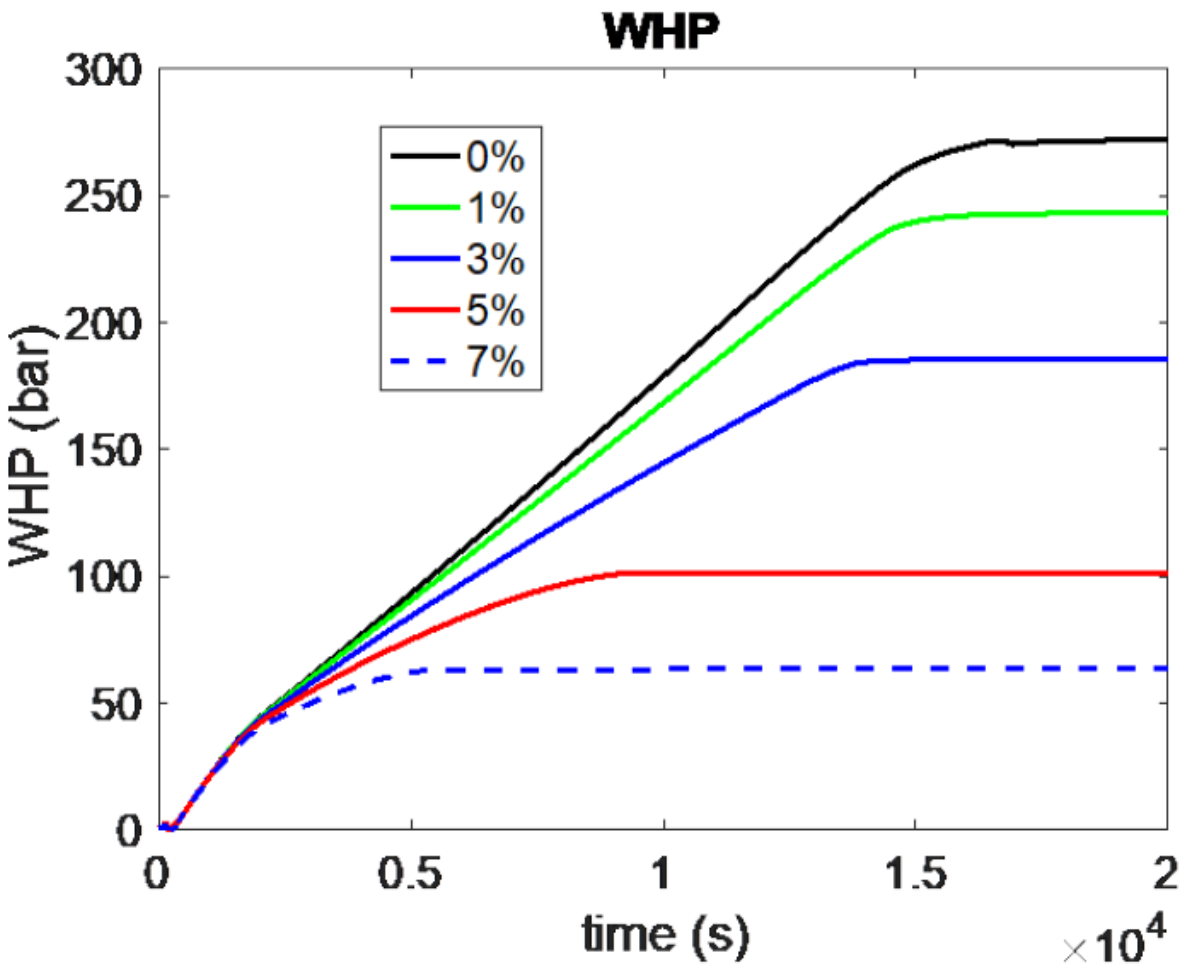

Figure 5.2.10: Pressure at BOP vs Time with different gas suspension in the fluid(Thea Hang Ngoc Tat, 2021)

6 Gas bubble speed modelling

6.1 Comparisons between gas bubble literature models and measurements

For the bubble speed prediction of the measured data, an equation derived by Li Zheng (Eq.above), wave equation (Eq.above) and Davies & Taylor equation (above) were used.

The reason for the selection of these models' comparison is that the models are a function of all the parameters that are available in the experimental well. The model considers the gas bubble and the well fluid properties such as viscosity, and densities.

Table 6.1.1: Measure data from physical testing

OD	ID	Fluid Density, [kg/m^3]	Air density, [kg/m^3]	Viscosity, [Pa*s]	Speed Measurements
Fluid 1					
30	25	1000	1,227	0,001	0,20247542
40	25	1000	1,227	0,001	0,21795146
50	25	1000	1,227	0,001	0,26047952
Fluid 2					
30	25	1000	1,227	0,006	0,15391043
40	25	1000	1,227	0,006	0,17578032
50	25	1000	1,227	0,006	0,20660383
Fluid 3					
30	25	1000	1,227	0,013	0,12747191
40	25	1000	1,227	0,013	0,1597186
50	25	1000	1,227	0,013	0,18476537
Fluid 4					
30	25	1170	1,227	0,0015	0,18682598
40	25	1170	1,227	0,0015	0,2084346
50	25	1170	1,227	0,0015	0,21984075
Fluid 5					
30	25	1180	1,227	0,0055	0,166
40	25	1180	1,227	0,0055	0,232
50	25	1180	1,227	0,0055	0,297
Fluid 6					
30	25	1020	1,227	0,0045	0,091
40	25	1020	1,227	0,0045	
50	25	1020	1,227	0,0045	
Fluid 7					
30	25	1020	1,227	0,0035	0,15329721
40	25	1020	1,227	0,0035	0,219
50	25	1020	1,227	0,0035	

Compare between all fluids

In Table 6.1.2 all fluids tested in the open well rig construction is represented. Three theoretical formulas were tested: The Li Zheng model, Wave equation and Davies and Taylor equation. The precent from the speed measurement and the theoretical formulas is also represented. The lower the percentage table shows, the better the formula works. The trend is also important here.

Table 6.1.2: Fluids Measure velocity from test and literature velocity from formulas, 15, 17 and 18

Clearance, [mm]	Speed Measurements	Li Zheng law	Wave analogy equation	Davies and	%Modified stokes	%Wave	%Davies and Taylor

				Taylor Equation			
Fluid 1							
2,5	0,20247542	3,402	61,237	0,157	1580,2	30144,3	-22,7
7,5	0,21795146	30,619	551,135	0,271	13948,4	252770,7	24,4
12,5	0,26047952	85,052	1530,932	0,350	32552,0	587635,9	34,4
Fluid 2							
2,5	0,15391043	0,567	10,206	0,157	268,4	6531,3	1,7
7,5	0,17578032	5,103	91,856	0,271	2803,1	52156,1	54,2
12,5	0,20660383	14,175	255,155	0,350	6761,1	123399,8	69,4
Fluid 3							
2,5	0,12747191	0,262	4,711	0,157	105,3	3595,4	22,8
7,5	0,1597186	2,355	42,395	0,271	1374,6	26443,6	69,7
12,5	0,18476537	6,542	117,764	0,350	3440,9	63637,0	89,4
Fluid 4							
2,5	0,18682598	2,654	47,774	0,157	1320,6	25471,2	-16,2
7,5	0,2084346	23,887	429,962	0,271	11360,1	206181,7	30,1
12,5	0,21984075	66,352	1194,340	0,350	30081,9	543175,0	59,2
Fluid 5							
2,5	0,166	0,730	13,141	0,157	340,7	7832,6	-5,5
7,5	0,232	6,570	118,266	0,271	2734,9	50927,6	17,0
12,5	0,297	18,251	328,516	0,350	6037,9	110381,8	17,7
Fluid 6							
2,5	0,091	0,771	13,881	0,157	746,9	15143,6	71,9
7,5		6,940	124,927	0,271			
12,5		19,279	347,020	0,350			
Fluid 7							
2,5	0,15329721	0,991	17,847	0,157	546,8	11541,9	2,1
7,5	0,219	8,923	160,620	0,271	3972,3	73202,2	23,7

Table 6.1.3: Fluids Measure velocity from test and literature velocity from formulas, 19 and 20

Clearance, [mm]	Speed Measurments	Slug flow regime	Harmathy's Equation	%Slug flow	%Harmathy's equation
Fluid 1					
2,5	0,20247542	0,236	0,254	16,367	25,3
7,5	0,21795146	0,259	0,254	18,754	16,4
12,5	0,26047952	0,280	0,254	7,684	-2,6
Fluid 2					
2,5	0,15391043	0,236		53,085	64,9
7,5	0,17578032	0,259		47,244	44,3
12,5	0,20660383	0,280		35,765	22,8
Fluid 3					
2,5	0,12747191	0,236		84,836	99,1
7,5	0,1597186	0,259		62,051	58,9
12,5	0,18476537	0,280		51,812	37,3

Fluid 4					
2,5	0,18682598	0,236		26,126	30,6
7,5	0,2084346	0,259		24,187	17,1
12,5	0,21984075	0,281		27,602	11,0
Fluid 5					
2,5	0,166	0,236		42,247	47,0
7,5	0,232	0,259		11,685	5,0
12,5	0,297	0,281		-5,659	-18,1
Fluid 6					
2,5	0,091	0,236		158,750	177,3
7,5					
12,5					
Fluid 7					
2,5	0,15329721	0,236		53,700	64,7
7,5	0,219	0,259		18,122	15,2

In

Table 6.1.3 the slug flow regime and the Harmathy's equation is represented with the percentage of the equation and the measure results. The Harmathy's equation uses gravity, density for liquid and gas and interfacial tension. The interfacial tension was not measured, but data from (Thea Hang Ngoc Tat, 2021) were used for water-air tension.

The slug flow regime doesn't use interfacial tension but have the same parameters and clearance as well. This formula still doesn't have viscosity measurements like the three other formulas.

The measurements data from the experiments is use in the result and then used to make an empirical model.

For modelling for the open wellbore simulation, the modified formula of Stokes law for terminal velocity is used. The key to make this work for this simulation is to find a curration factor to generate the correct model.

This is how it look like:

$$v_b = \mathrm{C} \cdot \frac{g d^2 (\rho_f - \rho_{air})}{18\mu} \qquad 24$$

Where:

- V_b = Velocity of bubbles, [m/s]
- C = Curalation factor, [-]
- g = gravity, [m/s^2]
- d = diameter, [m]
- ρ_{air} = density of air, [kg/m^3]
- ρ_f = density of fluid, [kg/m^3]
- μ = viscosity, [kg/m*s] or [Pa*s]

To make the Correlation factor for this model and see how the model works in a real physical simulation, then

The measurements data from the experiments are used in the result and then used to make an empirical model

For modeling for the open wellbore simulation, the modified formula of Stokes law for terminal velocity is used. The key to making this work for this simulation is to find a curation factor to generate the correct model.

This is how it will look like:

$$v_b = \mathrm{C} \cdot \frac{g d^2 (\rho_f - \rho_{air})}{18\mu} \qquad 25$$

Where:

- V_b = Velocity of bubbles, [m/s]
- C = Curalation factor, [-]
- g = gravity, [m/s^2]
- d = diameter, [m]
- ρ_{air} = density of air, [kg/m^3]
- ρ_f = density of fluid, [kg/m^3]
- μ = viscosity, [kg/m*s] or [Pa*s]

To make the Curation factor for this model and see how the model works in a real physical simulation, then the stoke formula is used to force theoretical values and then the value of velocity is divided.

The graph under shows the correlation factor vs the clearance to show how well this formula is respected on the simulated well.

The velocity of bubbles in wellbore theoretical formula:

$$v_b = \frac{g \cdot (0{,}5 \cdot (OD - ID)^2 \cdot (\rho_f - \rho_{air})}{18 \cdot \mu} \quad 26$$

Where:

- V_b = Velocity of bubbles, [m/s]
- g = gravity, [m/s^2]
- OD = inner diameter of inner tube, [m]
- ID = outer diameter of inner tube, [m]
- ρ_f = density of fluid, [kg/m^3]
- ρ_{air} = density of air in bubbles, [kg/m^3]
- μ = viscosity of fluid, [kg/m*s] or [Pa*s]

6.2 Correlation factor development

Correlation factor:

$$C = \frac{v_b(theoretical)}{v_b(experimental)} \quad 27$$

Where:

- C = correlation factor, [-]
- V_b(theoretical) = Velocity of bubbles from theoretical formula, [m/s]
- V_b(experimental) = Velocity of bubbles from experimental exercise, [m/s]

As a closer, the correlation factor is to 1 the better is the formula. As shown in the graph under, the correlation factor is low, and it is important to look at the dynamics in the bubble/slug and not only the velocity and the different parameters in the formula. The polymers act differently

with many same parameters, but the standard trend is the same. Higher viscosity tends to lower the velocity, lower density tends to lower the velocity and a higher value of the clearance tends to higher velocity of the bubbles in the same type of fluid (brine, Carbopol fluid, bentonite fluid). Starting speed from pump influx at the bottom of the system is meant to be the same but can be different from system to system. Counterforce from the walls from the pipe is also an important factor to take in place. The Counterforce and friction have been tried to minimize and the same material I use in every exercise to better compare. Below are the theoretical formulas with correlation factor vs Clearance for all fluids in the graphs and correlation factor equation and the R^2 in the tables. In the correlation factor equation the y is correlation factor and x is clearance.

Li Zheng model:

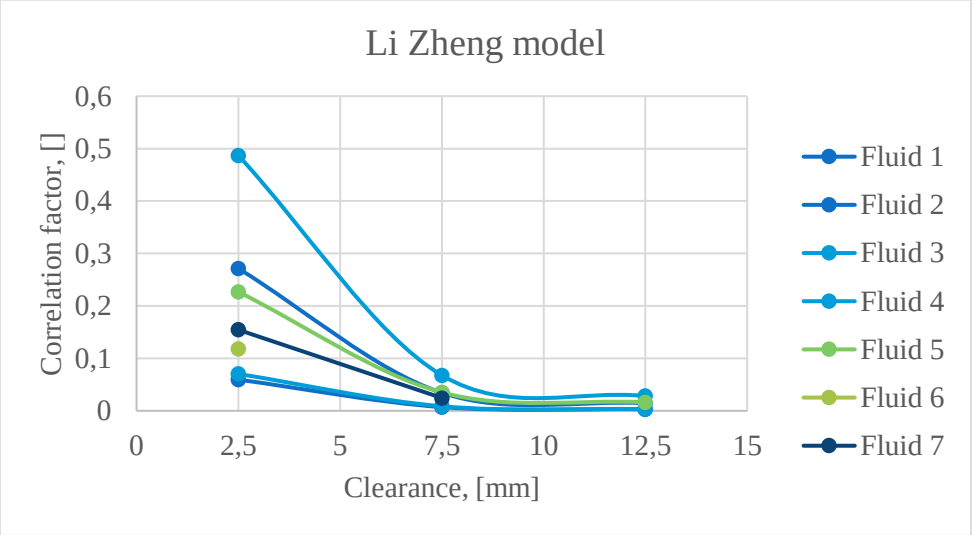

Figure 6.2.1: Li Zheng correlation factor vs clearance for Fluid 1-7

Table 6.2.1 Li Zheng model with Correlation factor and R^2

Li Zheng model		
Fluid	C-factor	R^2
Fluid 1	$y = 0{,}001x^2 - 0{,}0201x + 0{,}1038$	1
Fluid 2	$y = 0{,}0043x^2 - 0{,}0908x + 0{,}4714$	1
Fluid 3	$y = 0{,}0076x^2 - 0{,}1598x + 0{,}8391$	1

Fluid 4	$y = 0{,}0011x^2 - 0{,}0236x + 0{,}1223$	1
Fluid 5	$y = 0{,}0035x^2 - 0{,}0729x + 0{,}3875$	1
Fluid 6		
Fluid 7	$y = -0{,}026x + 0{,}2196$	1

Wave Equation:

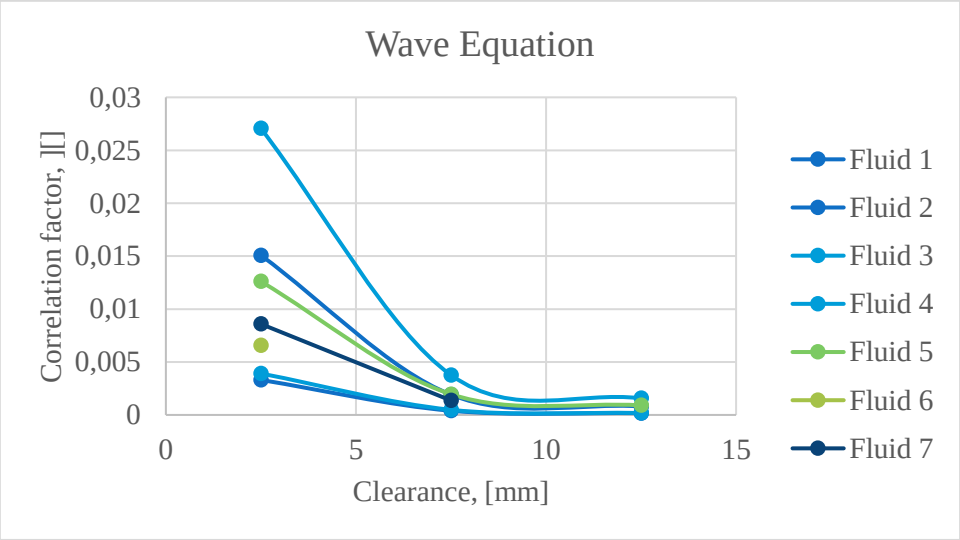

Figure 6.2.2: Wave equation correlation factor vs clearance for Fluid 1-7

Table 6.2.2: Wave equation with Correlation factor and R^2

Wave Equation		
Fluid	C-factor	R^2
Fluid 1	$y = 5E\text{-}05x^2 - 0{,}0011x + 0{,}0058$	1
Fluid 2	$y = 0{,}0002x2 - 0{,}005x + 0{,}0262$	1
Fluid 3	$y = 0{,}0004x^2 - 0{,}0089x + 0{,}0466$	1
Fluid 4	$y = 6E\text{-}05x^2 - 0{,}0013x + 0{,}0068$	1
Fluid 5	$y = 6E\text{-}05x^2 - 0{,}0013x + 0{,}0068$	1
Fluid 6		
Fluid 7	$y = 6E\text{-}05x^2 - 0{,}0013x + 0{,}0068$	1

Davies and Taylor Equation:

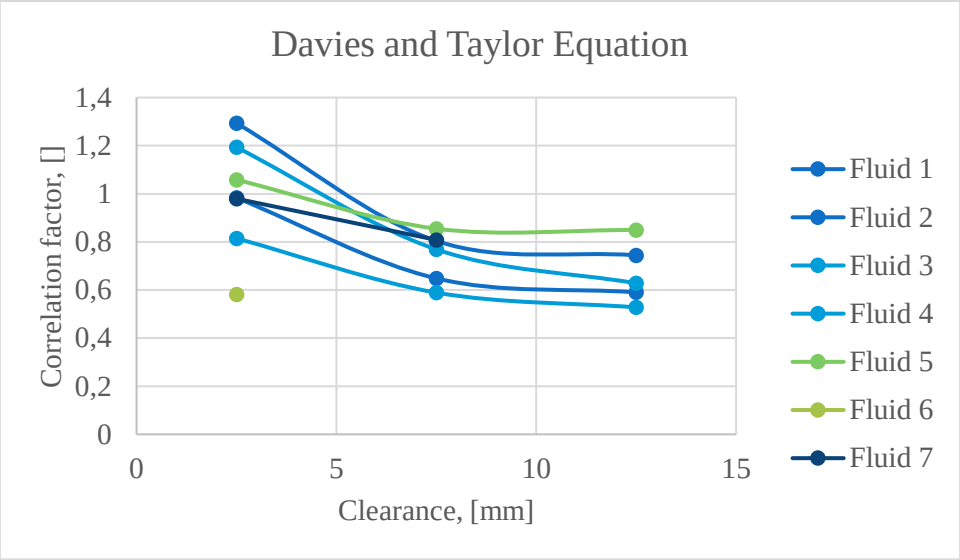

Figure 6.2.3: Davies and Taylor equation correlation factor vs clearance for Fluid 1-7

Table 6.2.3: Davies and Taylor Equation with correlation factor and R^2

Davies and Taylor Equation		
Fluid	C-factor	R^2
Fluid 1	$y = 6E\text{-}05x^2 - 0{,}0013x + 0{,}0068$	1
Fluid 2	$y = 0{,}0055x^2 - 0{,}1224x + 1{,}2547$	1
Fluid 3	$y = 0{,}0033x^2 - 0{,}0779x + 0{,}9886$	1
Fluid 4	$y = 0{,}0057x^2 - 0{,}1418x + 1{,}5125$	1
Fluid 5	$y = 0{,}004x^2 - 0{,}0803x + 1{,}2343$	1
Fluid 6		
Fluid 7	$y = -0{,}0342x + 1{,}065$	1

Slug flow regime:

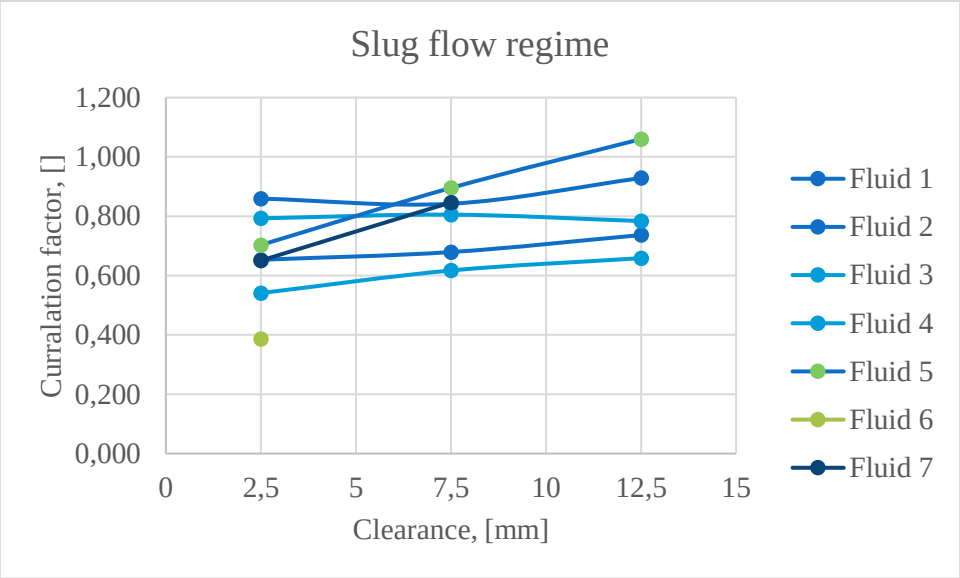

Figure 6.2.4: Slug flow correlation factor vs clearance for Fluid 1-7

Table 6.2.4: Slug flow regime with correlation factor and R^2

Slug flow regime		
Fluid	C-factor	R^2
Fluid 1	$y = 0{,}0021x^2 - 0{,}0242x + 0{,}9069$	1
Fluid 2	$y = 0{,}0006x^2 - 0{,}0011x + 0{,}6521$	1
Fluid 3	$y = -0{,}0007x^2 + 0{,}0221x + 0{,}4901$	1
Fluid 4	$y = -0{,}0007x^2 + 0{,}0093x + 0{,}774$	1
Fluid 5	$y = -0{,}0006x^2 + 0{,}044x + 0{,}5964$	1
Fluid 6		
Fluid 7	$y = 0{,}0392x + 0{,}5526$	1

Harmathy's Equation:

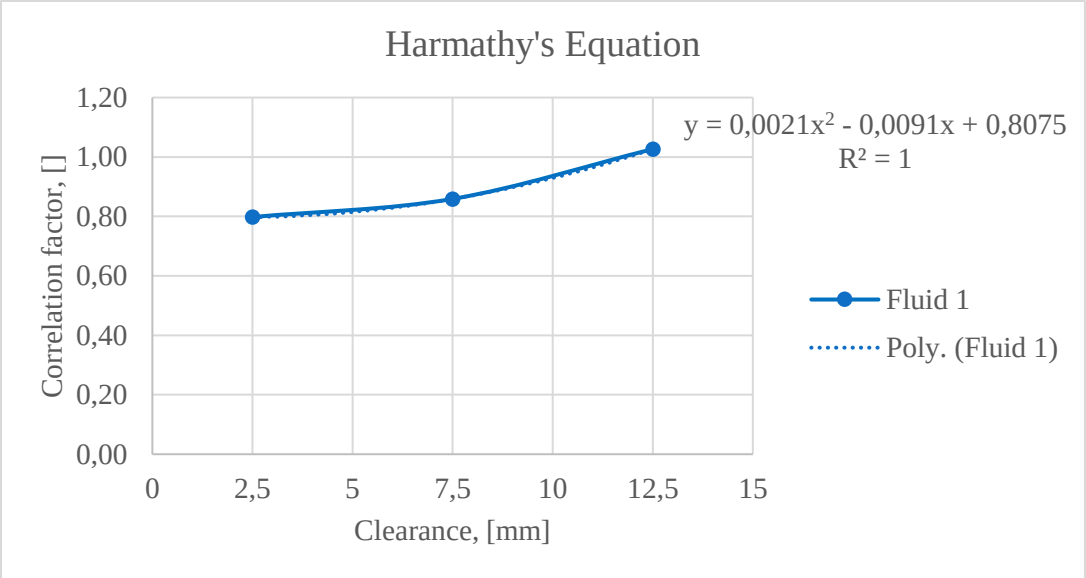

Figure 6.2.5: Harmathy's equation correlation factor vs clearance for Fluid 1-7

Table 6.2.5: Harmathy's Equation with Correlation factor and R^2

Harmathy's Equation		
Fluid	C-factor	R^2
Fluid 1	$y = 0{,}0021x^2 - 0{,}0091x + 0{,}8075$	1

7 Summary and discussion

After many experiments with many types of drilling fluid that have been searched and tested, one can conclude with the following:

1. Large diameter in a gas condition gives greater speed (large clearance in the annulus)

- From experiments with 3 different annulus sizes, the same trend in all experiments was that a larger annulus and thus a larger surface on the slug / bubble gave greater speed.

2. Larger Low shield yield stress gives lower speed.

- Generally larger viscosity measurements gave less kick speed up to Well head.

3. Higher kick intensity gives higher Well head pressure and faster time until pit gain is filled

- By looking at the graphs of Fluid Compare Well head finish pressure and Fluid Compare time to fill up pit gain 3m ^ 3 which is a summary of all the liquids run through the

program drillbench so there is a good connection between all attempts and that higher kick intensity provides higher Well head pressure and shorter time to fill up pit gain. Here in the graphs are all the experiments with the same size of well and drill pipe and there is the same pit gain volume (3m ^ 3).

4. Lighter and less viscous liquids fill up pit gain faster than heavier and viscous liquids.

- The liquid that took the longest time to fill up the pit gain was not the thinnest liquid, but the liquid that was most viscous.

All tests with fluid in room temperate. The next test experiment can be tested with different temperatures to see if the pressure build-up will increase or decrease. The same with velocity to see if it will increase or decrease. Results obtained from an open hole rig show that the speed of the bubbles bubble depends on the fluids' fluids properties (viscosity, density) and the annular clearance.

The 6 Fluid all represented the Stokes formula very well especially from the 40/25 and 50/25 diameter tubes with very small correlation factor. As mentioned, the brine vs water fluid comparison in the open wellbore simulation for velocity vs density with 30, 40 and 50mm outer diameter and 25mm inner diameter tube, shows at first glance that density affect the velocity with higher density will give lower velocity. Just to look at the graph, this can lie, but if you look at the viscosity measurements on brine, you must take that into account. According to stokes low, the viscosity has a lot to say to the velocity and consider the density that increases with salt injection in the water that forms brine and higher density.

More clearance in the annulus or bigger diameter of the outer tube (inner tube is constant) has also a big identification for that the formula works in practice.

The slug and bubbles in all fluids, except the bentonite mud, have the same dynamics from bottom to top of the borewell. Regardless of whether the density, viscosity, or diameter of the pipe changes. There are no splits of the slug, there are bubbles that have nearly the same velocity of the slug if there are tail-bubbles and if the bubbles are small, they will not merge with the slug. In the bentonite mud there were a big dynamic change where the slug split and had to fight the fluid to reach the top of the well. Then the velocity dropped significantly when this occurs. To compare this liquid with the others, it is important to take this into account when the dynamics of the bubble / slug changes so much.

Therefore, the same viscosity, density of the liquid and the same diameter of the pipe can give different results in the end with different particles and polymer in the mud.

Open well experiment:

Gas bubbles velocity depends on the rheological parameters including density and viscosity. It also depends on annular wellbore clearance. The gas bubbles require correlation factor. The bubble and slug test determined that small bubbles have lower velocity than big bubbles. Slugs have higher velocity than big and small bubbles. Small bubbles in tail formation behind slugs have almost the same velocity as slugs. The diameter (Clearance) for the slugs/bubbles has the most influence for velocity in condition of the size of the slugs/bubbles. Length and volume have also an influence, but the diameter and the surface area have the biggest influence on speed. This is logical combined with the buoyancy force up and downwards. For the density, as higher density value and weighted polymer added to the fluid, the viscosity also increased. Comparing heavier and low-density fluids with almost the same viscosity, it shows that heavier density mud, the bubble/slug velocity increased.

The viscosity measurements shows that both, plastic viscosity, Yield Stress and Low Shear yield stress all had an increase in this value had a decrease in velocity.

Closed well experiment:

Well head pressure depends on rheological parameters, kick influx and annular clearance. The dynamic measurements shows that WHP reduces 8-10% from the BHP.

Drillbench shows trends where methane had higher WHP vs Dry air as kick influx gas with same kick intensity. Especially with higher kick intensity. The reason for this is higher saturation and density of the gas vs fluid. Drillbench also shows that low annular clearance had high WHP vs bigger annular clearance.

Table 6.2.1: Summary of fluids type, Clearance in annulus, Rheology, and measured velocity

Bubble type	Clearance, [mm]		Drilling Fluid	Fluid rheology						
Bubble type	Outer radius	Inner Radius	Liquid	yield Point, lb/100sqft	Plastic Viscosity, cp	LSYS, lb/100sqft	Liquid density, sg	n	k	Bubble velocity, m/s

bubble	30	25	water	0,000	1,000	0,000	1,000	1,000	1,000	0,187
slug			water	0,000	1,000	0,000	1,000	1,000	1,000	0,218
Avg			water	0,000	1,000	0,000	1,000	1,000	1,000	0,202
bubble	40		water	0,000	1,000	0,000	1,000	1,000	1,000	0,197
slug			water	0,000	1,000	0,000	1,000	1,000	1,000	0,239
Avg			water	0,000	1,000	0,000	1,000	1,000	1,000	0,218
bubble	50		water	0,000	1,000	0,000	1,000	1,000	1,000	0,232
slug			water	0,000	1,000	0,000	1,000	1,000	1,000	0,289
Avg			water	0,000	1,000	0,000	1,000	1,000	1,000	0,260
bubble	30		Water+2,5cp	3,000	6,000	0,500	1,000	0,737	0,091	0,120
slug			Water+2,5cp	3,000	6,000	0,500	1,000	0,737	0,091	0,188
Avg			Water+2,5cp	3,000	6,000	0,500	1,000	0,737	0,091	0,154
bubble	40		Water+2,5cp	3,000	6,000	0,500	1,000	0,737	0,091	0,129
slug			Water+2,5cp	3,000	6,000	0,500	1,000	0,737	0,091	0,223
Avg			Water+2,5cp	3,000	6,000	0,500	1,000	0,737	0,091	1,176
bubble	50		Water+2,5cp	3,000	6,000	0,500	1,000	0,737	0,091	0,155
slug			Water+2,5cp	3,000	6,000	0,500	1,000	0,737	0,091	0,258
Avg			Water+2,5cp	3,000	6,000	0,500	1,000	0,737	0,091	0,207
bubble	30		Water+30cp	8,500	13,000	1,500	1,000	0,682	0,306	0,087
slug			Water+30cp	8,500	13,000	1,500	1,000	0,682	0,306	0,167
Avg			Water+30cp	8,500	13,000	1,500	1,000	0,682	0,306	0,127
bubble	40		Water+30cp	8,500	13,000	1,500	1,000	0,682	0,306	0,110
slug			Water+30cp	8,500	13,000	1,500	1,000	0,682	0,306	0,209
Avg			Water+30cp	8,500	13,000	1,500	1,000	0,682	0,306	0,160
bubble	50		Water+30cp	8,500	13,000	1,500	1,000	0,682	0,306	0,149
slug			Water+30cp	8,500	13,000	1,500	1,000	0,682	0,306	0,220
Avg			Water+30cp	8,500	13,000	1,500	1,000	0,682	0,306	0,185
bubble	30		Brine	1,500	1,200	0,500	1,170	0,637	0,051	0,172
slug			Brine	1,500	1,200	0,500	1,170	0,637	0,051	0,202
Avg			Brine	1,500	1,200	0,500	1,170	0,637	0,051	0,187
bubble	40		Brine	1,500	1,200	0,500	1,170	0,637	0,051	0,184
slug			Brine	1,500	1,200	0,500	1,170	0,637	0,051	0,233
Avg			Brine	1,500	1,200	0,500	1,170	0,637	0,051	0,208
bubble	50		Brine	1,500	1,200	0,500	1,170	0,637	0,051	0,189
slug			Brine	1,500	1,200	0,500	1,170	0,637	0,051	0,251
Avg			Brine	1,500	1,200	0,500	1,170	0,637	0,051	0,220
slug	30		Bentonite 1	4,000	4,500	2,500	1,020	0,613	0,186	0,091
slug	30		Bentonite 2	4,000	3,500	1,000	1,020	0,552	0,240	0,153
slug	40		Bentonite 3	4,000	3,500	1,000	1,020	0,552	0,240	0,219
slug	30		Modified mud	9,000	5,500	2,500	1,180	0,464	0,805	0,166
slug	40		Modified mud	9,000	5,500	2,500	1,180	0,464	0,805	0,232
slug	50		Modified mud	9,000	5,500	2,500	1,180	0,464	0,805	0,297

7.1 Summary of top open rig experimental works

Table 7.1.1: Summary of

Type	Clearance	Drilling fluid	Fluid rheology					Density	Velocity
			n	k	PV	LSYS	YS		
Small Bubbles	30x25	Water	1	1	1	0	0		
	40x25								
	50x25								
Slug	30x25	2.5 cP							
	40x25								
	50x25								

From experimental studies the velocity is affected of density, viscosity, and clearance. From these formulas will the open rig simulations velocity and the measure data be compared and the positive and negative effect of these models to calculate the velocity of the slug in the annulus. All formulas use density and gravity.

Table 7.1.2: Compare theoretical models

Models	Positive	Negative
Li Zheng model	-uses Viscosity, density, and clearance - A trend from viscosity, density and clearance between measure velocity and result - - -	- extremely large discrepancy in percent between measure result and calculated result 3500-543 000% - - -
Wave Equation	-Uses density, Clearance, and viscosity -18 times smaller result than Li Zheng equation - -	-large discrepancy in percent between measure result and calculated result 100-30 000% - -
Davies and Taylor Equation	-Density and Clearance -Great trend with clearance	-doesn't use viscosity -bad trend with wiscous fluid - -

	-Okey discrepancy in percent between measure result and calculated result -22-89% - -	-
Slug flow Regime	-uses density and clearance -Great trend with clearance -Good discrepancy percent between measure result and calculated result with -5-160% -great result for Newtonian fluid - - -	-doesn't use viscosity -bad connection between real result whe -worst result for more viscous fluds compared to smaller and Newtonian fluid. - - -
Harmathy's Equation	-uses density -uses interfacial/surface tension -Good discrepancy percent between measure result and calculated result with -3-25% -great result for fluid 1, water Newtonian fluid -	-don't use viscosity and clearance -Bad trend for viscosity and clearance -Didn't have interfacial tension so could only register for fluid 1 with water - - - -

Compare Fluid 1 and Fluid 3 with different theoretical models :

Clearance, [mm]	Speed Measurments	%Li Zheng	%Wave	%Davies and Taylor	%Slug flow	%Harmaty's equation
Fluid 1						
2,5	0,202	1580	30144	-22,702	16,367	25,316
7,5	0,218	13948	252771	24,377	18,754	16,418
12,5	0,260	32552	587636	34,354	7,684	-2,589
Fluid 3						
2,5	0,127	105	3595	22,779	84,836	
7,5	0,160	1375	26444	69,724	62,051	
12,5	0,185	3441	63637	89,410	51,812	

Clearance, [mm]	Speed Measurments	Li Zheng	Wave	Davies and Taylor	Slug flow	Harmaty's equation
Fluid 1						
2,5	0,202	3,40	61,24	0,16	0,236	0,254
7,5	0,218	30,62	551,14	0,27	0,259	0,254
12,5	0,260	85,05	1530,93	0,35	0,280	0,254
Fluid 3						
2,5	0,127	0,26	4,71	0,16	0,236	
7,5	0,160	2,36	42,40	0,27	0,259	
12,5	0,185	6,54	117,76	0,35	0,280	

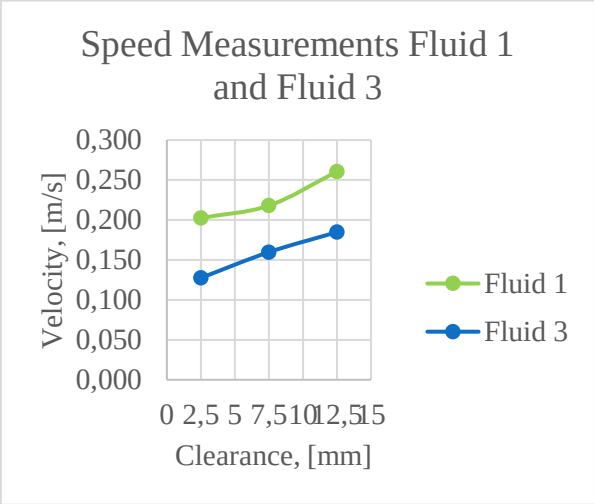

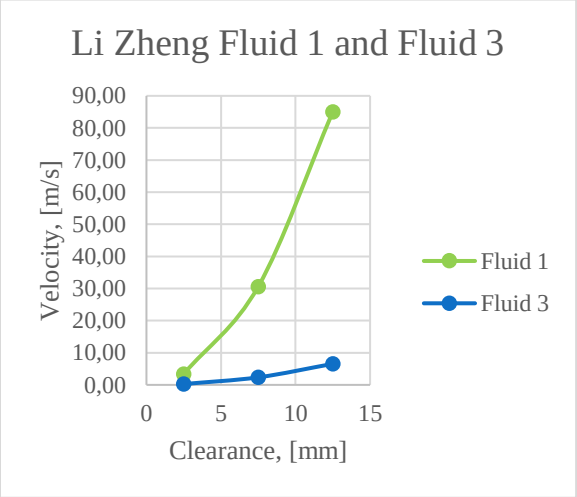

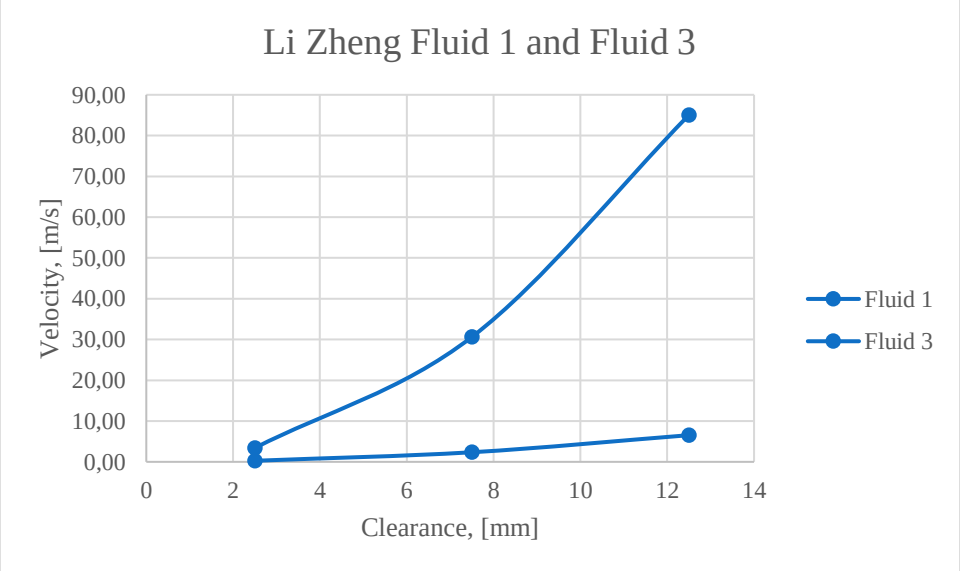

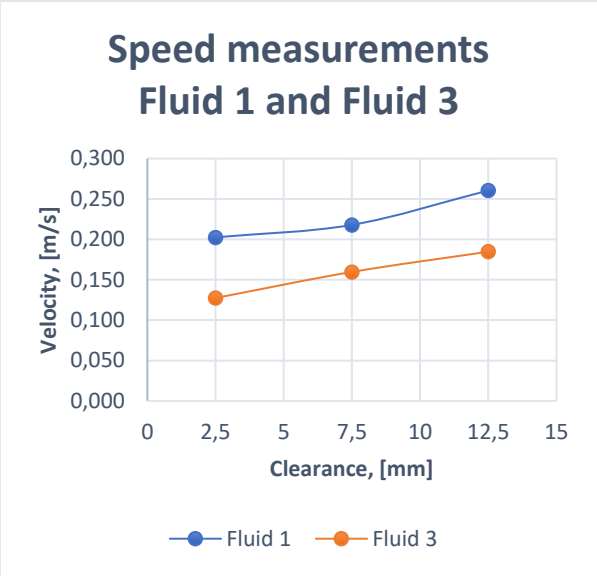
Speed measurements Fluid 1 and Fluid 3
Velocity, [m/s]
0,300
0,250
0,200
0,150
0,100
0,050
0,000
0
2,5
5
7,5
10
12,5
15
Clearance, [mm]
Fluid 1
Fluid 3

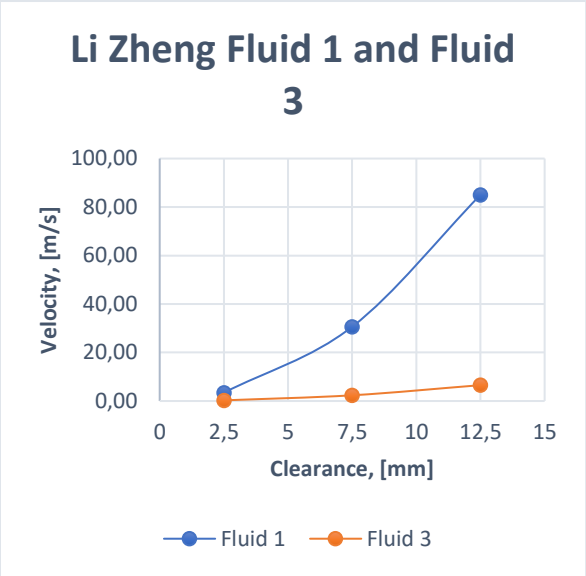
Li Zheng Fluid 1 and Fluid 3
Velocity, [m/s]
100,00
80,00
60,00
40,00
20,00
0,00
0
2,5
5
7,5
10
12,5
15
Clearance, [mm]
Fluid 1
Fluid 3

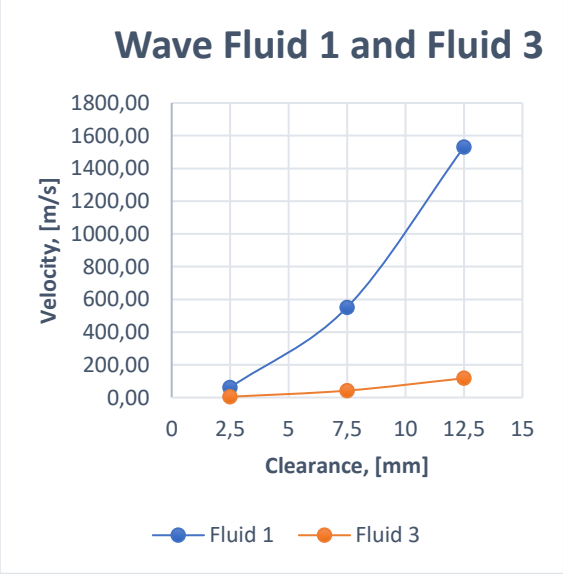
Wave Fluid 1 and Fluid 3
Velocity, [m/s]
1800,00
1600,00
1400,00
1200,00
1000,00
800,00
600,00
400,00
200,00
0,00
0
2,5
5
7,5
10
12,5
15
Clearance, [mm]
Fluid 1
Fluid 3

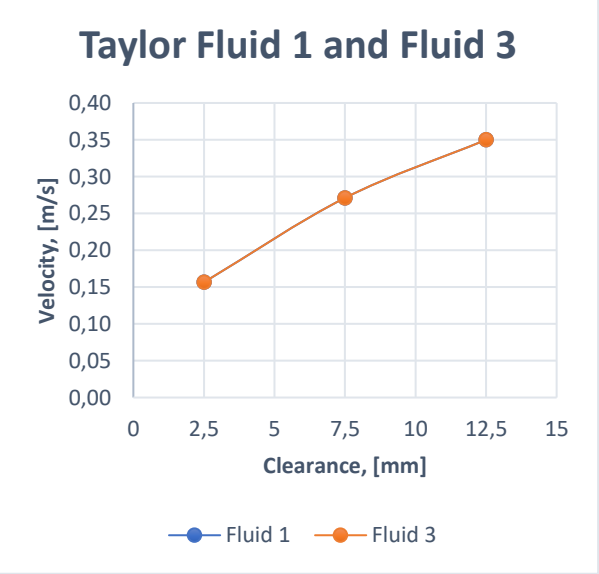
Taylor Fluid 1 and Fluid 3
Velocity, [m/s]
0,40
0,35
0,30
0,25
0,20
0,15
0,10
0,05
0,00
0
2,5
5
7,5
10
12,5
15
Clearance, [mm]
Fluid 1
Fluid 3

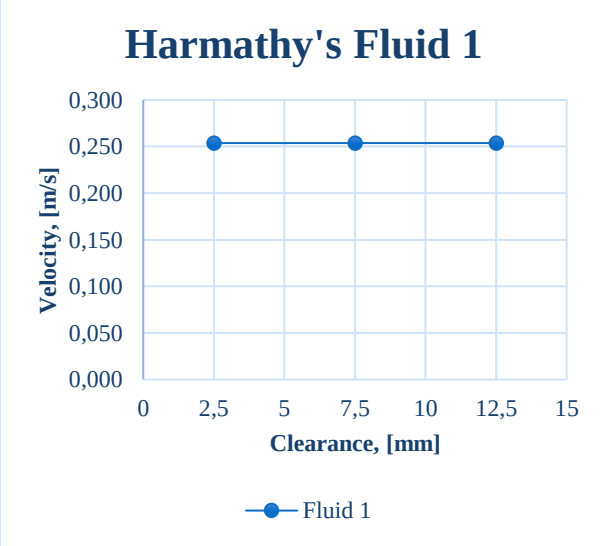
Harmathy's Fluid 1
Velocity, [m/s]
0,300
0,250
0,200
0,150
0,100
0,050
0,000
0
2,5
5
7,5
10
12,5
15
Clearance, [mm]
Fluid 1

Fluid 1 is the base fluid witch only contains water, have 1sg as density and is a Newtonian fluid. Fluid 3 is a non-Newtonian fluid, have the same density as fluid 1 but contains CP and is a more viscous fluid. To compare the models for the result there are three things that are compared.

1. Measured speed vs model calculated speed
2. Trend from the speed measurements vs trend from the model calculated speed
3. Parameters included.

Clearance, [mm]	Speed Measurments	Li Zheng	Wave	Davies and Taylor	Slug flow	Harmathy's equation
Fluid 1						
2,5	0,202	3,40	61,24	0,16	0,236	0,254
7,5	0,218	30,62	551,14	0,27	0,259	0,254
12,5	0,260	85,05	1530,93	0,35	0,280	0,254
Fluid 2						
2,5	0,154	0,57	10,21	0,16	0,236	
7,5	0,176	5,10	91,86	0,27	0,259	
12,5	0,207	14,18	255,16	0,35	0,280	
Fluid 3						
2,5	0,127	0,26	4,71	0,16	0,236	
7,5	0,160	2,36	42,40	0,27	0,259	
12,5	0,185	6,54	117,76	0,35	0,280	
Fluid 4						
2,5	0,187	2,65	47,77	0,16	0,236	
7,5	0,208	23,89	429,96	0,27	0,259	
12,5	0,220	66,35	1194,34	0,35	0,281	
Fluid 5						
2,5	0,166	0,73	13,14	0,16	0,236	
7,5	0,232	6,57	118,27	0,27	0,259	
12,5	0,297	18,25	328,52	0,35	0,281	
Fluid 6						
2,5	0,091	0,77	13,88	0,16	0,236	
7,5						
12,5						
Fluid 7						
2,5	0,153	0,99	17,85	0,16	0,236	
7,5	0,219	8,92	160,62	0,27	0,259	

Clearance, [mm]	Speed Measurements	%Li Zheng	%Wave	%Davies and Taylor	%Slug flow	%Harmathy's equation
Fluid 1						
2,5	0,202	1580	30144	-22,702	16,367	25,316
7,5	0,218	13948	252771	24,377	18,754	16,418
12,5	0,260	32552	587636	34,354	7,684	-2,589
Fluid 2						
2,5	0,154	268	6531	1,688	53,085	
7,5	0,176	2803	52156	54,216	47,244	
12,5	0,207	6761	123400	69,389	35,765	
Fluid 3						
2,5	0,127	105	3595	22,779	84,836	
7,5	0,160	1375	26444	69,724	62,051	
12,5	0,185	3441	63637	89,410	51,812	
Fluid 4						
2,5	0,187	1321	25471	-16,220	26,126	
7,5	0,208	11360	206182	30,067	24,187	
12,5	0,220	30082	543175	59,204	27,602	
Fluid 5						
2,5	0,166	341	7833	-5,511	42,247	
7,5	0,232	2735	50928	16,973	11,685	5,045
12,5	0,297	6038	110382	17,706	-5,659	-18,123
Fluid 6						
2,5	0,091	747	15144	71,877	158,750	177,272
7,5						
12,5						
Fluid 7						
2,5	0,153	547	11542	2,096	53,700	64,702
7,5	0,219	3972	73202	23,714	18,122	15,225

7.2 Summary of top closed rig experimental works

The trend from WHP vs BHP experimental work shows that all test gives lower pressure than WHP. In average 8-10% reduction from all injection rates combine. Because of small length of the well, the different fluid characterization didn't have the massive impact for the pressure sensor. Yet, it was surprising to get these results for all the fluids.

From the closed well simulation with bigger scale like a realistic wellbore, the result is clearer. Higher density and viscosity show that the WHP decreases. Increase in annular

clearance also has a big effect for the well head pressure with the same kick intensity. The bigger the clearance is then the lower is the finish WHP.

Table 7.2.1: Summary of fluids tested in the closed well simulation with rheology, BHP, WHP and difference between WHP and BHP (Delta)

Table xx closed rig construction pressure data with different fluids and their rheology measurements

							WHP			
		Rheology				BHP	Test		Delta	
Fluids	Density	PV	YS	LSYS	RHE-Apar (mPa/s)	Pump pressure	LR	HR	Delta_LR	Delta_HR
Water	1	1	0	0	1,06	500	469	350	31	150
Fluid 1						1000	867	800	133	200
						1500	1299	1331	201	169
						2000	1851	1902	149	98
						2500	2404	2338	96	162
2,5 CP	1	6	3	0,5	47,5	500	483	398	17	102
Fluid 2						1000	871	873	129	127
						1500	1383	1442	117	58
						2000	1913	1856	87	144
						2500	2390	2431	110	69
30 CP	1,09	3	2	0,5		500	434	298	66	202
Fluid 12						1000	806	893	194	107
						1500	1320	1324	180	176
						2000	1883	1871	117	129
						2500	2281	2285	219	215
50 CP	1,18	5,5	9	2,5	918	500	415	382	85	118
Fluid 5						1000	852	798	148	202
						1500	1410	1355	90	145
						2000	1873	1811	127	189
						2500	2289	2321	211	179
Brine	1,17	1,5	1,2	0,5	1,53	500	412	412	88	88
Fluid 4						1000	876	767	124	233
						1500	1387	1274	113	226
						2000	1877	1845	123	155
						2500	2331	2361	169	139
Bentonite	1,02	3,5	4	1	1060	500	411	409	89	91

Fluid 7						1000	889	792	111	208
						1500	1383	1290	117	210
						2000	1921	1839	79	161
						2500	2324	2362	176	138
Weighted Bentonite	1,28	6	33,5	25,5		500	359	441	141	59
Fluid 13						1000	874	824	126	176
						1500	1371	1378	129	122
						2000	1873	1918	127	82
						2500	2363	2362	137	138

From (Otto L. A Santos, 2021) they tested how 2 barrels and 5 barrels volume gas injected in the bottom hole of an wellbore with 2180 psi as BHP. The finish WHP were 97 psi for 2 barrels and 297 psi for 5 barrels.

From the closed wellbore experiment, comparing 2 meter to 1 meters pressure test with water as fluid, the WHP was significant lower for the longer length experiment. The 2 meter high wellbore had logically more fluid volume than the 1 meter experiment with same clearance and BHP.

From the drillbench simulation comparing small and big clearance, the WHP were much lower for the big clearance experiment with the same length and kick intensity.

Reviewing an ongoing SPE paper shows that the

8 Conclusion

For all models used to determine the velocity of the slug in the annulus, they need both a correlation factor and should be modified. No models where good enough to measure the velocity from the exercise but some were close. The Li Zheng and Wave equation uses all the parameters conducted in this thesis in their formulas and varied the same way as the speed measured. In relation to the experiment the speed increased too much considering the clearance difference. The Davies and Taylor equation had a nice trend considering clearance difference and were close to the measure speed but didn't vary when the viscosity increased. Same with the slug flow that had a nice trend with clearance and were closed to measure speed but didn't vary enough with viscosity. The Harmathy's Equation were also close to speed measure but didn't vary from clearance.

The Slug flow is the theoretical formula that had the best result. This formula doesn't have the viscosity measurement so to modify it to be even better than a correlation factor can be used or use equation from velocity vs PV. The trend where summarize for all clearance to (0,0006x^2-0,01496x+0,2409) with x as PV. Change (0,2409) with the slug flow equation and set in PV:

$$S = 0{,}35\sqrt{\frac{g\cdot(\rho_l-\rho_g)\cdot d_{out}}{\rho_l}}\cdot\left(1+\frac{0{,}29d_{in}}{d_{out}}\right)+0{,}0006x^2-0{,}01496x \qquad 28$$

Clearance	Speed measured	Slug flow	Modified Slug flow	%slug flow	%Modified slug flow
Fluid 1					
2,5	0,202	0,236	0,22065487	16,3668525	8,97859759
7,5	0,218	0,259	0,24386652	18,7539267	11,8902883
12,5	0,260	0,280	0,26553645	7,68441422	1,94139075
Fluid 2					
2,5	0,202	0,236	0,22065487	53,0853188	-5,2202814
7,5	0,218	0,259	0,24386652	47,2439676	-3,8074812
12,5	0,260	0,280	0,26553645	35,7650755	-7,6699373

With easy adjustment and modified equation, the velocity can calculate with 10-50 % error to -7-11% error in these two fluids.

From (Otto L. A Santos, 2021) experiments with Full-scale well the accomplished Build-up pressure trend and different pressure between BHP and WHP. The same trends were conducted in this experiment and also different pressure between BHP and WHP, even in a 1 meter tube the reduction of pressure to the WHP were 8-12 % vs 5000 meter full scale wellbore with 88-95%. With this, the theory is confirmed with compression of fluid and reduction of pressure up to WHP.

For next exercise:

For the next test of these experiments, you may want to look at friction in the well in the annulus between the drill string and the drill wall. The different between smooth and ruff wellbore. Another thing that can be examined is if the experiment is performed at an angle or horizontally. Will the result be the same or will it be totally different? In many formulas and article, the parameter that we didn't use in this thesis because of hard to measure it, the surface tension.

The next person who wants to continue the research on this thesis should, if they have the equipment, measure, and calculate with this parameter as well. Reynolds number…

Incline…

Table 7.2.1: Table of average measurements units from BHP, continuous, low rate and high rate with procent of difference between BHP and WHP measurements

Fluids	BHP	Continuous	LR	HR	% Continuous	% LR	% HR
Water	1500	1358	1378	1344,2	-9,5	-8,1	-10,4
2CP	1500	1356,6	1408	1400	-9,6	-6,1	-6,7
30CP	1500	1369,2	1344,8	1334,2	-8,7	-10,3	-11,1
50CP	1500	1358	1367,8	1333,4	-9,5	-8,8	-11,1
Brine	1500	1353,2	1376,6	1331,8	-9,8	-8,2	-11,2
Bentonite	1500	1354,4	1385,6	1338,4	-9,7	-7,6	-10,8
Weighted	1500	1364	1368	1384,6	-9,1	-8,8	-7,7

9 References

(Havnegjerde et al., 1992; Skjeggestad, 1989; Stavanger, 2021)

A. R. Hasan, C. S. K., Morteza Sayarpour. (2007). A Basic Approach to Wellbore Two-Phase Flow Modeling. *SPE Annual Technical Conferance and Exhibition*. https://doi.org/https://doi.org/10.2118/109868-MS (California, USA)

A.C.V. Martins Lage, E. Y. N., A.G.D.P. Cordovil. (1994). Experimental Tests for Gas Kick Migration Analysis. *Society of Petroleum Engineers (SPE)*, Article SPE-26953-MS. https://doi.org/https://doi.org/10.2118/26953-MS

Ambrose, S. (2015). The rise of Taylor bubbles in vertical pipes. *The University of Nottingham*, *307*(July).

Ashley Johnson and lan Rezmer-Cooper, S. C. R. T. B., Sedco Forex; and Dominic McCann, Anadrill. (1995). Gas Migration: Fast, Slow or Stopped. *SPE/IADC Members, Copyright 1995, SPE/IADC Drilling Conference.*, Article SPE/IADC 29342.

Batchelor, G. K. (2012). *An introduction to fluid dynamics*.

Britannica, T. E. o. E. (2022). Boyle's Law. In T. E. o. E. Britannica (Ed.), *Boyle's Law chemisty*. Britannica.com.

Bugg, J. D. (2002). The Velocity field around a Taylor bubble rising in a stagnant fluid: numerical and experimental results. *International Journal of Multiphase Flow*, *28*(5), 791-803.

Fattnes, L. (2020). New Nanoparticle Based Drilling Fluid Formulation and Characterization: Experimental and Simulation Studies. *Master's Thesis*, 189.

Frank Hovland, R. R. (1992). Analysis of Gas-Rise Velocities From Full-Scale Kick Experiments. *Society of Petroleum Engineers (SPE)*, Article SPE-24580-MS. https://doi.org/https://doi.org/10.2118/24580-MS

Ghajar, J. (2005). Non-boiling heat transfer in gas-liquid flow in pipes. *Journal of the brazilian Society of Mechanical Sciences*.

Gregersen, E. (2020). Archimedes' principle. *Britannica History*. https://www.britannica.com/science/Archimedes-principle

Guangzhao Zhou, C. L., Veerabhadra S. Denduluri, George K. Wong, Amit Amritkar, Ramanan Krishnamoorti, Andrea Prosperetti. (2021). Pressure-Difference Method for Gas-Kick Detection in Risers. *SPE Journal, SPE J. 26 (05): 2479–2497.*, Article SPE-205362-PA. https://doi.org/ https://doi.org/10.2118/205362-PA

Gucuyener, I. H. (1983). A Rheological Model for Drilling Fluids and Cement Slurries. *Paper presented at the Middle East Oil Technical Conference and Exhibition, Manama, Bahrain*, Article SPE-11487-MS https://doi.org/https://doi.org/10.2118/11487-MS

Guo, P. B., & Liu, G. (2011). *Applied Drilling Circulation Systems : Hydraulics, Calculations and Models*. Elsevier Science.

Hall, A. R. W. (1992). Multiphase Flow Of Oil, Water And Gas In Horizontal Pipes. *Imperical College of Science, Thechnology and Medicine, University of London, 300*.

Hamarhaug, M. (2011). *Well Control and Training Scenarios* University of Stavanger]. uis.brage.no. https://uis.brage.unit.no/uis-xmlui/bitstream/handle/11250/183373/Hamarhaug%2cMarianne.pdf?sequence=1&isAllowed=y

Harmaty, T. Z. (1960). Velocity of large drops and bubbles in media of infinite or restricted extent. *AIChE Journal The Global Home of Chemical Engineers, 6*, 281-288. https://doi.org/https://doi.org/10.1002/aic.690060222

Havnegjerde, B., Skjeggestad, O., & Omdal, P. I. (1992). *Øvelser i boreslamteknologi : vannbasert og oljebasert boreslam, tilleggsinformasjon om oljebasert boreslam, kort om nyere boreslamsystemer, saltlake-tabeller, "brine"-tabeller*. Alma Mater.

Islam, M. T. (2020). Single bubble rising behaviors in Newtonian and non-Newtonian fluids with validation of emperical correlations: A computational fluid dynamics study. *Wildy Online Libary*. https://onlinelibrary.wiley.com/doi/full/10.1002/eng2.12100

J. Tsamopoulos, Y. D., N. Chatzidai, G. Karapetsas, M. Pavlidis. (2008). Steady bubble rise and deformation in Newtonian and viscoplastic fluids and conditions for bubble entrapment. *Journal of Fluid Mechanics, 601*(Cambrige.org). https://www.cambridge.org/core/journals/journal-of-fluid-mechanics/article/steady-bubble-rise-and-deformation-in-newtonian-and-viscoplastic-fluids-and-conditions-for-bubble-entrapment/B44D808070E07F99D7DC3D23E2A3DEBC

Li Zheng, P. d. Y. (2000). Buoyant Velocity of Spherical and Non-Spherical Bubbles/Droplets. *Members ASCE, Department of Civil and Envir. Engineerin, Clarkson University, Postdam, NY 13699, A summary of the paper*.

M. Zamora, R. B. (1977). Prediction of Drilling Mud Rheology Using a Simplified Herschel-Bulkley Model. *J. Pressure Vessel, 485-490*.

Mobley, R. K. (2000). Characteristics of compressed air. *ScienceDirect*, 194-202. https://www.sciencedirect.com/science/article/pii/B9780750671743500640

Otto L. A Santos, W. C. W., Jyotsna Sharma, Mauricio A. Almeida, Mahendra K. Kunja, Charles E. Taylor. (2021). Use of Fiber Optic Information to Detect and Investigate the Gas-in-Riser Phenomenon. *SPE/IADC*, 25.

P. Skalle, A. L. P., J. Tronvoll. (1991). Experimental Study of Gas Rise Velocity and Its Effect on Bottomhole Pressure in a Vertical Well. *Society of Petroleum Engineers (SPE)*. https://doi.org/https://doi.org/10.2118/23160-MS

Pavlina Basarova, M. H. (2014). The collision efficiency of small bubbles with large particles. *Minerals Engineering, 66-68*, 230-233. https://www.sciencedirect.com/science/article/pii/S0892687514002040

R. M. Davies, S. G. T., F.R.S. (1949). the mechanics of large bubbles rising through extended liquids and through liguids in tubes. *royal society, London, 376-390*(200), 390.

Rolv Rommetveit, K. S. B., Jan Einar Gravdal, Clemente J.C. Goncalves, Antonio Carlos V.M. Lage, Jose E.A. Campos, Átila F.L. Aragão, Alberto Arcelloni, Shiniti Ohara. (2003). Ultra-Deepwater Hydraulics and Well Control Tests with Extensive Instrumentation: Field Tests and Data Analysis. *Society of Petroleum Engineers (SPE)*, Article SPE-84316-MS. https://doi.org/https://doi.org/10.2118/84316-MS

Schlumberger Oilfield, G. L. (2022). Saltwater mud. *Schlumberger Oilfield Glossary*. https://glossary.oilfield.slb.com/en/terms/s/saltwater_mud

Shahram Amirnia, J. R. d. B., Maurice A. Bergougnou, Argyrios Margaritis. (2013). Continuous rise velocity of air bubbles in non-Newtonian biopolymer solutions. *Chemical Engineering Science, 94*, 60-68. https://www.sciencedirect.com/science/article/pii/S0009250913001334

Skjeggestad, O. (1989). *Boreslamteknologi : teori og praksis*. Alma Mater.

Software, S. (2022, 28.04.2022). *Drillbench Dynamic Drilling Simulation Software*. https://www.software.slb.com/products/drillbench

Stavanger, U. i. (2021). Øvinger i Bore- og Brønnvæsker (PET210). In. Stavanger: Universitetet i Stavanger.

Strand, S. (1998). *Øving i bore-og brønnvæsker*. Høgskolen i Stavanger.

Tarvin, J. A. (1994). Gas Rises Rapidly Through Drilling Mud. *Society of Petroleum Engineers (SPE)*, Article SPE-27499-MS. https://doi.org/https://doi.org/10.2118/27499-MS

Terry, R. E. a. R., J. B. (2014). *Applied Petroleum Reservoir Engineering, 3rd Edition*.

The Bureau of Ocean Energy Managment, R. a. E. (2011). *Report Regarding the Causes of the April 20, 2010 Macondo Well Blowout*. https://www.bsee.gov/sites/bsee.gov/files/reports/blowout-prevention/dwhfinaldoi-volumeii.pdf

Thea Hang Ngoc Tat, D. G., Kjell Kåre Fjelde. (2021). Use of Transient Model for Studying Kick Migration Velocities and Build-up Pressures in a Closed Well. *OMAE2021-61143*, 8.

Tomiyama, A. (2002). Single bubbles in stagnant liquids and in linear shear flows [Graduate School of Science & Tech, Kobe University, Japan]. *Semantic Scholar*, 17.

Vikra, S. *Trykkontroll modul 1 & 2*.

Warren L. Lloyd, M. D. A., John R. Kozicz. (2000). New Considerations for Handling Gas in a Deepwater Riser. *Paper presented at the IADC/SPE Drilling Conference, ,* Article SPE-59183-MS. https://doi.org/https://doi.org/10.2118/59183-MS

10 Appendix